Design and Validation of a Polyaxial Knee Mechanical Prosthesis Alignment Protocol, Based on a Multivariate Biomechanical Model

Andrés Mauricio Cárdenas Torres

Tesis doctoral presentada para optar al título de Doctor en Ingeniería Electrónica y de Computación

Director
Alher Mauricio Hernández, PhD.

Codirector
Juliana Uribe Pérez, PhD.

Asesor

Jesús Alberto Plata Contreras, MD.

Universidad de Antioquia
Facultad de Ingeniería

Doctorado en Ingeniería Electrónica y de Computación

Medellín, Antioquia, Colombia

2022

Cita		Cárdenas Torres [1]
Referencia Estilo IEEE (2020)	[1]	A. M. Cárdenas Torres, “Design and Validation of a Polyaxial Knee Mechanical Prosthesis Alignment Protocol, Based on a Multivariate Biomechanical Model”, Tesis doctoral, Doctorado en Ingeniería Electrónica y de Computación, Universidad de Antioquia, Medellín, Antioquia, Colombia, 2022.

Doctorado en Ingeniería Electrónica y de Computación

Grupo de Investigación Bioinstrumentación e Ingeniería Clínica (GIBIC).

ABSTRACT

The above-knee lower limb loss is a common and complex amputation type, which compromises the loss of two fundamental joints for bipedal walking, thus limiting the person's autonomy. Its etiology is associated with health problems, mainly vascular or traumatic.

The transfemoral prosthesis is a supportive orthopedic device for the rehabilitation and adaptation of the amputee to their new mobility condition. Typically, the prosthesis is assembled with a socket, suspension system, prosthetic knee or joint unit, pylon, and prosthetic foot.

The adaptation to the prosthetic device is imperative for the amputee's functionality to improve; therefore, the proper performance of the prosthesis must be ensured. Prosthetic alignment is a procedure for adjusting the prosthesis according to the anatomical and biomechanical conditions of the amputee. The alignment procedure typically is conducted in three stages: bench, static, and dynamic alignment. The bench alignment includes the prosthesis assembling and the components aligning according to the load lines of the prosthesis to lock the joint unit. The purpose of static alignment is to match the prosthesis' load lines to the amputee's anatomical lines to ensure balance during standing. Dynamic alignment studies the amputee's gait to identify deviations associated with prosthetic misalignment; so, a fine adjustment of the prosthesis is performed.

The prosthetic alignment procedure is considerably dependent on the prosthetist's knowledge and skills in gait analysis and prosthetic alignment, as well as the amputee's communication skills and the rehabilitation center's assistive technologies. This decreases the likelihood of achieving nominal prosthetic alignment, making gait deviations the first sign of prosthetic misalignment. If the gait deviation is sustained over time, the amputee changes his or her gait patterns, resulting in diseases of the amputee's musculoskeletal system.

Multiple measurement systems are used to analyze the gait of humans. The recording of spatio-temporal, kinetic, kinematic, thermal, and muscle activity parameters provides information to detect gait deviations associated with prosthetic misalignment; however, there are no devices dedicated to alignment assessment. Often prosthetic fitting centers do not have access to gait and standing analysis technology; therefore, subjective strategies such as standing observation, visual gait analysis and verbal feedback from the amputee are used to adjust prosthesis alignment. Under this consideration, prosthetic alignment is highly subjective, so the integrity of the amputee's health is at risk. Computational approaches have been proposed to support transtibial prosthetic alignment procedures; however, the scientific literature does not report computational models dedicated to assess the alignment of transfemoral prostheses, so there is still a delay in this subject.

In this thesis, we consider that prosthetic gait is a multivariate system in which qualitative and quantitative variables of the patient and prosthesis are affected by prosthetic alignment and their relationship can be recognized with the gait and standing analysis. Under this premise, we proposed to develop a new protocol for the alignment of

transfemoral mechanical prostheses supported by computational models for the prosthetist's aid during the prosthetic alignment.

Initially, a literature review was performed to identify the qualitative and quantitative parameters, and the technologies typically used during the gait analysis and prosthetic alignment procedure. A prevalence was found in the use of kinetic, spatiotemporal, muscle activity, body balance, comfort, and stump temperature parameters for the evaluation of prosthetic gait. Likewise, the study allowed us to recognize the magnitude and direction of the alignment variations, the prosthetic elements aligned, the characteristics of the alignment tests, and the population size for recording. The literature review found a lag in the dynamic alignment research, particularly for transfemoral prostheses.

Based on the literature review findings, we proposed to record twenty-eight (28) parameters of the Ground Reaction Force (GRF), twelve (12) spatiotemporal parameters, six (6) electromyography parameters of the *tibialis anterior*, *gastrocnemius medialis*, *rectus femoris*, and the *biceps femoris*, and nineteen (19) stump temperature parameters. Additionally, a seventeen (17) question survey was applied to evaluate the prosthetic comfort, and anthropometric and sociodemographic information of the volunteers was asked. Random alignment variations of the socket were ranged between -18.0° to 28.0° in flexion-extension, adduction-abduction, and internal-external movements. The foot alignment variations ranged between -13.0° to 11.0° in dorsi-plantar flexion, eversion-inversion, and internal-external rotation.

Five (5) alignments were variated on the prosthesis for each amputee, one (1) nominal alignment and four (4) misalignments. The nominal alignment was judged by a senior prosthetist at the Mahavir Kmina Artificial Limb Center. The alignment test was double-blind, as neither amputees nor prosthetists were aware of the prosthetic misalignments. The alignments order was random. Each amputee walked down a hallway for fifteen (15) minutes and all parameters were recorded.

All parameters were processed to identify inter-subject statistically significant differences between nominal alignment and misalignments, to find the descriptive variables of the static and dynamic prosthetic alignment procedure. The prosthetic misalignment produces statistical differences of the GRF for the prosthetic limb during walking trials; however, no differences were observed in standing. The misalignments did not produce significant differences in the amputees' balance, comfort, and muscular activity of the sound limb, during gait and standing trials. Generally, the prosthetic gait of the transfemoral amputees was faster, more unstable, and fatiguing than the normal gait of the control group.

Parameters associated with the stump temperature did not show significant differences between both alignment conditions; however, the intra-subject analysis of the temperature's variation coefficient was different between nominal and misalignment for more than 70.0% of amputees. The inter-subject analysis of the Ground Reaction Force (GRF) showed statistical differences between both alignment conditions.

Statistical analysis showed no significant differences between nominal alignment and misalignments during static alignment. This limited the scope of the alignment protocol proposed in this thesis to dynamic alignment. From the statistical analysis, it was

identified that the following parameters behave as differentiating descriptors between nominal alignment and misalignment during dynamic alignment: the braking force impulse (I_3), propulsion force impulse (I_4), duration of the stance phase (t_1), duration of the braking phase (t_4), duration of the propulsion phase (t_5), time to propulsion peak (t_7), time to midstance valley (t_9), the impulse of terminal stance and pre-swing (I_6), the loading rate (LR), the braking (BI_V), and propulsion impulse (PI_V).

The alignment protocol proposed in this thesis includes two computational models. The Support Machine Vector (SMV) with Gaussian Kernel was used to classify GRF parameters of the amputee's gait between nominal and misalignments. The dataset was divided into 80% for training and validation, and 20% for model testing. The SVM model separated the dataset between nominal alignment and misalignment with 95.5% accuracy. The confusion matrix shows a 5.5% false-negative rate (FNR) for the misalignment class and a 1.8% FNR nominal class.

A Bayesian Regularized Artificial Neural Networks with 30 hidden layers was trained to estimate the magnitude and direction of prosthetic misalignment in flexion-extension, abduction-adduction, and internal-external rotation of the socket, and dorsiflexion-plantarflexion, inversion- eversion, and medial-lateral rotation of the prosthetic foot. The model could reproduce 94.11% of the information. The histogram shows 0.51° error for the estimated parameters; therefore, using both models, we propose the alignment protocol.

The computational alignment protocol was validated in the Mahavir Kmina Artificial Limb Center. Two (2) transfemoral amputees were recruited for the trials. One junior and

one senior prosthetist accompany the validation tests. The alignment protocol was iterated a maximum of 3 times, to limit interactions with the amputee by COVID-19 biosafety standards. During each iteration, junior and senior prosthetists evaluated the amputees' gait on a scale from zero (0) to ten (10).

The nominal alignment of the first amputee was not achieved throughout the three iterations, and prosthetists finally rated the prosthetic gait as 8.0. The prosthetists and computational protocol matched in the misalignment prosthesis for all three iterations. The non-convergence of the nominal alignment could be due to the precision of the prosthetists in adjusting the angles suggested by the computational protocol, and the learning curve in the use of the protocol.

In the validation session of the alignment protocol for the second amputee recruited, the prosthetists were more skilled in the alignment’s adjustments, so the nominal alignment was achieved in the second iteration, ranging the amputee’s gait at 9.6.

The prosthetists on average scored 8.18 on the prosthetic gait after applying the computational alignment protocol. The natural amputees' gait patterns affected gait quality; therefore, the correction of gait deviations should be done with a posterior treatment. Prosthetists scored 8.52 for this kind of computational aid of the prosthetic alignment, and they stated that the alignment protocol allowed them to do a better job, rating it with an 8.58. The senior prosthetist stated that the protocol made him take 37 minutes longer than usual and the junior prosthetist stated that computational protocol did not take him longer.

The result of our computational alignment protocol presents an advance in the study of dynamic prosthetic alignment for transfemoral amputees; however, the prosthetic alignment protocol should continue to be studied to clarify the uncertainties caused by the intersubjectivity of the data and to find new strategies to support prosthetists. The rate of convergence of the protocol could be improved by retraining the computational models with a larger dataset; however, the accuracy of angles adjustment is perhaps affecting the convergence of the nominal alignment. Therefore, further research should be focused on the development of more precise alignment tools.

Index

Figures Index

Tables Index

Chapter 1

General Introduction

This chapter describes the main characteristics of the prosthetic alignment procedure and highlights the problematic elements that motivated this research. The hypothesis is presented, and the objectives were developed throughout this doctoral thesis. Likewise, the methodological structure and development of experiments that were used in this research to confirm the investigative hypothesis are disclosed. Finally, a general outline of the thesis is presented.

1.1. Problem statement.

According to the World Health Organization (WHO) and The World Bank, worldwide there are more than one billion people affected by some kind of disability [1], [2]. Some estimates suggest between 5% and 10% of the Colombian population has some type of

disability [3]; however, in more recent data an estimated 7.2% is reported at the national level [4]. The number of worldwide amputees is not known; for instance, the WHO estimates forty million people need a prosthesis, orthosis, or rehabilitation treatment [5]. Other reports suggest that in developed countries there are more than fifty-seven million amputees [6]. In Colombia, more than 120.000 people with upper or lower limb problems were reported in 2014 [7].

Amputation is associated with different causes, such as vascular disease, trauma, infections, diabetes mellitus, and cancer [8]. The unilateral lower limb amputation is a generalized and common case and it is classified according to the amputation height [9]–[11]. Transfemoral amputation is a complex injury that comprises the portion of the lower limb, which is necessary for human locomotion. The goal of surgery is to supply muscle balance and to position the femur for weight-bearing and ambulation [12]. Adaptation of transfemoral amputees can be significantly achieved with proper medical treatment and psychological support. The artificial limbs allow the amputee to adapt to the new mobility conditions; however, only 10% of the worldwide amputees can access the prosthesis [13], [14].

The components of the transfemoral mechanical prosthesis are socket, suspension system, joint unit (knee), shank, and a terminal device (foot) [15]. The prosthetic alignment is a procedure to position the prosthetic components to achieve the most suitable limb geometry, and amputees' functionality and comfort [16], [17]. The alignment protocol is an experimental procedure consisting of three stages: bench alignment, static alignment, and dynamic alignment [18]–[20].

The bench alignment implies the assembly of the prosthetic components seeking the balance of anterior and sagittal load-lines. During the prosthetic assembly and bench alignment procedure, the prosthetist takes care of the prosthetic weight balance to keep the knee locked while the prosthesis is upright. The static alignment procedure aims at a correct integration of the prosthesis and the patient. This procedure consists of aligning the anatomical lines of the amputee with the load lines of the prosthesis to ensure a correct distribution of the amputee's weight on the residual limb [21]. The dynamic alignment implies a complex amputee gait assessment procedure of the prosthetic gait to detect deviations such as circumduction, lateral trunk tilt, abduction gait, pistoning, swinging movement of the whip, among others [22]–[24].

Bench alignment is developed by using lasers or plumb lines to align the prosthesis from distal to proximal component [25]. Manufacturers such as Ottobock and Fillauer have developed sliding adapters that align the socket line in the frontal and sagittal to the stump angles. Typically, these devices are used for contracted residual limbs [26], [27]. The L.A.S.A.R system (Ottobock, Germany) is used to perform static alignment. This device uses load cells to align the anatomical lines of patients with the prosthesis lines to improve the weight distribution lines. Inertial measurement units [28], motion capture systems [29], and the Europa + system (Orthocare, USA) are used to assist the prosthetist during gait analysis and assess dynamic alignment.

The previously described devices help to perform the alignment procedures; however, some problems remain. For example, sliders must be integrated into the prosthesis, so the final alignment is affected when they are removed from the prosthesis. Any device that allows analysis of balance or human gait performance can be useful in assessing the effect

of prosthesis alignment; however, there are no devices completely dedicated to assisting the prosthetist during alignment.

The definition of the optimal prosthetic alignment depends on multiple characteristics of the amputee such as anatomical features, residual limb morphology. and the degree of adaptation to the prosthesis. Likewise, the nominal alignment depends on the type of prosthesis used and its particularities. For this reason, prosthetic fitting centers include gait and standing analysis devices, amputee feedback, and procedural observation to assess prosthetic alignment. The prosthetist's skills to perform the alignment directly affects the likelihood of misaligning the prosthesis. These phenomena increase the uncertainty and subjectivity during the definition of the optimal or nominal alignment.

Computational models reported in the literature were able to identify between nominal alignments and misalignments of transtibial prostheses during walking, and suggesting the alignment angle of the prosthetic foot to achieve the optimal alignment during standing [30]; however, there is a gap in the knowledge of transfemoral alignment [31]–[33]. Computational models are unknown to aid the prosthetist during static or dynamic alignment of transfemoral mechanical prostheses that include socket and prosthetic foot angle changes simultaneously.

Commercial support systems and those reported in the literature are scarce, so the prosthetist uses observation as the main evaluation mechanism [34]. Therefore, the alignment of transfemoral mechanical prostheses could be summarized as an iterative, qualitative, and complex procedure in which the prosthetist analyzes multiple biomechanical variables during standing and walking of the amputee. The subjectivity

during the definition of alignment quality, i.e., nominal or misaligned, produces negative effects on the amputee's health and prosthetic fitting. The prosthetic misalignment triggers diseases such as osteoarthritis, back pain, and stump ulcerations [35], additionally affects the energy expenditure [36], and increased pressure on the skin that is in contact with the socket [27].

To conclude, the main problem with alignment protocols is the subjectivity involved in identifying the nominal or optimal alignment, taking into account the particularities of the amputee. Also, the absence of computational alignment models for transfemoral prostheses is the motivation for developing this research.

1.2. Scope, hypothesis, and proposed solution.

Considering the limitations of alignment procedure of the mechanical transfemoral prostheses and the negative effect on the amputee's wellness when misalignments occur; furthermore, the experience of the research group in bioinstrumentation and clinical engineering (GIBIC) [37] and the Mahavir Kmina Artificial Limb Center in prosthetic limbs research, the following hypothesis is considered: "*An alignment protocol based on a computational model will predict the value of the angles with which a transfemoral mechanical prosthesis should be aligned during the prosthetic gait analysis"*, based on a literature review and a statistical analysis that identifies the gait parameters significatively affected by the prosthetic alignment procedure.

The alignment protocol proposed will reduce the subjectivity of the prosthetic alignment procedure, providing the prosthetist a greater control of the alignment procedure. A new

alignment protocol will be the basis for new prosthetic procedures and the continuous improvement of the transfemoral and transtibial alignment protocols.

1.3. Main objective.

To propose an alignment protocol that helps the prosthetist during the static and dynamic alignment procedure, relating the biomechanical variables of the interaction between the patient and the users of the transfemoral mechanical prosthesis with a polyaxially knee.

1.4. Specific objectives.

I. To identify the set of biomechanical variables that characterize the static and dynamic alignment of transfemoral mechanical prostheses.

II. To propose a qualitative and quantitative measurement method for the biomechanical variables set that are characteristics in the static and dynamic alignment of transfemoral mechanical prostheses.

III. To design a protocol for patients' selection and the biomechanical variables record of the amputee and the prosthesis, during the static and dynamic alignment procedure.

IV. To propose and evaluate a computational model based on the biomechanical variables recorded during the static and dynamic analysis of the transfemoral mechanical prostheses.

V. To propose an alignment protocol to support the prosthetist during the static and dynamic alignment of transfemoral mechanical prostheses, based on the computational model.

VI. To validate the alignment protocol of transfemoral mechanical prostheses by a statistical evaluation with transfemoral amputees.

1.5. General methodology.

To achieve the aim of this thesis, the methodology outlined in Figure 1 is followed. As well as the methodology helps to understand the development of the chapters in the presented thesis document.

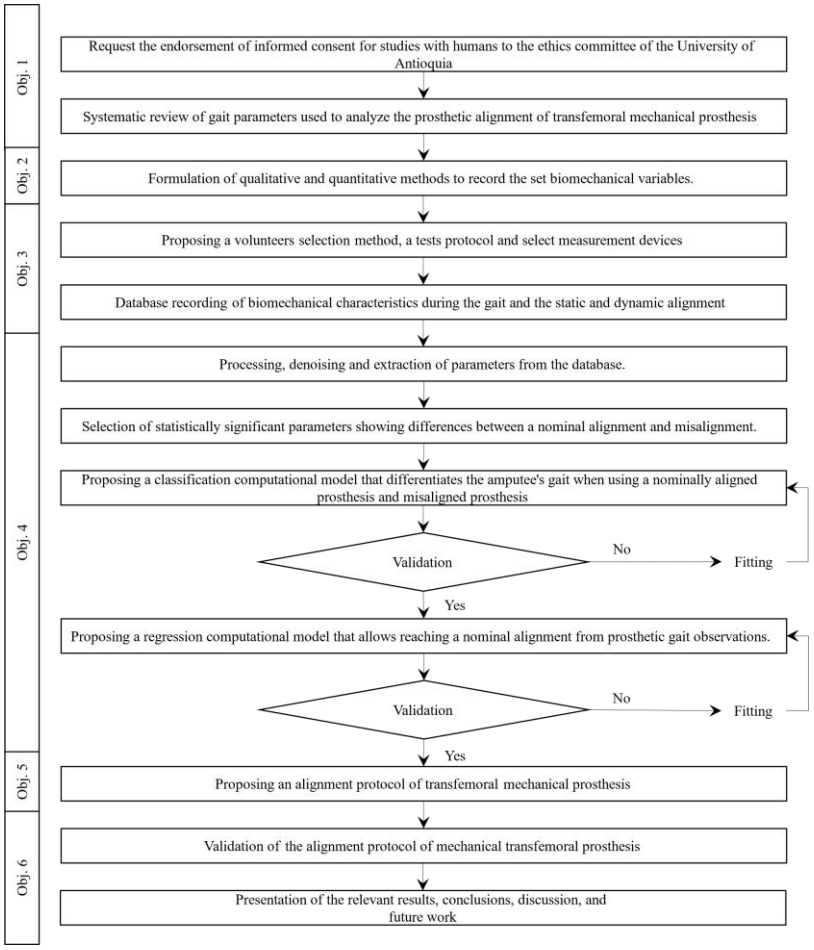

Figure 1. Thesis methodology.

1.5.1. Ethics committee endorsement request and database registration.

The bioethics committee of the University of Antioquia requested the endorsement of the informed consent approval. This study registered a set of anatomical and biomechanical variables from a population of healthy adults with transfemoral amputation. The risk for the amputee was minimal during the tests. The volunteers were recruited by Mahavir Kmina Artificial Limb Center. Participation in the study was conditional on the endorsement of Mahavir Kmina and the inclusion-exclusion criteria.

Sixteen transfemoral amputees were enrolled with the preselection of the Mahavir Kmina Artificial Limb Center (MK) and a control group of fifteen non-amputee volunteers. The transfemoral amputees included in the study were adults with at least one year of amputation surgery, more than six months of experience wearing a transfemoral prosthesis, being over 18 years old and under 70 years old. The exclusion criteria for both groups were diagnosis of neuromuscular or bone diseases, consumption of intoxicating drinks or hallucinogenic substances in the last three days, and not being pregnant.

For the database construction, sociodemographic and anthropometric information, amputation cause, morphological characteristics of the residual limb, and parameters of the prosthesis were asked to the volunteers. The approval of the people was requested for video recording, photography, and biomechanical parameters collection.

1.5.2. Gait parameters associated with the study of prosthetic alignment.

The understanding of biomechanical parameters that describe a clinically acceptable alignment of transfemoral mechanical prosthesis is an essential previous stage to propose

a computational model for prosthetic alignment. A literature systematic review was completed following the checklist Preferred Reporting Items for Systematic and Meta-Analyses – PRISMA [38]. Thirty-eight articles were chosen for the quantitative analysis. The quality assessment of the papers was performed using an adaptation of the Downs & Black criteria [39], focusing mainly on the population information, the alignment variation magnitudes, and the alignment experiment procedure. The quality level of the studies was divided among A, B, and C, according to the number score calculated by the Van der Linde et al. method [40].

The literature review allowed us to identify that the clinically accepted protocol to perform prosthetic alignment consists of changing the socket and foot angles to adjust the amputees' biomechanical to normal gait patterns [41]; however,. In addition, insufficient studies were found to explain the effects of prosthetic misalignment in transfemoral amputees. The results of the literature review are deepened in **Chapter 3.**

1.5.3. Selection of parameters related to the alignment procedures and test protocol formulation.

The parameters that would be recorded during the alignment tests were defined during this stage. The literature review was the input for the test protocol construction because it allowed the identification of clinically accepted conditions. The test protocol defined the parameters to be recorded for the patient, the prosthesis, and, in general, the gait analysis.

The parameters that would be recorded during the alignment tests and the formulation of the test protocol were defined during this stage. The literature review allowed us to

identify the parameters clinically accepted to assess the prosthetic gait. The muscle activity, kinetic, and kinematic parameters were chosen to record the standing and walking. Anthropometric and sociodemographic data of the volunteers, characteristics of the stump, and the prosthesis in the amputee group were recorded. The thermography of the residual limb was recorded. The Prosthesis Evaluation Questionnaire (PEQ) was used to assess the amputees' comfort [42], [43]. The test protocol defined the characteristics of the walking test environment, the measurement instruments, and procedure for data capture, the amounts of alignment variations, the sequence of the tests, among others. **Chapter 4.** and **Chapter 5.** explain and develop the parameters choice and the alignment experimentation

1.5.4. Database recording for amputees and the control group.

The characteristic gait parameters were recorded when dynamic alignment for transfemoral amputees was performed. The facility of Mahavir Kmina Artificial Limb Center (MK) was used as a gait analysis laboratory for ten months. The amputee records took three days. The clinical evaluation of the patient and their inclusion assessment were performed by the MK experts during the first day. If the patient had been approved by MK and agreed to take part in the study, their anatomical parameters were recorded, and informed consent was presented. On the second day, the MK prosthetists built the prosthesis, and the bench alignment was done. On the third day, the volunteer was prepared for walking trials. The walking trials took around 8 hours. Four misalignments and one nominal alignment were performed. The gait trials will be expanded on **Chapter 4.** and **Chapter 5.**

1.5.5. Statistical significance analysis of gait parameters collected.

The parameters statistically most affected by prosthetic misalignment were identified and showed statistically significant differences between nominal alignments and prosthetic misalignments. Kurtosis-bias analysis [44] and Kolmogorov-Smirnov test [45] were applied to identify the normal distribution of data. The one-way analysis of variance ANOVA [46], Kruskal-Wallis test [47], and Kolmogorov-Smirnov tests [48] was used to identify statistically significant differences between nominal alignments and misalignments, including within and between subjects analysis. The Bonferroni test was used to perform a multiple comparison test between volunteers to compare nominal alignments and misalignments. The statistical analysis will be expanded in **Chapter 4.** and **Chapter 5.**

1.5.6. Novel alignment protocol for transfemoral mechanical prostheses.

The alignment protocol for transfemoral mechanical prostheses proposes the use of two computational models. Vector support machines [49] are used to identify whether a prosthetic alignment is correctly performed (nominal) or incorrectly performed (misalignment). A regression model using neural networks [50], [51] allows estimating the misalignment angles in frontal, lateral, and transverse rotation of the socket and foot. The prosthetist uses the alignment protocol to support his assessment criteria of the alignment quality. The alignment protocol used both alignment models to estimate the magnitude and direction of prosthetic misalignment. With this information, prosthetists can adjust the prosthesis to achieve nominal alignment. The development of the models and the alignment protocol is expanded in **Chapter 6.**

1.5.7. Alignment protocol validation.

One junior and one senior prosthetist to perform the alignment protocol validation tests. The prosthetists align the prosthesis using the angles estimated by the models and the walking test is repeated three times or until the smallest misalignment tolerance is reached. During the alignment tests, the prosthetists evaluate the gait of the amputee. If in the last protocol iteration, the models and prosthetists disagree with the prosthetic alignment, the protocol ends, and a failure is reported.

The Mahavir Kmina artificial limb center provides the prosthetist and the new prostheses for the volunteers participating in the study. A group of two transfemoral volunteers was recruited for two days to validate the protocol. The population characteristics were as follows: the average age of 49.3 (±3.2) years, a weight of 65.8 (±10.3) kg, the height of 166.7 (±7.7) cm, and a body mass index of 23.7 (±3.0). The prosthetists evaluated the effectiveness of the alignment protocol. The results of the modification of the model can be observed in **Chapter 6.**

1.6. Thesis outline.

This thesis is a compendium of 6 articles developed in the framework biomechanics, prosthetic gait analysis, and prosthetic alignment procedures. This doctoral thesis is part of the research line in biomechanics, and modeling and simulation of biomedical systems in the Bioinstrumentation and Clinical Engineering Research Group - GIBIC. The doctoral student was a beneficiary of the COLCIENCIAS grant-727 of 2015. It also received support from the University of San Buenaventura Medellín.

Additionally, this work received funding from the following projects:

- Fondo Nacional de Regalías de la República de Colombia-Project code Ruta N 139C "*Fortalecimiento de plataforma tecnológica para la formación especializada en el área de la salud y el desarrollo de tecnología biomédica*".
- Fondo Nacional de Regalías de la República de Colombia-Project code Ruta N 470C "*Sistema integrado para el monitoreo continuo de pacientes en los ambientes domiciliarios, intrahospitalario y de movilidad para nuevos modelos de atención y de mercado*".

The development of this thesis is presented as a compendium of articles that are being evaluated and submitted to indexed journals in the biomechanics area. Chapters 3 to 6 list the articles proposed for the journals:

1. *Biomechanical variables used during static and dynamic alignment of transfemoral mechanical prostheses.* (**Chapter 3.**).
2. *The effect of prosthetic alignment on the stump's temperature and the ground reaction force.* (**Chapter 4.**).
3. *Evaluation of the prosthesis alignment effects on spatiotemporal, comfort, balance, and muscle activity information of transfemoral amputees during gait and standing.* (**Chapter 4.**).
4. *Computational protocol to assist the prosthetist during the alignment of transfemoral prosthesis.* (**Chapter 6.**).
5. *Parametric Modeling of Kinetic-Kinematic Polycentric Mechanical Knee.* (Chapter 6).

6. *Gait parameters identification for the differentiation of neurodegenerative diseases using classifiers.* (Chapter 6).

Chapter 2.

Theoretical background

Understanding the prosthetic alignment procedure and proposing a prosthetic alignment model involves a set of theoretical knowledge. Figure 2 shows the schematic used to present the conceptual framework.

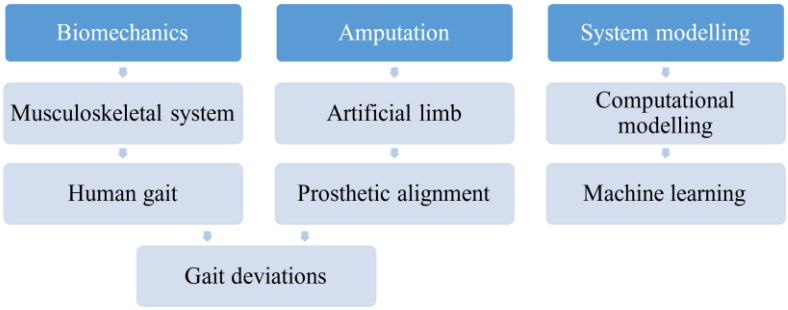

Figure 2. The generality of the conceptual framework.

2.1. Biomechanics of the human gait.

The bipedal gait involves the activation and synchronization of the musculoskeletal system to move forward the body's center of gravity in such a way that the energy expenditure is minimized [52]. A set of bones, joints, and muscles handle producing the power necessary to articulate the lower limbs and support the body weight. A brief explanation of the system that regulates human movement will be presented below.

2.1.1. Musculoskeletal system.

The human lower limbs involve three main joints: the hip, knee, and ankle. The hip joint transfers the forces and weight of the trunk to the lower limbs. It is a synovial type of ball joint with three rotational degrees of freedom. This joint can perform 120° flexions, 20° extensions, 120° adductions, 30° abductions, and internal or external rotations between 30° and 45º, respectively. The femoral head is two-thirds of a solid sphere that inserts into the acetabulum [53]. Figure 3(a) shows the inclination of the femoral head concerning the diaphysis (close to 125°).

Figure 3(b) shows the knee which is a synovial joint included by the tibia's proximal end, the femur's distal end, and the patella. From a mechanical perspective, this joint is a hinge-type joint with one degree of freedom. The knee can perform 120º flexions and hyperextension between 5° to 10º. The asymmetry of the femoral condyles produces flexions and extensions combined with medial-lateral rotations. The knee articulates the thigh and leg to support and stabilize the human body. The head of the femur has an inclination angle (θ) in relation to the diaphysis. Angles greater than $\theta > 125°$ result in *genu valgum* and angles less than 125° produce a *genu varum*.

The hip joint has three ligaments: on the anterior side, the iliofemoral and pubofemoral ligaments, and on the posterior side the ischiofemoral ligament. The pelvic walls have a set of muscles: the internal obturator, piriformis, levator ani, and coccygeus. The internal obturator laterally rotates the thigh and helps to fit the head of the femur into the acetabulum. The ligament of the femoral head connects the acetabulum to the femoral head. The medial collateral ligaments and the tibial collateral ligament connect the femur with the tibia and fibula, respectively [54].

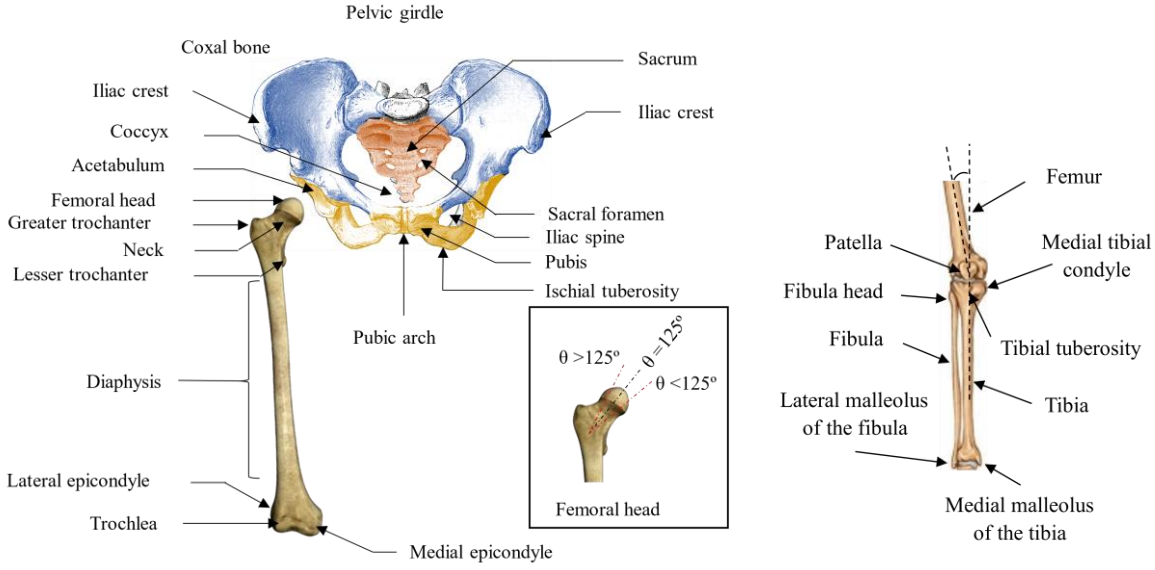

(a) pelvic girdle[1]

(b) knee joint [2].

Figure 3. Lower torso of the human skeletal system.

To understand the muscular system, we must recognize the characteristics of the human motor system, which produces movement. The cerebral cortex and the musculoskeletal system form a feedback loop that controls and adjusts movement. A motor unit is

[1] Image adapted from [276].

[2] Image adapted from [277].

composed of a motor neuron in the spinal cord and muscle fibers. A muscle is formed by thousands of fibers [55]. The lower limb muscle system is described in Figure 4.

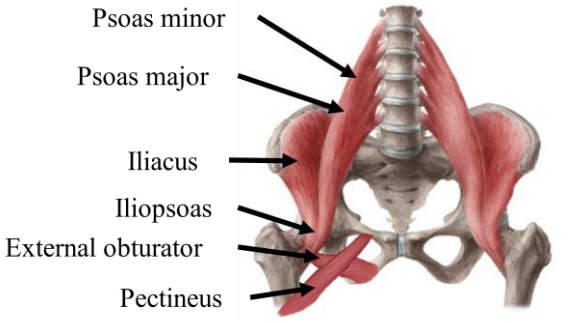

a) Pelvic muscles [3].

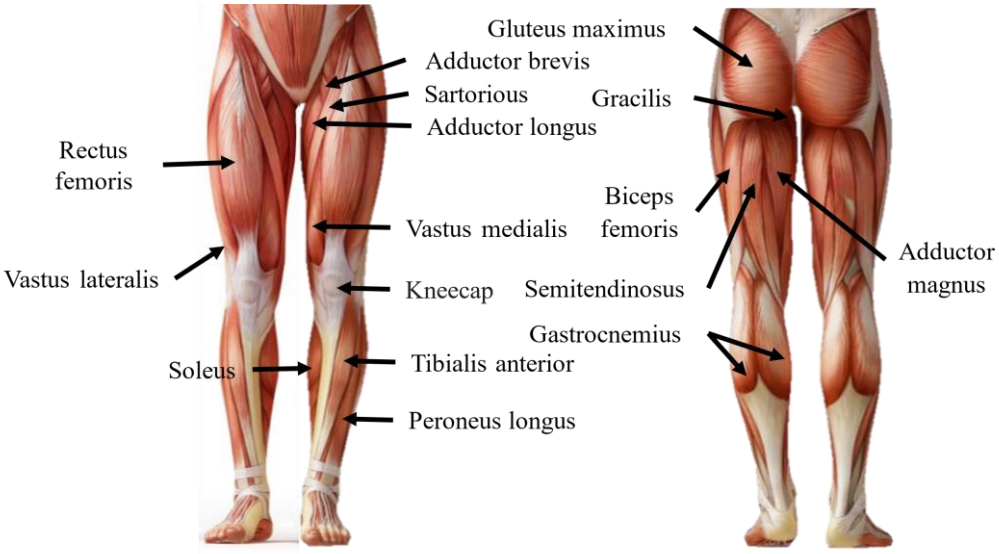

b) Muscles of lower limbs [4].

Figure 4. Muscle information of the lower limbs.

The hip muscles are strong and supportive of locomotion, stability, and posture of human gait. Muscles are organized according to their location, for instance in the anterior,

[3] Image adapted from [278].
[4] Image adapted from [279].

medial, and posterior compartments are considered as extensor, adductor, and flexor, respectively. The thigh walls include three intermuscular septa in anterior, posterior, and lateral sides. The anterior compartment of the thigh includes the pectineal, iliopsoas, sartorius, and quadriceps femoris. The pectineus muscle produces adduction and flexion of the thigh, as well as medial rotation. The iliopsoas is a powerful muscle considered the main flexor of the thigh; it includes the psoas major and the iliac. These muscles connect the spine and pelvis to the femur's trochanter. The sartorius is a biarticular muscle, considered the longest muscle of the body. It produces flexion movements of the hip and knee joints, abductions of the thigh, and lateral rotations to a lesser extent. The quadriceps femoris includes four portions, the *rectus femoris*, *vastus lateralis*, *vastus medialis*, and *vastus*. It is a biarticular muscle influencing the hip and knee, and it is considered the main extensor of the lower limb.

The medial compartment is composed of the *adductor longus*, *adductor brevis*, a*dductor magnus*, *gracilis*, and *external obturator*. The *adductor longus* causes adduction of the thigh. This muscle arises proximally from the body of the pubis below the pubic crest and inserts on the femur's *linea aspera*. The *adductor brevis* helps in the adduction of the thigh; however, it also flexes it. Raise from the body and lower branch of the pubis and is inserted in the upper third part of the femur's *linea aspera*. The adductor magnus flexes the thigh and the hamstring extends it. The *gracilis* adducts the thigh flexes the leg and helps the medial rotation. The muscle originates from the ischium and pubis and inserts into the trochanteric fossa of the femur. The external obturator is a muscle deeply located; produces lateral rotation of the thigh and stabilizes the femur’s head in the acetabulum;

muscle originates on the external obturator membrane and the surrounding hollow of the pelvis and is inserted on the rear of the greater trochanter.

Muscles such as the biceps femoris, popliteal, semimembranosus, sartorius, gracilis, semitendinosus, and gastrocnemius take part in knee flexion. Except for the gastrocnemius, the anterior muscles allow for extension and hyperextension of the knee during standing. The popliteus and biceps femoris rotate and flex the tibia over the femur. The knee extensors are grouped into the rectus femoris and the vastus. The Rectus Femoris is a biarticular muscle that extends the leg and flexes the hip. The vastus medialis, lateral, and medial rotate the knee.

2.1.2. Human gait cycle.

The gait cycle has two main phases: the stance phase and the swing phase (Figure 5). The stance phase represents 60% of the gait cycle and during the 40% remaining the swing phase is performed. The human body weight is supported by one lower limb throughout the stance phase. The single support is divided mainly into five moments: the heel strike, the loading response, the midstance, the heel off, and the toe-off. After this, the foot leaves the ground, and the swing phase begins. The lower limb is brought back in hip extension, from where it advances forward until it reaches the flexion of the hip and a progressive extension of the knee until the heel has contact with the ground [56].

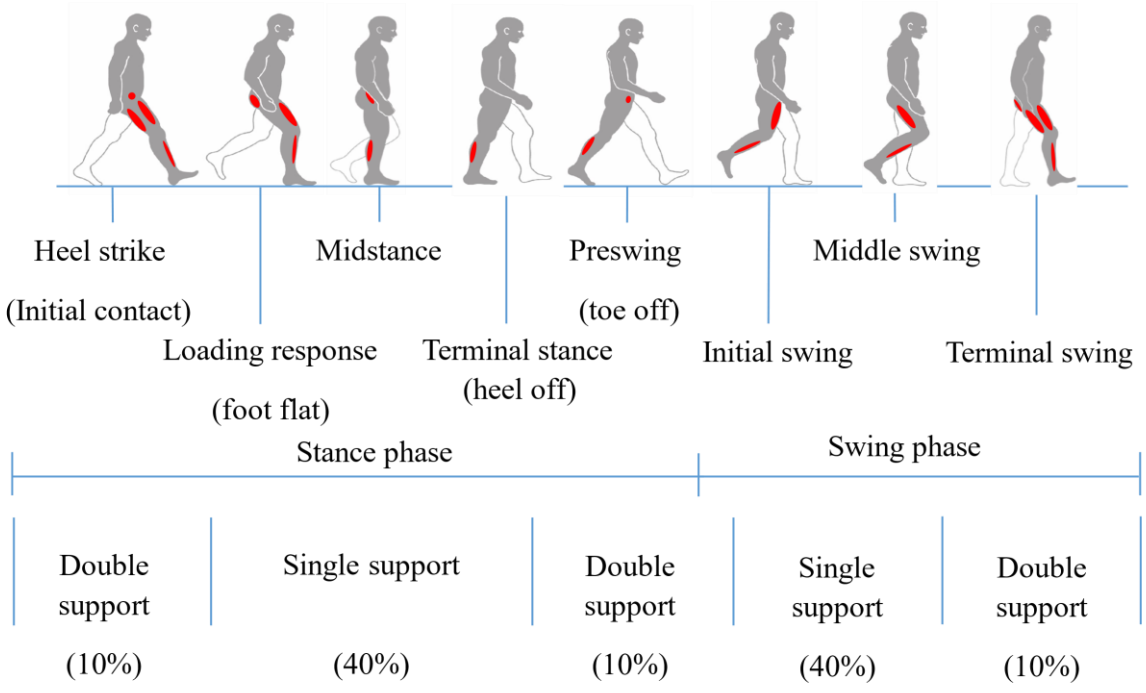

Figure 5. Gait phases and muscle activation during human gait.

The biomechanics of human gait can generalize into a set of specific movements, however, each person adapts their gait by making their gait patterns unique [57]. Table 1 shows the parameters typically used to assess human locomotion [58].

Spatiotemporal parameters	Kinematics	Kinetics	Muscular activity
Stance duration (s), stride duration (s), double stance duration (s), swing duration (s), swing phase (%), double stance phase (%), stance phase (%), double stance phase (%), cadence (step/min), flight speed (m/s), average speed (m/s), stride length (m), step length (m), step width (m), and gait deviation index [59].	Pelvic obliquity (deg), pelvic tilt (deg), pelvic rotation (deg), hip abduction-adduction (deg), hip rotation (deg), knee flexion-extension (deg), hip flexion-extension (deg), ankle dorsi-plantarflexion (deg), foot progression (deg), and gait profile score (deg) [60].	Ground reaction forces and moments on tree components: vertical, mediolateral, and anteroposterior [61].	Timing and the intensity of muscle contraction during gait cycles [62].

Table 1. Parameters for gait assessment.

2.1.2.1. Spatiotemporal and kinematic parameters of the gait

Spatiotemporal data describe temporal characteristics, distance, and speed of the lower limbs during walking. The individuality of the foot tread, the rhythm and gait patterns are studied during the support and swing phases of walking, which allows to find possible gait disorders of the evaluated subject. Table 1 shows an example of spatiotemporal parameters.

The kinematic analysis allows the analysis of the angular position and orientation of the body segments such as the hip, pelvis, knee, and foot during the gait performing. The spatiotemporal and kinematics parameters provide diagnosis support and therapy considerations for postural problems, musculoskeletal disorders, and neurological injuries [63].

The motion analysis systems use reflective markers to calculate spatiotemporal and kinematics analysis of gait. The Helen Hayes [64] and Davis [65] are protocols for positioning reflective markers on bony landmarks. The gait patterns for a normal gait have already been previously found [66]. Figure 6 shows the typical ranges of kinematics parameters that are usually used to assess human gait.

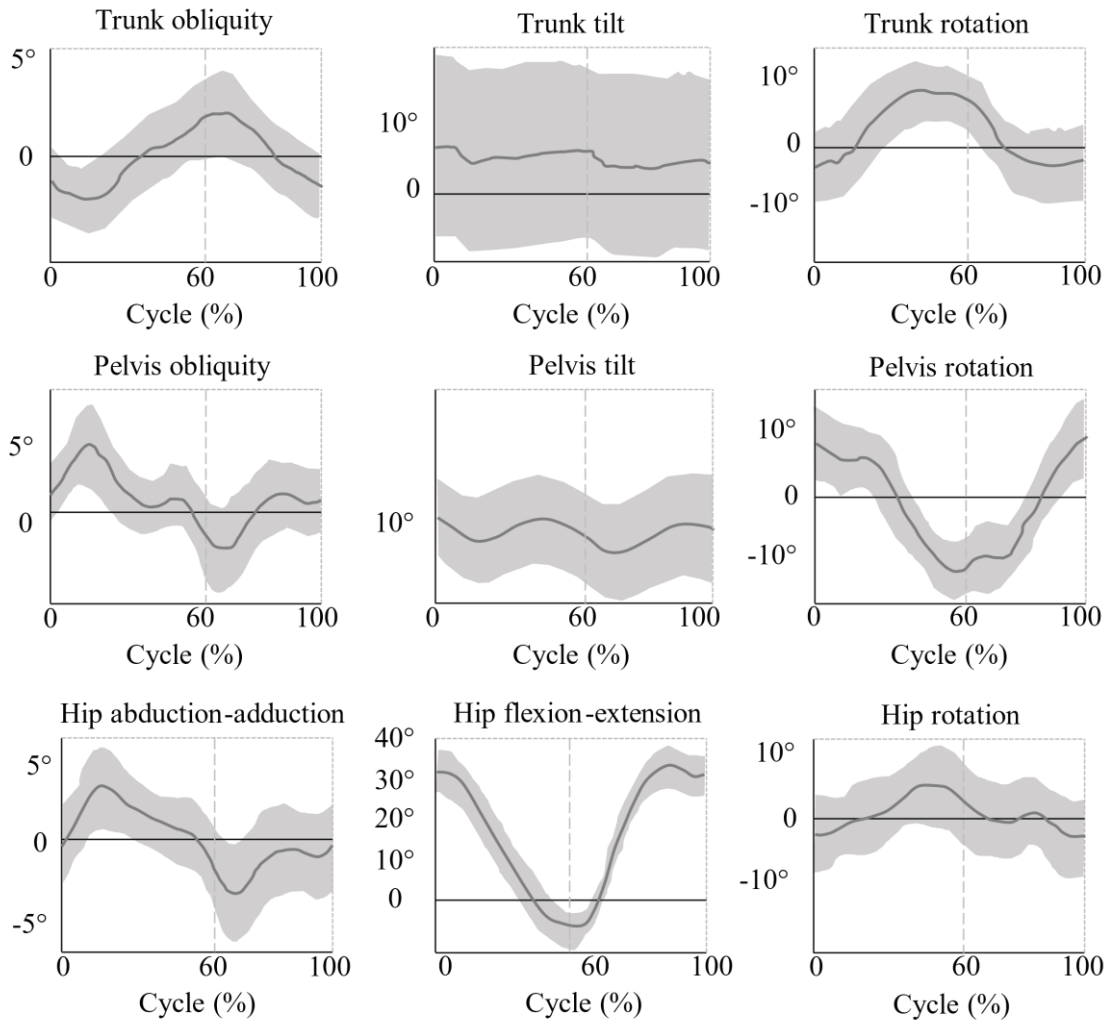

Figure 6. Example of kinematic curves for gait analysis.

2.1.2.2. Kinetics parameters of the gait

The forces exerted by the human body during walking are related to the ground reaction force (GRF). The GRF is the force exerted by the ground on the body. As any reaction force, this vector has the same magnitude but opposite direction and sense that the force exerted by the supporting foot on the floor [67]. The GRF vector has three components: vertical, anteroposterior, and mediolateral (Figure 7). The vertical force explains the effect of gravitational force on the human body. The anteroposterior shows the

acceleration and deceleration of the body. Finally, the mediolateral component helps to explain the balance of the human body.

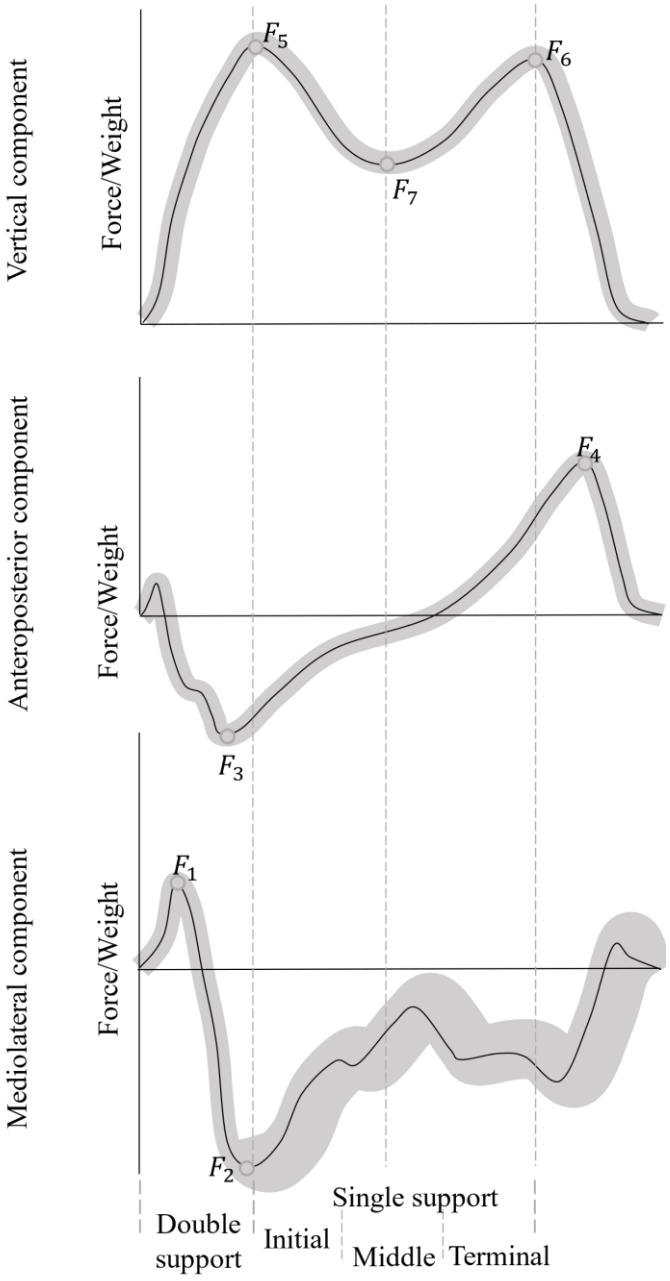

Figure 7. Curves of ground reaction force components.

The most important force peaks of the vertical component represent the maximum weight acceptance (F_5), the total support of the total weight in the middle stance (F_7), and the

push-off force to start the swing phase (F_6) [68]. The anteroposterior force peaks are the braking force (F_3) showing a decrease of bodies forward speed. As well as, the propulsive force (F_4) push the center of gravity forward to produce the swing phase [69]. The mediolateral shape shows the maximum medial force peak (F_1) and lateral force (F_2) [61], [70].

2.1.2.3. Muscular activity of the gait.

During an eccentric (lengthening) or concentric (shortening) contact of the muscle, changes in the activation patterns of motor units can be observed. Likewise, muscle fatigue can be recognized when the amplitude of the electrical signals produced by the muscles is progressively increased. Finally, the oxygen availability and energy metabolism affect the regulating motor unit recruitment firing frequency [55].

Surface electromyography (SEMG) is a particular way of studying the bioelectrical signals produced on muscles. The muscle activation in healthy subjects has also been previously found by electromyography (Figure 8), so any perturbation of the activation sequence or differences of muscular energy could mean a gait deviation [71]. Throughout the gait cycle, there is concentric and eccentric activation of muscles for the joint the hip, knee, and foot. Concentric muscle activation of the hip occurs in the initial contact, foot flat, toe-off, and mid-swing. Eccentric contraction happens during mid-stance, heel-off, and initial contact. Dorsiflexors contract eccentrically during the initial contact and eccentrically to control dorsiflexion in the foot flat. During the joint of the knee, the hamstrings and hip extensors activate concentrically in the initial contact. For the foot flat gait subphase, the knee extensors work in eccentrical activation. Plantar flexors activate

concentrically during the transition of the middle stance to heel off. From foot flat to mid-stance, the knee moves into extension, therefore knee extensors work concentrically. The hamstring contracts eccentrically during the middle stance followed by a concentric activation in the heel-off transition. From toe-off to mid-swing the dorsiflexors work concentrically to return the foot to a neutral position. From mid-swing to initial contact, the dorsiflexors work in isometric activation. Quadriceps works eccentrically from heel-off to toe-off. From mid-swing to initial contact the hamstrings activate briefly in eccentric [72].

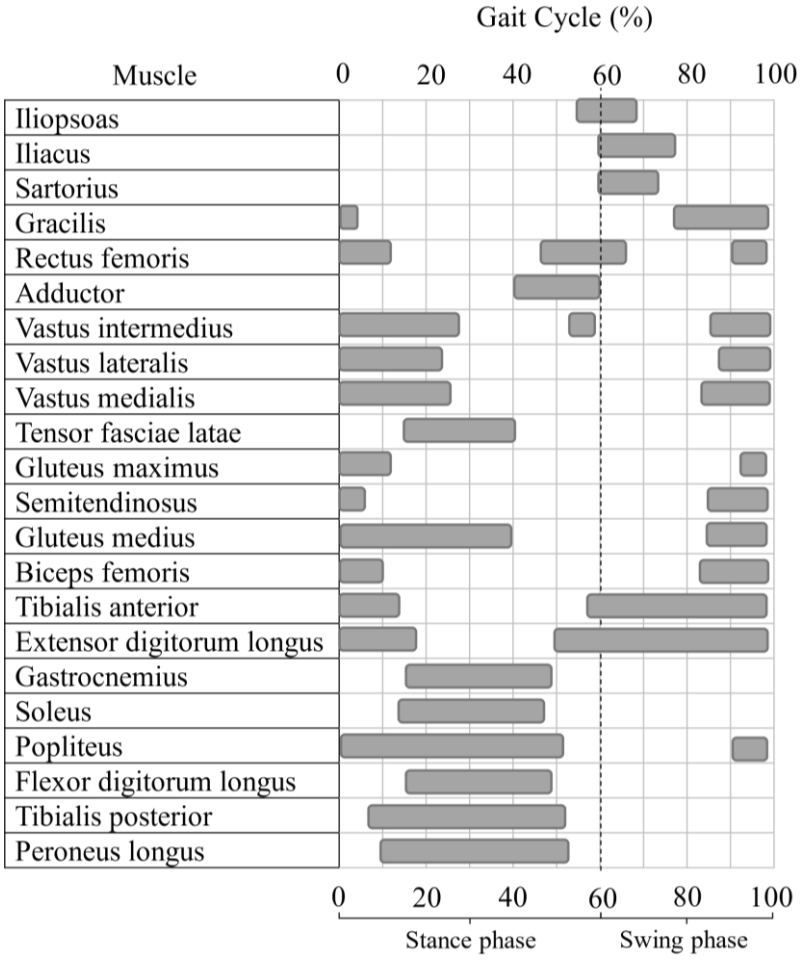

Figure 8. Muscle activation sequence of a normal gait [66], [73].

The muscle activation sequence makes it possible to perform gait analysis, muscle load analysis, and even to find pathophysiological factors. Literature reports frequency analysis of electromyographic signals makes it possible to recognize muscle activation and muscle fatigue to assess the normal gait [74].

2.1.3. Gait Deviations.

Human gait abnormalities can be found by quantitative or qualitative techniques. Motion capture systems, electromyography, inertial and force measurement systems, allow obtaining specific data on human biomechanics. Furthermore, the observation of gait and patterns detection can help during disease diagnostics [63], [75]. Hemiplegic gait is recognized by fixed plantar flexion of the ankle and a knee extension, producing a circumduction of one lower limb. A lesion of the nervous system could cause this gait pattern. A diplegic gait is characterized by similar effects to those mentioned above, affecting both lower limbs, producing a scissoring gait. The foot dorsiflexion, high steppage gait, and muscle weakness prevail in people diagnosed with neuropathic gait. Features like tremors, flexed neck, and trunk, short steps, reduced swing of arms, are found in a parkinsonian gait [76]. Neurological diseases such as Parkinson's, multiple sclerosis, post-stroke, among others can be detected by observation of muscular activity during gait [77].

The use of prosthetic devices affect the normal gait of amputees because they learn strategies to compensate for the new conditions for walking [78]. The observation of prosthetic gait allows finding characteristic patterns that could suggest gait deviations. The gait deviations on lower limb amputees include those associated with causes to

specific amputation, the patient, and others to the prosthesis. Muscle contractures, residual limb pain, muscle weakness, amputation scar, and psychological disorders are some of the causes associated with the patient [79]. The prosthetic malalignment and the socket fitting are the cause of most gait deviations due to the prosthesis.

2.2. Amputation.

Amputation is the surgically cutting off a limb from the rest of the body, resulting in a residual limb, also known as a stump [80]. Various causes produce amputation, but the most predominant are vascular issues, trauma, tumor lesions, thrombosis, diabetes mellitus, embolisms, infections, or trophic disorders [81]. Amputation can be divided into two large groups: upper limb amputation and lower limb amputation; however, lower limb amputations have a 10 to 1 ratio to their upper counterparts [82].

The amputation is classified according to the amputation height. The upper limb amputation is divided into amputation of the hand or fingers, disarticulation of the wrist, amputation of the forearm, elbow, arm, scapula-temporal, and interscapulum-humeral. The lower limb amputations are divided according to the affected joint. Amputation at the hip joint is known as hemipelvectomy or disarticulation of the hip; similarly, amputation through the knee is called knee disarticulation. Amputations above the knee are also known as transfemoral (TF) amputations. These occurring below the knee are called transtibial (TT) or below-knee amputations. Below ankle amputations can be metacarpal, trans metatarsal, tarsal-metatarsal, midtarsal, and transmalleolar.

2.2.1. Transfemoral amputation.

Transfemoral amputation involves the loss of the foot, tibia, fibula, and some biarticular muscles between the hip and knee, hence the amputation height substantially affects the residual limb functionality. During the amputation surgery, the thigh is cut between 25 cm and 30 cm from the greater trochanter to the knee [83] or also up to 10 cm above the joint interline of the knee [84].

The level of amputation must be correctly estimated because less tissue loss will preserve the balance between the abductors and adductors and the residual limb will have adequate strength and sensitivity. Figure 9 shows the muscles affected according to the height of transfemoral amputation; divided into thirds (1/3), that means, upper, middle, and lower thirds.

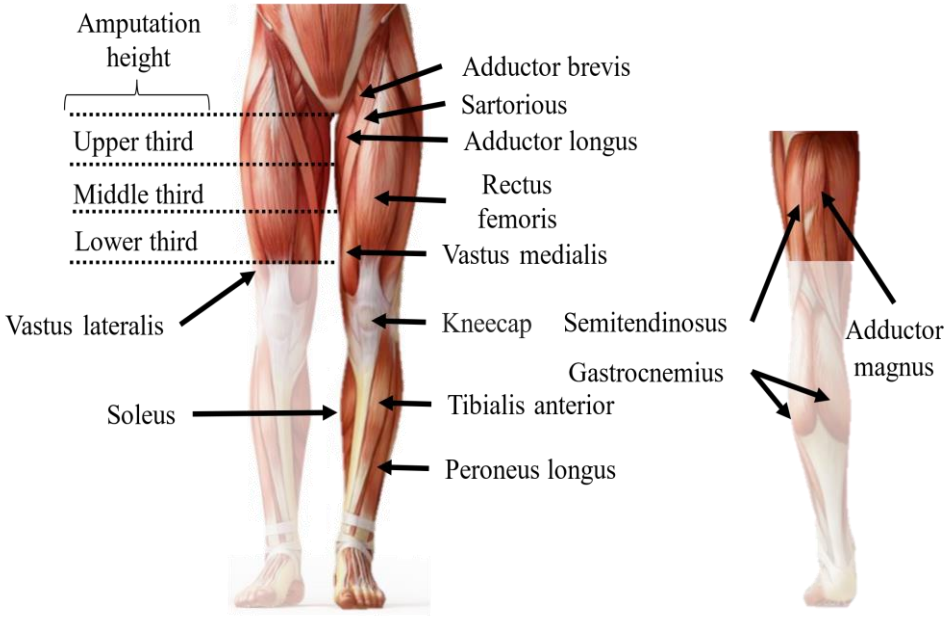

Figure 9. Muscles affected by a transfemoral amputation. [5]

[5] Image adapted from [279].

Upper third amputations will produce a short residual limb with less muscle tissue, lower muscle strength, and a natural tendency for the stump to flex and abduct. Lower third amputations will produce a stump too long, with increased muscle strength, but tending to abduction. A good amputation height is at the middle third level because a stump with the proper tissue and muscle strength is achieved. In addition, the scar location will influence the socket design, the prosthetic interface, and the amputee's rehabilitation. For instance, a poor position of the amputation scar could lead to a new surgery to release pressure on the tissue [85].

2.2.2. Artificial limbs: transfemoral prosthesis.

Artificial limbs are prosthetic devices performing the functions of a limb with different efficiency degrees. The device characteristics and prosthetic adaptation help people during their integration to activities of daily living. Transfemoral prostheses are assistive technologies for the amputee that fulfill the function of an artificial leg. The basic components of a transfemoral prosthesis include (1) socket, (2) suspension system, (3) joint unit (artificial knee), (4) pylon, (5) prosthetic foot, and (6) pyramidal adaptors to align the prosthesis [86]; Figure 10 helps to recognize prosthetic components. Each of the elements of the prosthesis fulfills a specific function and is related to the patient's mobility, confidence, stability, and even comfort [87].

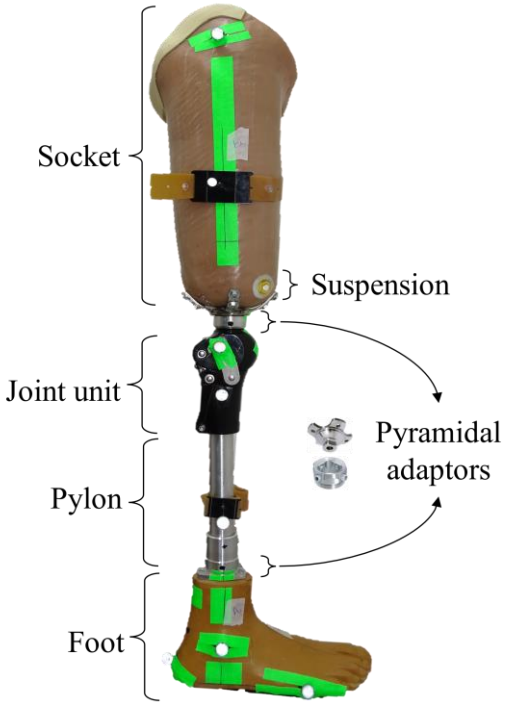

Figure 10. Mainly components of above-knee prostheses.

2.2.2.1. Prosthetic socket

The socket is a prosthetic component that contains the residual limb, providing structural integrity to the prosthesis, and acting as an interface between stump and prosthetic device. The socket is customized according to the residual limb shape, the bony prominences, the scar location, and the muscle tissue. There are two generalized types of sockets, the ischial containment, and quadrilateral [88], [89]. Figure 11 shows the inside shape of the sockets. The ischial containment type uses the ischial tuberosity for bearing amputees' weight. On the contrary, the quadrilateral distributes the body weight over the surface of the residual limb.

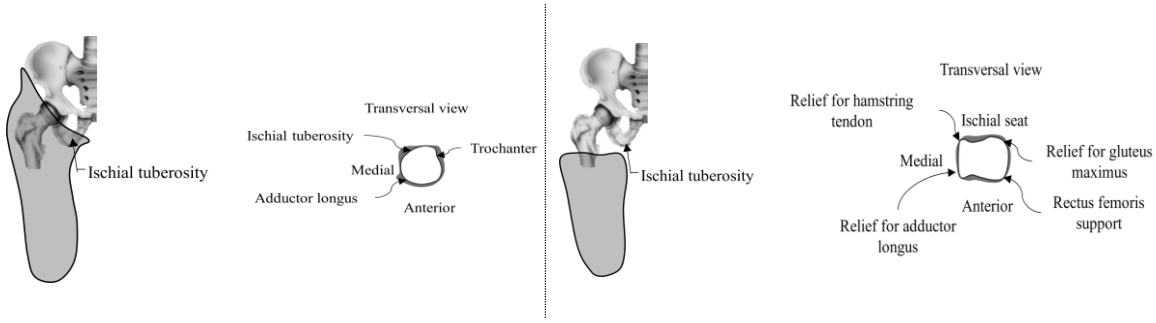

(a). Ischial containment socket

(b). Quadrilateral socket

Figure 11. Socket types for transfemoral prosthetic devices.

Sockets are usually built in a single structure and a rigid material such as Nylon, polypropylene, polyethylene, and carbon fiber; however, research on the socket continually advances, considering their effects on amputee's gait performance and comfort [90]–[92]. To provide stability and confidence, there are silicone socks or liners to improve the adhesion between residual limb and socket [93]. The residual limb is under constant pressure since it supports body weight, therefore the socket is a common generator of skin problems in the stump [94], [95]. For instance, authors in [96] analyzed the ulcers caused by pressure on the residual limb. The electromyography has been used to identify excessive activation of residual limb muscles suggesting problems associated with socket pressure [97].

The stump-socket interface is susceptible to changes in temperature which cause perspiration. The increase in humidity leads to bacteria growth that in the short term, causes infections on the skin [98]. Thermal cameras have been used to identify hot spots on the stump, select better materials, define new socket construction techniques, and increase prosthetic adherence [98], [99].

2.2.2.2. Suspension system

The suspension system holds the prosthesis in place to avoid the pistoning effect. There are two types of suspension: suction, locking pin, and straps. A valve on the socket is used to generate negative pressure (suction) and fit the socket over the stump, otherwise, it will be necessary to use elastic straps to fix the prosthesis to the hips. The locking pin suction system uses a liner/cushion interface along with a pin; therefore, the stump is directly fixed to the prosthetic device and avoids movements of the stump and rotation of the socket. The silicone liners cover the stump and improve comfort and increase the suction [100].

2.2.2.3. Joint unit: prosthetic knee

The joint unit is a mechanism that fulfills various purposes. For instance, during the stance phase and on standing, the prosthetic knee must be kept rigid to provide stability. During the swing phase, when sitting, bending, and kneeling, the joint unit must be able to flex [101], [102]. Prosthetic knees are essentially classified into two types, mechanical and computerized or microcontrolled [103]. In addition, features such as friction control, pneumatic control, hydraulic control, manual knee locking, among others, provide improvements in amputee stability and movement.

There are two general types of knee mechanisms, the monocentric and the polycentric [101], [104]. The monocentric (single rotation axis) knee behaves like a hinge, so they are suitable for children or people learning to walk using prosthetic devices. Polycentric knees have multiple axes of rotation, generally four. Figure 12 shows an example of a prosthetic knee with a four-bar mechanism. The link between axes A and B is named the

base a, so it remains blocked as shown in Figure 12(a). A double rocker formed by links A to D, and B to C, produce rotations on axis C and D producing the rotation of the knee as shown in the Figure 12(b). When line formed by links b and c is projected, the convergence point $P(x, y)$, named the Instantaneous Center of Rotation (*CIR*) achieve the maximal value when the flexion is completed Figure 12(c).

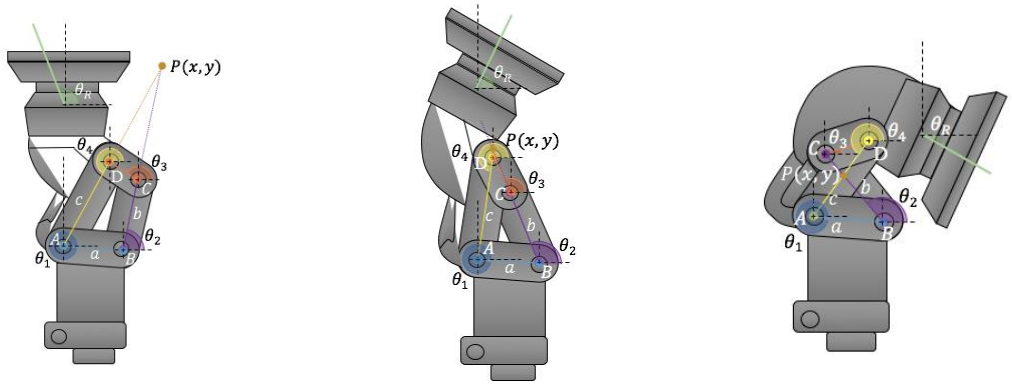

(a). Position in extension. (b). Beginning of the flexion. (c). Flexion completed

Figure 12. Four-bar polycentric knee.

The mechanical characteristics of the polyaxial system supply biomechanical versatility, gait stability, natural walking, and confidence. For instance, the vertical load line of the prosthesis, during the stance phase, is frontal and proximal to the anatomical line, meaning that the polycentric knee will not flex. When the swing phase begins, the prosthetic load line lies behind the anatomical one, causing a knee flexion. In the swing phase, the knee is flexed, and the prosthetic length is reduced, avoiding stumbling over obstacles.

2.2.2.4. Prosthetic foot.

The prosthetic foot is the support of the amputee on the floor which provides stability, dissipates, returns, or directs energy towards the other prosthetic components. The construction material foot and their performance will depend on the activities that the amputee carries out daily. For example, the SACH foot (Solid Ankle Cushioned Heel) is a basic foot built with elastic materials and a non-articulated ankle, suitable for people with low physical activity. For people with high physical activity is recommended a prosthetic foot built with stronger materials to provide stability in uneven environments and shock forces tolerance. High-performance athletes often need thrust force, therefore prosthetic feet with dynamic responses are recommended. Finally, electronic feet can adapt to varying ground conditions, providing a more efficient gait for the amputee [105].

The prosthetic foot used in this research was the Jaipur foot (Figure 13). This prosthetic component is manufactured by Bhagwan Mahaveer Viklang Sahayata Samiti (BMVSS) in Jaipur, India. The Jaipur foot is a modification of the Solid Ankle Cushioned Heel (SACH) foot. Jaipur foot is composed of three blocks: the forefoot, heel, and ankle blocks, which simulate the anatomy of the human foot. The forefoot and heel are made with sponge rubber, and the ankle block is made of wood. The prosthetic foot is covered with high density polyethylene.

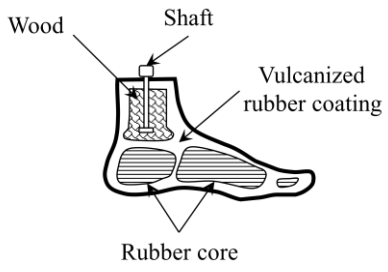

Figure 13. Jaipur foot cross section.

2.2.2.5. Pyramidal adaptors.

Pyramidal adapters connect the socket with the prosthetic knee and pylon with the prosthetic foot. Generally, pyramidal adapters are made of steel, aluminum, and titanium. The male adapter is inserted into the female adapter and four screws secure the joint (Figure 14). To modify the socket or foot alignment, the four screws are threaded to fix the position of the female adapter on the male, which produces a rotation of the connected prosthetic elements in the vertical, longitudinal and lateral axes.

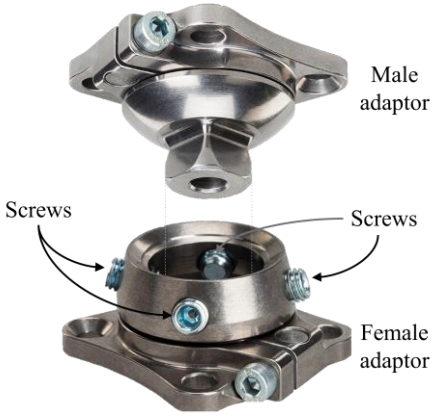

Figure 14. Examples of female and male pyramidal adapters.

2.2.3. Prosthetic alignment procedure.

Prosthesis alignment is the most critical procedure during the prosthetic and post-prosthetic phases of the amputee patient. There is no physical mechanism to perform prosthetic alignment, instead prosthetists follow a procedure that consists of three steps: alignment is divided into three stages: bench alignment, static alignment, and dynamic alignment. The alignment procedure balances the load line of the prosthesis with the biomechanical and anatomical lines of the amputee. To achieve this purpose, a

biomechanical analysis, gait observations, and feedback of the patients must be performed [16].

The bench alignment includes the assembly of the prosthesis, from the most distal to proximal prosthetic component [106]. After the prosthesis has been assembled, it is checked that the weight of the prosthesis is completely balanced. Figure 15 shows the load line of the prosthesis in the side view, which must be anterior to the prosthetic knee joint line, producing a knee blocking. As well as in the frontal and lateral view, the line must cross the socket in the middle.

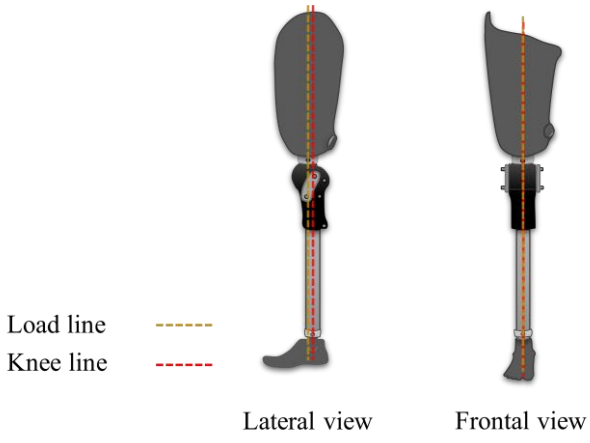

Figure 15. Knee line fitting with the prosthetic load line for bench alignment.

The amputee wears the prosthesis during static alignment. Static alignment adjusts the load lines of the prosthesis to the anatomical lines of the amputee to ensure correct posture and weight distribution during standing. The load line of the prosthesis is shifted to be parallel to the anatomical line as is shown in Figure 16 (a). The posture of the patient is constantly supervised to avoid knee flexions during standing. The lower limbs must be in similar conditions in adduction or abduction, both knees must be at the same height, the shoulders and iliac crests must be parallel. The dimensions and rotation of feet must be

similar, the socket midline will be distributed 50% medial and lateral, and the weight distribution must be at least 35% on the prosthetic side and 65% intact side.

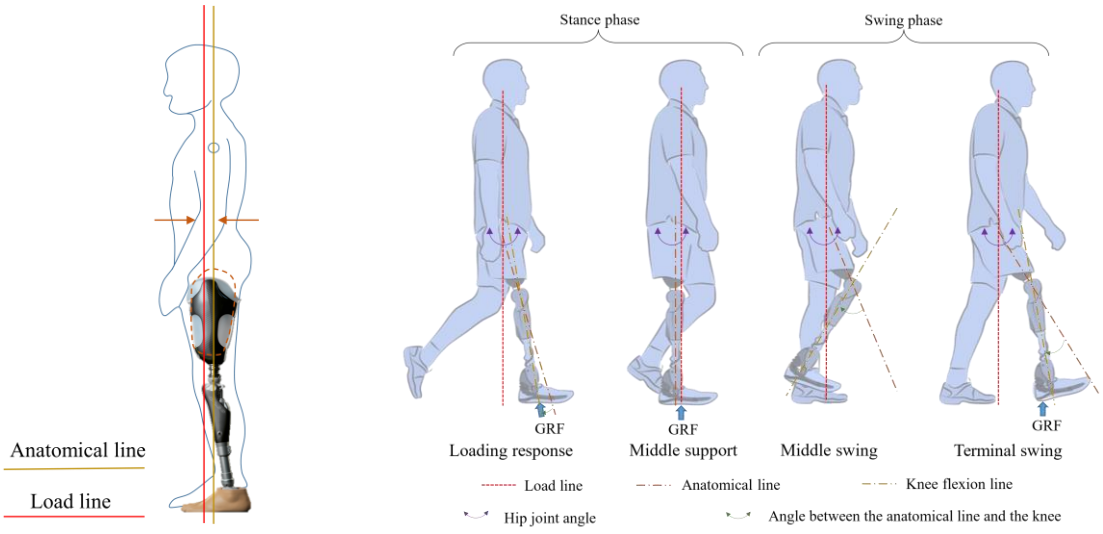

(a). Static alignment. (b). Dynamic alignment. [6]

Figure 16. Sagittal view of the standing and gait of the amputee during the prosthetic alignment procedure.

The dynamic alignment procedure fine-tunes the prosthesis to avoid gait deviations of amputees. The prosthetist checks the amputee's gait, to have the shoulders, the iliac crests, and the sacral foramina at the same height. An example of the sagittal view of this process is shown in Figure 16 (b). Displacement of the stump in the socket (pistoning) and excessive knee and foot rotations are avoided. In general, the prosthetist rectifies the prosthetic alignment to avoid gait deviations. The prosthetist asks the amputee for information about the comfort of the prosthesis and their perception of gait performance.

A poor alignment triggers deviations in the amputee's gait such as lateral flexion of the trunk, swinging in abduction, among others [107], leading to health problems such as

[6] Image adapted from [280].

osteoporosis in the stump, osteoarthritis in the healthy knee and hip joints, pain back, lordosis, among others. For this reason, static and dynamic alignment during walking is essential to achieve the adaptation of the patient to his activities of daily life.

Mechanical devices are used to assist the alignment procedure. Manufactures such as Ottobock and Fillauer have developed sliding adapters to reposition prostheses in the frontal and sagittal plane, allowing prosthetists to better translate components on the prosthesis [26], [27].

Electronic devices such as the *L.A.S.A.R* system (Ottobock, Germany) help the prosthetist to perform the standing analysis. The static alignment could be assessed by projecting reference lines on the prosthesis and using load cells to measure the weight distribution lines. This allows the prosthetist to evaluate the weight distribution over both lower limbs. Although this tool assists the technician during static alignment, it does not support them during dynamic alignment. The *Europa* + system (Orthocare, USA) is an instrument to perform gait analysis. It uses a load cell to measure vertical forces and moments developed during standing and walking. This device is integrated into the prosthesis. At the end of the gait analysis, the device must be removed from the prosthesis, which makes the evaluation of the alignment complex.

There is prosthetist assistance technology to analyze the standing and the gait performance. Motion capture systems record spatiotemporal [108] and kinematics parameters and inertial -systems capture kinetics information for gait analysis [109]. Electromyography and inertial data have been used to predict temporal spatiotemporal parameters [110]. Synchronization of an optoelectronic system and electromyographic

signals were used to measure the elevation angulation parameters of the prosthetic limb [111]. The energy cost [112], brain activation signals [113], the stump temperature [98] have been useful to analyze the gait and comfort measuring. Those kinds of tools could be used in the alignment procedures of a transfemoral prosthesis to detect prosthesis length problems, socket in abductions, poor socket support, a prosthetic knee that is too stiff, limp by pain, discomfort signals, and an unreliable gait [114]–[116].

Regardless of the electronic devices used to analyze gait or standing, the optimal prosthetic alignment depends on the amputee's own characteristics such as anatomy, biomechanics, residual limb morphology and degree of adaptation to the prosthesis. For this reason, fitting centers evaluate prosthetic alignment through dialogue with amputees and observation of standing and gait. The prosthetist skills to perform the alignment also affects the quality of the alignment. These phenomena add uncertainty and subjectivity during the definition of the optimal or nominal alignment.

2.3. Systems modeling.

A system is an interrelated element set that reacts according to intrinsic rules of behavior (Figure 17); therefore, the system theory separates between the structure and behavior. The structure refers to the inner architecture of the system. The behavior alludes to the response of the system to excitation variables and observable variables called outputs in a timestamp [117].

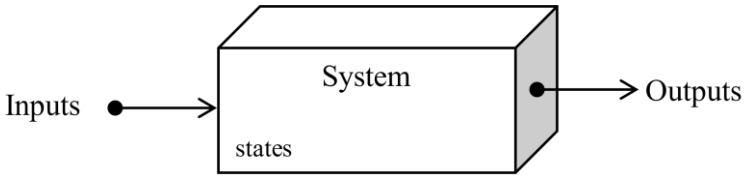

Figure 17. Basic diagram of the system concept.

The structure includes the states and the transition states mechanisms. The structured knowledge allows recognition of the system behavior over time. The conceptual model and the operational model are stages to describe a real system. Identifying the descriptor variables, the interaction of the components, and the scenarios variation, are necessary to define a conceptual model. The operation model is a computational model that uses mathematics, physics, and computer science to implement the conceptual model.

Computational power has improved the adaptation of conceptual models to computational models and has paved the way for systems identification theory and machine learning.

2.3.1. Computational modeling.

Systems identification aims to find a numerical description of the system behavior by the measurement of input excitations and the effects it produces at the output. To achieve the identification success, the experimental process must be performed seeking to achieve a good extraction of the system features. The identification scheme is depicted in Figure 18. Computational models can be used for simulation, prediction, classification, or controlling systems; therefore, the experimentation protocol will depend on the model aim [118]. Model validation could produce three situations: the model must be fitted, the modeling technique does not explain the system, and the experimental test was not enough.

In this thesis we used the system identification procedure to quantify the effect of prosthetic alignment on standing and gait in transfemoral amputees. Unsupervised and supervised machine learning techniques were used for modeling.

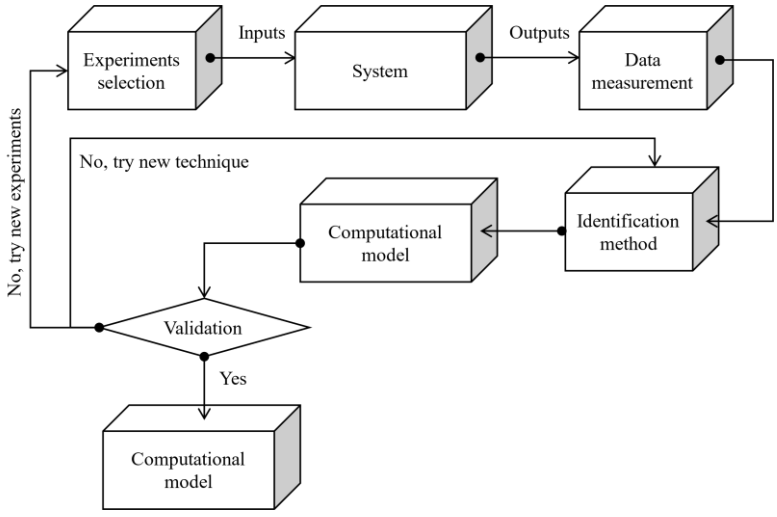

Figure 18. System identification structure.

2.3.2. Machine learning techniques.

Machine learning finds the system behavior by the recognition of the data patterns and trends. The selection of a suitable algorithm for machine learning will depend on the model aim, for example, a classification model will be different from a regression model and in turn to a clustering model. Therefore, the objective of the model must be clearly defined before carrying out the identification process. The supervised learning aim is to find system models for the classification and regression of the data. The unsupervised techniques are used in clustering and dimensionality reduction. Reinforcement learning is based on rewarding desired behaviors and punishing unwanted ones [119].

The supervised classification techniques assign test data to specific labels or previously known categories. The most common classification methods include Logistic Regression,

Naïve Bayes, Decision Trees, the K-nearest Neighbor, and Support Vector Machine. The supervised regression techniques predict continuous variables. Regression techniques include, among others, Gaussian Regression, Neural Networks, Support Vector Regression [120].

The dataset in unsupervised machine learning is not labeled and categorized, so its attributes are unknown; therefore, the model automatically finds the hidden patterns of the data. This algorithm can be divided into clustering and association. During clustering, objects are grouped into clusters according to the similarity between characteristics of the commonalities. Common unsupervised algorithm techniques are K-means Clustering, K-nearest Neighbors (KNN), Neural Networks, Singular Value Decomposition, and Factor Analysis [121].

In this doctoral thesis, the unsupervised learning technique K-means was used to identify the residual limb hot spots during walking trials of amputees wearing a correctly aligned or misaligned prosthesis. The Factor Analysis technique was used to reduce the parameters of the anterior, posterior, and lateral sides of the stump's thermography. The Vector Support Machines were used to classify the prosthetic alignment between nominal and misaligned, by using the dataset of the Ground Reaction Force of the prosthetic limb. Furthermore, a regression model with Neural Networks was identified to calculate the prosthetic misalignment angles in the socket and the foot from the dataset of Ground Reaction Force of the prosthetic limb.

2.3.2.1. K-means clustering method.

The k-means partitions a dataset in k clusters according to the mean distance separation of the commonalities. The clustering is achieved when the distance between objects is minimized; therefore, there are different distance functions to measure the separation between clusters. The k-means algorithm is summarized in three steps: (1) defining the number of centroids, (2) assigning objects to the centroid, and (3) updating the centroids.

The k-means algorithm optimization problem repeats (2) and (3) until the centroids move below a threshold distance. The minimization function is the sum of the quadratic distances of each group from the centroid of its cluster (eq. 2.1), where S is a vector containing x_j attributes. There are k clusters with a μ_q centroid.

$$\min_S E(\mu_q) = \min_S \sum_{q=1}^{k} \sum\nolimits_{x_j \in S_q} \|x_j - \mu_q\|^2 \tag{2.1}$$

The definition of the number of centroids is a complex process since there is no prior knowledge of the grouping of the data. Therefore, methods such as Calinski-Harabasz [122] and Davies-Bouldin [123] help to find the clustering efficiency and to select an appropriate number of centroids.

The Calinski-Harabasz score is the relation between the mean inter-cluster variation and the intra-cluster variation for all clusters (eq. 2.2). Where n_E is the size of the dataset clustered into k clusters. Trace function $t_r()$ is calculated for the inter-cluster variation matrix W_k solved in equation 2.3. and the intra-cluster variation matrix B_k in equation 2.4. Variable x is a qth cluster centroid c_q. The mean of the dataset is named μ and n_q is the number of elements in the qth cluster.

$$CH = \frac{t_r(B_k)}{t_r(W_k)} \frac{n_E - k}{k - 1} \tag{2.2}$$

$$W_k = \sum_{q=1}^{k} \sum_{x \in C_q} (x - c_q)(x - c_q)^T \tag{2.3}$$

$$B_k = \sum_{q=1}^{k} n_q (c_q - \mu)(c_q - \mu)^T \tag{2.4}$$

The Davies-Bouldin index is shown in equation 2.5. This metric explains the similarity between clusters by comparing the clusters' distance between them and their size. Where, σ_q is the mean distance between the qth cluster and their cluster centroid. The mean distance of the jth cluster and their centroid is named as σ_j.

$$DB = \frac{1}{k} \sum_{q=1, q \neq j}^{k} \max \left(\frac{\sigma_q + \sigma_j}{(\sigma_q - \sigma_j)(\sigma_q - \sigma_j)^T} \right) \tag{2.5}$$

The smallest value of the DB index and the highest value of the Calinski-Harabasz score means a compact cluster with sufficiently separated centroids. Hence, the clustering exercise is reduced to minimizing these indexes.

2.3.2.2. Factor Analysis.

Factor analysis is a multivariate statistical technique to describe the relationship between variables or factors observed in a dataset. The resulting equation will relate the highly correlated variables to each other; therefore, the resultant factor number will be smaller than the original ones [124].

Consider an observable variable k with a mean (μ), covariance matrix (Σ), and contained in a randomly sampled data set. Variable k can be expressed as a linear combination (eq

2.6) of m common factors $(f_1, f_2, \cdots, f_m)$ and a specific error for each factor $(e_1, e_2, \cdots e_k)$.

$$\begin{Bmatrix} Y_1 = d_{11}f_1 + d_{12}f_2 + \cdots + d_{1m}f_m + \varepsilon_1 \\ Y_2 = d_{21}f_1 + d_{22}f_2 + \cdots + d_{2m}f_m + \varepsilon_2 \\ \vdots \\ Y_k = d_{21}f_1 + d_{22}f_2 + \cdots + d_{2m}f_m + \varepsilon_2 \end{Bmatrix} \quad (2.6)$$

The resultant factor analysis in (eq. 2.7)

$$Y_i = \{d_{i1}f_1 + d_{i2}f_2 + \cdots + d_{im}f_m + \varepsilon_i\} \quad (2.7)$$

The resulting common factors (f_1) will be less than the number of original variables (Y_i). Values of d_{ij} represent the contribution level of each factor. Factors $f_1, f_2, \cdots, f_m$ are not correlated with zero mean and unit variance.

2.3.2.3. Neural Networks.

A neural network system (NN) refers to an artificial neural network interconnected by nodes that simulate the human brain's behavior. Typically, neural networks are defined under four parameters: (1) the type of neuron, (2) the archetype of the connection, (3) the learning algorithm, and (4) the recall algorithm.

The combination of NN and fuzzy logic proposes one of the types of neurons or nodes in which NN graphs. The neuro-fuzzy network uses a set of fuzzy rules for the learning method, the weights estimation, and the activation functions [125]. The perceptron is a linear binary qualifier, so it is used in both supervised and unsupervised learning. The perceptron is conceptualized in 4 elements: an input layer, a set of weights and biases, a network of sums, and an activation function [126]. The connection architecture is related to the way the neural network is organized, its topology, and the internal interconnections.

The auto-associative, hetero-associative, feedforward, and backpropagation architectures are the most recognized [127]. The learning algorithms can be supervised, unsupervised, and reinforced [128], [129]. The retrieval function refers to the knowledge extracted by the neural network.

2.3.2.4. Multilayer Neural Networks.

The architecture of a feedforward multilayer perceptron with backpropagation error is presented in Figure 19. The mathematical representation is presented in Eq. 2.8. This technique uses layers (g_i) to describe the neuron interconnection and a set of weights (w_i) is defined to represent the interconnection strength between neurons. Each node uses an activation function (f); usually being the sigmoid function. The neural network learning is achieved when a cost function (eq. 2.9) is minimized. Parameter w denotes weights, b is the bias, N is the training examples, a is the activation output vector produced by each input x, and y is the target output.

$$y(\bar{X}) = f\left(\sum_{i}^{N} w_i g_i(\bar{X})\right) + B \tag{2.8}$$

$$C(w,b) = \frac{1}{2N}\sum_{x} \|y(x) - a\|^2 \tag{2.9}$$

The purpose of this topology is to find a weight matrix that explains the interactions between neural network layers. The weight matrix is iteratively fitted until the prediction error between the estimated and real output is minimized. Backpropagation is an iterative process that minimizes the root mean square error between the predicted output and the actual value. The algorithm for backpropagation network training implies the weights initialization and activation function (e.g. the logistic function), calculation of hidden

layer outputs, computation of output layer outputs, the output error calculating, the weight fitting of the output and hidden layers, and repeating the procedure until to minimize a cost function [130].

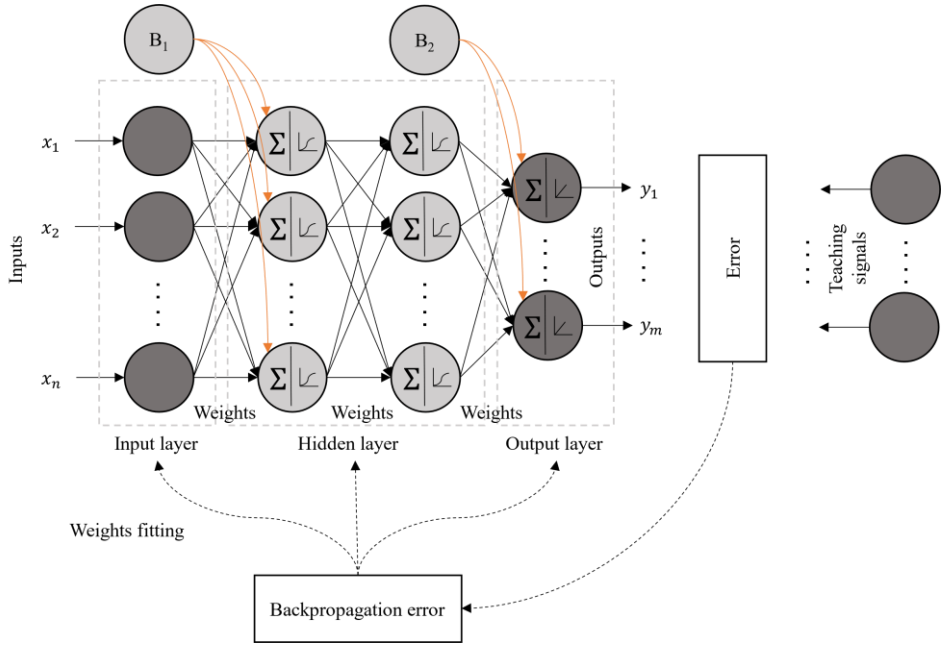

Figure 19. Structure of a feed-forward multilayer neural network.

Overfitting and underfitting are typical problems of NN. Overfitting occurs when the model follows noisy data, and the order is increased to achieve a better fitting, therefore, the resulting neural network learns local data behavior but cannot explain added information. A neural network underfitting does not properly explain the problem and the estimated output does not follow the targets [131]. Model simplifying, early stopping, regularization using, and dropout are techniques to avoid the overfitting error.

2.3.2.5. Bayesian Regularization Neural Networks.

Overfitting is an unavoidable problem without regularization, especially when the observations in the dataset training are less than the parameters to be estimated [132]. The

algorithm proposes the minimization of an objective function (eq. 2.10), considering a mean squared error function (eq. 2.11) and a weight attenuation function (eq. 2.12). The α and β are distribution control hyper-parameters. Value of w_i are the *ith* weight of neural network and m is the number of weights. N is the total number of the input-output sets; finally, the *ith* output is named as y_i.

$$F = \beta E_D + \alpha E_W y(\bar{X}) \tag{2.10}$$

$$E_D = \frac{1}{N}\sum_{i}^{N}(y_i - t_i)^2 = \frac{1}{N}\sum_{i}^{N} e_i^2 \tag{2.11}$$

$$E_W = \frac{1}{2}\sum_{i}^{m} w_i^2 \tag{2.12}$$

The weight initialization is randomly set. Iterations of the density function (eq. 2.13) update the weight values according to Bayer's rule. In other words, equation 2.13 is the rate between likelihood multiplying prior and the evidence. M is the architecture of the neural network. $P(w|\alpha, M)$ is the prior knowledge of the weights. $P(D|w, \beta, M)$ is the likelihood function of the data occurrence given the weight w. $P(D|\alpha, \beta, M)$ is a normalization factor calculated by equation 2.13.

$$P(w|D, \alpha, \beta, M) = \frac{P(D|w,\beta,M).P(w|\alpha,M)}{P(D|\alpha,\beta,M)} \tag{2.12}$$

$$P(D|\alpha, \beta, M) = \int_{-\infty}^{\infty} P(D|\alpha, \beta, M)P(w|\alpha, M)dw \tag{2.13}$$

Assuming a Gaussian distribution for the noise in the weight and training dataset, the probability densities $P(D|\alpha, \beta, M)$ and $P(w|\alpha, M)$ are calculated by equations 2.14 and 2.15.

$$P(D|w,\beta,M) = \left(\frac{\pi}{\beta}\right)^{-N/2} e^{(-\beta E_D)} \tag{2.14}$$

$$P(w|\alpha,M) = \left(\frac{\pi}{\alpha}\right)^{-m/2} e^{(-\beta E_W)} \tag{2.15}$$

Using equations 2.13 to 2.15 in 2.12, the density function to update the weight values is transformed in 2.16. The maximization of 2.16 means minimizing regularization objective function [133], [134].

$$P(w|D,\alpha,\beta,M) = \frac{1}{Z_F(\alpha,\beta)} e^{(-F(w))} \tag{2.16}$$

The iteratively synaptic updating is calculated with equation 2.17. The error vector is labeled as $e = [e_1, e_2, \dots, e_N]$. The number of iterations is labeled as k and μ is an iterative damping parameter. The variable J means the Jacobian matrix (eq. 2.18) and the Hessian matrix is denoted by $H = [J^T J]$.

$$w^{k+1} = w^k - [H + \mu I]/Je \tag{2.17}$$

$$J = \begin{bmatrix} \partial e_1(x_1,w)/\partial w_1 & \cdots & \partial e_1(x_1,w)/\partial w_m \\ \vdots & \ddots & \vdots \\ \partial e_N(x_N,w)/\partial w_1 & \cdots & \partial e_N(x_N,w)/\partial w_m \end{bmatrix} \tag{2.18}$$

2.3.2.6. Vector Support Machine.

The support vector machines (SVM) are supervised algorithms used in regression and classification modeling. It is a technique based on the statistical learning theory proposed by Cortes & Vapnik [135]. To understand the operation of the Support Vector Regression, please refer to [136].

The purpose of SVM is to find a plane to separate a dataset into groups known a priori, maximizing the distance (margin) between the values closest to the plane, called support

vectors. Figure 20 shows a two-dimensional data set; however, the group's separation is becoming increasingly difficult when the dataset size increases; therefore, hyperplanes are used to represent an n-dimensional plane [137].

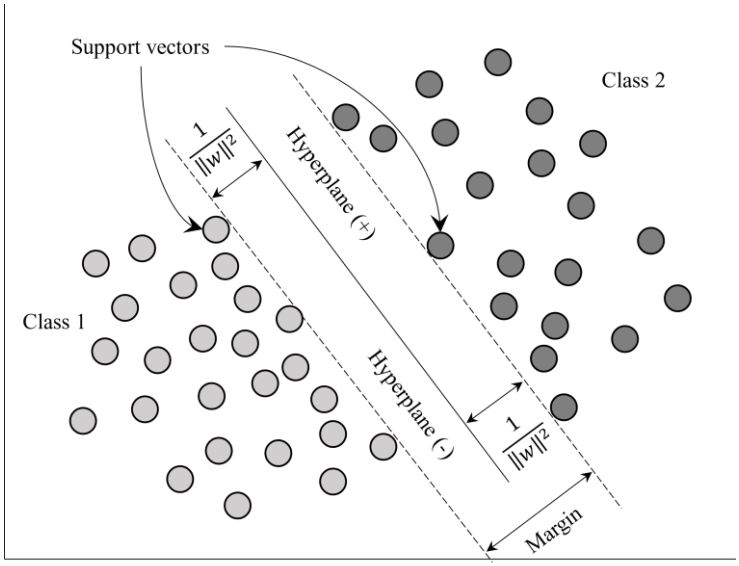

Figure 20. Decision boundary hyperplane of Support Vector Machines linearly separable.

A linearly separable data set can be represented as shown in equation 2.19, which is typically named as hard margin SVM. The training dataset is the vector $x = [x_0, x_1, \dots, x_m]$, the bias is labeled as b, the categories as y_i and the weighted vector is w. The dataset is linearly separable if there exists a pair w, b such that the inequality 2.20 is satisfied. Thus, the solution is achieved when the objective function $J(w) = 1/2\,\|w\|^2$ is minimized. The Lagrangian function is used to minimize or maximize the objective function augmented (eq. 2.21). Parameters w and b are renowned as primal variables, and λ_i are the Lagrange multipliers [138].

$$f(x) = w^T x + b \tag{2.19}$$

$$\begin{cases} (w \cdot x_i + b) \geq 1 & y_i = 1 \\ (w \cdot x_i + b) \leq -1, & y_i = -1 \end{cases} \quad i = 1, \dots N \tag{2.20}$$

$$\mathcal{L}(w, b, \lambda) = \frac{1}{2} w^T w - \sum_{i=1}^{N} \lambda_i [y_i (w^T x_i + b) - 1] \tag{2.21}$$

The most common is to find a dataset not completely separable; therefore, data appears inside the hyperplane, so a non-negative slack parameter ($\xi \geq 0$) and a cost value C are introduced in the objective function of the SVM (eq. 2.21) for N pairs input-output; this case is typically named soft margin SVM [139]. The new optimization problem is shown in equation 2.22 and transformation 2.23.

$$J(w, b, \xi) = \frac{1}{2} \|w\|^2 + C \sum_{i=1}^{N} \xi_i \tag{2.22}$$

$$\begin{cases} (w \cdot x_i + b) \geq 1 - \xi_i & y_i = 1 \\ \xi_i \geq 0, & y_i = -1 \end{cases} \quad i = 1, \dots N \tag{2.23}$$

Values of $\xi_i = 0$ in 2.22 mean that input parameters were correctly classified and when $\xi_i > 0$ suggests data wrongly classified. The variable xi is associated with an index to measure the classification error. Therefore, the problem of finding the best hyperplane is reduced to the solution of 2.23 constrained to 2.24.

$$\min_{w,b} \left\{ \frac{1}{2} \|w\|^2 + C \sum_{i=1}^{N} \zeta_i \right. \tag{2.23}$$

$$\left\{ \sum_{i=1}^{N} \lambda_i \; y_i = 0 \quad 0 \leq \lambda_i \geq C, i = 1,2, \dots, N \right. \tag{2.24}$$

The Kernel method is used when the soft SMV problem cannot be solved because it can not find a hyperplane that minimizes the number of unclassified data. The kernel transforms the input data to a higher-dimensional space, in which data is linearly separable [140]. This method is remarkably interesting because the computational burden of the data oversizing is less than solving a nonlinear surface, which makes this algorithm

efficient. The kernel satisfied the Mercer's theorem (eq. 2.25), where $\phi(x_i)$ is a function belongs to Hilbert space to project x_i to a high-dimensional space [141].

$$K(x_i, x_j) = \phi(x_i)\phi(x_j) \tag{2.25}$$

The most popular kernel is the Gaussian radial basis function (2.26). The solution of equation 2.27 will allow finding the hyperplane of separation between classes subject to $\sum_{i=1}^{K} \lambda_i y_i = 0$ for $0 \leq \alpha_i \leq C$.

$$K(x_i, x_j) = e^{\left(-\frac{\|x-u\|^2}{\sigma^2}\right)} \tag{2.26}$$

$$\max_{\lambda} \sum_{i=1}^{N} \lambda_i - \frac{1}{2} \sum_{i=1}^{N} \sum_{j=1}^{N} \alpha_i \alpha_j y_i y_j K(x_i, x_j) \tag{2.27}$$

2.3.2.7. Validation methods for computational models.

The K-Fold cross-validation is a common method to train and assess computational models. The algorithm randomly divides the dataset into k groups of similar sizes. The training process uses k-1 groups, and the remaining group is used for validation. This procedure is repeated k times and a different validation group is chosen. At the end of the algorithm, k error values and performances would be calculated and this information is used to select the final model [142].

Confusion matrices are a strategy for evaluating the performance of supervised classification algorithms. The row of the matrix means the true class and columns show the predicted class. The positions of each matrix report the number or percentage of false positives or true positives. This helps evaluate classification models [142]. The receiver

operating characteristic curve (ROC) shows the classification model performance using the information of false positive and true positive rates [143].

Chapter 3.

Biomechanical variables used during static and dynamic alignment of transfemoral mechanical prostheses.

Contribution to Ph.D. research: The purpose of this chapter is to present the fulfillment of the first, second, and third specific objective of the Ph.D. thesis "*To identify the set of biomechanical variables that characterize the static and dynamic alignment of transfemoral mechanical prostheses*", "*To propose a qualitative and quantitative measurement method for the biomechanical variables set that are characteristics in the static and dynamic alignment of transfemoral mechanical prostheses*", and "*To design a*

protocol for patients' selection and the biomechanical variables record of the amputee and the prosthesis, during the static and dynamic alignment procedure".

The literature review presented in this chapter made it possible to find the parameters, measurement systems, and characteristics of the alignment experiments that should be used in the protocol for recording and evaluating the prosthetic gait of amputees during alignment variations. The literature review showed a lag in the alignment studies in transfemoral amputation compared to transtibial amputation and allowed to confirm the subjectivity of the alignment procedures. The findings described in this chapter were analyzed in cooperation with Dr. J Jan Andrysek, senior scientist at the Bloorview Research Institute, Holland Bloorview Kids Rehabilitation Hospital, Toronto, ON, Canada. This chapter has one supporting appendix. Refers to **Appendix RP** for more information about the protocol for selection of volunteers, biomechanical variables recording of the amputee and the prosthesis, and qualitative and quantitative measurement methods for the biomechanical variables. Refers to **Appendix IC** to observe informed consent.

Title of research paper: Technical and procedural considerations relating to the prosthetic alignment of transfemoral and transtibial prostheses: A systematic review.

Published in: Prosthetics and Orthotics International (Under Review)

Cited as: Andrés M. Cárdenas, Jan Andrysek, Juliana Uribe, Alher M. Hernández, and Jesús A. Plata, "Technical and procedural considerations relating to the prosthetic alignment of transfemoral and transtibial prostheses: A systematic review.,", pp. 1–10.

DOI: NA

3.1. Abstract.

Background: Prosthetic alignment plays a key role in the rehabilitation and patient outcomes of individuals with lower-limb loss.

Objective: The goal of this chapter was to systematically review the state-of-the-science related to prosthetic alignment research, and specifically to find the primary outcomes associated with prosthetic alignment as well as considerations for the implementation of alignment procedures.

Study design: Systematic review.

Methods: The reviewing process was conducted following the PRISMA methodology. Data from papers were extracted and categorized based on population attributes, used outcome measures and metrics, alignment procedure characteristics, and the effects of prosthetic alignment on rehabilitation outcomes. The quality of the papers was assessed using thirteen predetermined criteria.

Results: The literature review showed a lag in the alignment studies in transfemoral amputation compared to transtibial amputation and allowed to confirm the subjectivity of the alignment procedures. Changes in socket reaction moment, ground reaction force, socket-stump interface pressure, spatiotemporal data, and patient comfort were typically affected by socket and foot angulations and translations. Considerations in alignment research were mainly directed towards the ambulation method, footwear use, accommodation time, and the number of trials.

Conclusion: Existing literature provides somewhat limited information about the considerations and outcomes of alignment procedures. The evidence is not of high-quality and primarily relates to individuals with transtibial amputation.

3.2. Introduction.

Lower-limb amputations (LLA) account for 85% of all significant limb amputations [144], [145]. Transtibial (TT) and transfemoral (TF) amputations are the most common LLAs [146], [147]. Prostheses are most used to restore the mobility of individuals with lower-limb amputations. Most individuals with LLA face challenges such as stump pain [148], osteoarthritis, osteopenia, osteoporosis, and low back pain [107]. These may be related to abnormal movement, and loading patterns during gait typically referred to as gait deviations [78], [149].

To achieve an amputee's comfortable and natural gait, the prosthesis must be correctly aligned relative to the anatomy of the musculoskeletal system [20]. The procedure is divided into three stages [150]. Bench alignment is focused on balancing the load lines of the prosthesis. Static alignment is focused on optimizing the distribution of weight over the sound limb and the prosthesis to improve balance during standing. Dynamic alignment is conducted during walking and targets the minimization of gait deviations. Prosthetic alignment, which typically includes these three stages, is a critical and iterative procedure that is highly dependent on the skills of the prosthetist [151]; therefore, a plurality of methods have been proposed to improve upon this procedure. Several examples of these methods include: an axis system to set the socket alignment position and orientation

allowing the assessment of the significance and repeatability of an optimal alignment [152], prior alignment techniques such as anatomically based-alignment (ABA) standing, ABA supine, and the vertical alignment axis (VAA) to reduce the time and skills to perform alignment [153], and the dynamic alignment procedure optimization using gait parameters, socket geometry, and information of the artificial leg components [154].

The most significant risk for a patient using a misaligned prosthesis is gait deviations or abnormal gait patterns. These include gait, and biomechanical anomalies such us such as vaulting, circumduction, drop off, medial/lateral whip, and lateral trunk bending [24], [155], some alterations in plantar foot pressures [156], asymmetries in step length [157], changes in the stump pressure [158], standing balance deviations [159], a moderate asymmetry between spatiotemporal gait parameters of lower limbs [160], [161]. Gait deviations are associated with pain and long-term musculoskeletal problems, increased energy consumption [36], as well as user dissatisfaction [162] and the need for continuous visitations to prosthetics centers for prosthesis adjustments [16].

It is crucial to develop an understanding of the variables that can be used to find clinically acceptable prosthetic alignments. Several systematic reviews have compiled such information [163]–[166]. However, these former studies do not specifically outline the considerations for achieving prosthetic alignments towards optimized patient outcomes. Additionally, the focus of these prior reviews is primarily on transtibial amputations, and other levels of amputation are not addressed. Furthermore, the previous reviews do not explicitly explore important factors such as ambulation methods, type of footwear, population attributes, accommodation time to a new alignment condition, the prosthetic elements, among others, in the alignment procedure. In this paper, a meticulous analysis

of literature was performed to highlight the factors related to prosthetic alignment, patient and the prosthesis, aspects of prosthetic alignment testing, and the influences on amputee performance. This systematic review aims to inform clinical practices and research relating to the alignment of lower-limb prostheses.

3.3. Methods.

The search strategy for this systematic review was focused on papers dated between 2000 and 2020, for considering most new dynamic alignment techniques. Databases explored were IEEE, Scopus, and PubMed. A. M. C. and J. U. perform the papers searching following the strategy depicted in Table 2.

Database	Search Strategy
IEEE	Alignment AND Prosthesis AND Amputee
Scopus	TITLE-ABS-KEY (alignment) AND TITLE-ABS-KEY (prosthesis OR prosthetic OR amputee OR amputees) AND TITLE-ABS-KEY (transtibial OR trans-tibial OR transfemoral OR trans-femoral) AND PUBYEAR > 2000 AND PUBYEAR < 2020
PubMed	((Alignment[Title/Abstract] AND (Amputee[Title/Abstract] OR Amputees[Title/Abstract])) AND (Prosthesis[Title/Abstract] OR prosthetic[Title/Abstract])) AND (transtibial[Title/Abstract] OR trans-tibial[Title/Abstract] OR transfemoral[Title/Abstract] OR trans-femoral[Title/Abstract]) AND ("2000"[PDAT]: "2020"[PDAT])

Table 2. Information about the electronic literature search.

The eligibility criteria were full papers written in English and studies focused on TF or TT dynamic prosthesis alignment. All articles were analyzed by using the Preferred Reporting Items for Systematic and Meta-Analyses – PRISMA checklist [38].

The quantitative synthesis of papers includes extraction and categorization of information following 1) population attributes, 2) alignment procedure characteristics, and 3) effects of prosthetic alignment on amputee performance. The first one includes information about the population sampled, prosthetic groups, sociodemographic characteristics, details of amputation, or residual limb information. In the next topic were described standard requirements during prosthetic alignment experimentation and typical magnitudes and orientations of the prosthesis in the study of alignment. The last one represents the effects of prosthetic alignment on amputee performance.

The quality assessment of articles was performed using 13 criteria [39]: The population information (M1) composed by the inclusion and exclusion criteria (Q1), sociodemographic information (Q2), amputation information (Q3), prosthetic elements used (Q4); the intervention and assessment procedures (M2) divided in the alignment variation experiments (Q5), number of prosthetic element links aligned (Q6), years using a prosthesis (Q7), and reported accommodation time (Q8); the methodological procedures (M3) composed by the information about alignment experiment procedure (Q9), randomization of alignment variations (Q10), and participant blinding during alignment test (Q11); finally the evaluation of article results (M4) divided by study limitation description (Q12), and statistical tests description (Q13).

Each condition Q could take two values, zero for requirements not satisfied or one in the opposite case, excepting $Q_{6,}$ which could take three states: zero, one, or two variations of prosthetic adaptor links. The quality level of the studies is divided among A, B, and C, and the scores were calculated by following a similar procedure to the suggested by Van der Linde et al. [40]. Index A would represent studies with a total score higher than 11 having fulfilled the criteria Q_2, Q_3, Q_5, and Q_{10}. Index B corresponds to an overall rating greater than or equal to six and less or equal than eleven, and a positive Q_1, Q_5, Q_{10} criteria. Finally, index C shows papers with a total score of less than six.

3.4. Results.

A total of 176 papers were extracted from databases using the search strategy, distributed as follows: 115 from Scopus, 47 from PubMed, and 14 articles from IEEE database. Figure 21 shows the PRISMA flow diagram developed for the information assessment.

Papers [167], [168] were grouped in the A-level (5.3%) with a quality mean value of 11.5(±0.7), B-level clustered 21.1% of articles [169]–[176] with 8.1(±0.8), and finally the 73.7% of documents [33], [36], [183]–[192], [157], [193]–[200], [160], [177]–[182] were grouped in C-level having a quality of 6.0(±2.5). Quality parameters as test blinding (patient) and randomization of alignment variations were critical criteria, explaining in a considerable extent the small number of articles classified in A-level.

Figure 21. The flow of information followed on the systematic review using the PRISMA method.

The prosthetic misalignment topic have been commonly reported in the Prosthetics and Orthotics International Journal [157], [160], [169], [181], [189], [191], [192], Journal of Biomechanics [172], [182], [184], [194], [198], Gait & Posture [36], [171], [173], [178], and Clinical Biomechanics [177], [195], [197].

3.4.1. Population attributes.

Transtibial amputees (TTA) were mentioned in 86.8% of articles, transfemoral amputees (TFA) in 15.8%, and a non-amputee control group (NAC) in 7.9% of papers. The quality of documents focused on TF was mainly in C significantly lower than the TTA. Not all articles fully disclosed sociodemographic data. Most reports showed sociodemographic data (age, height, weight, and gender), but no significant relationships were observed between the parameters; however, even though 44.7% of papers recruited both genders, being just 14.9% females and among these, only 11.1% were TF, indicating a disparity in results. The amputation etiology was mostly trauma. The mean value of time using prosthesis was 8.6±7.3 years; nevertheless, in most cases, this value was not announced explicitly; instead, they reported times greater than one, three, or five years. The time since the amputation was typically 14.4(±4.5) years.

3.4.2. Characteristics of the alignment procedure.

The information of the alignment procedure was grouped into three categories: standard requirements during prosthetic alignment experimentation, typical magnitudes or orientations of prosthetic elements, and the gait alterations by prosthetic alignment variations.

3.4.2.1. The standard requirements during the prosthetic alignment experiments.

The research in prosthetic alignment demands long and strenuous work sessions; therefore, the definition of minimum requirements of alignment changes, accommodation time, and resting time will facilitate the interaction with the patient. 42.1% of papers declared less than four alignment changes, 13.2% informed a range between five and ten, and 44.7% did not report data. The accommodation time of the patient to a new alignment condition was less than ten minutes for 26.3% of papers, 15.8% said between ten and thirty minutes, and 57.9% did not announce. Few documents inform resting times for patients to recover after each alignment, for instance, in [160] and [36] reported 20 and 30 minutes respectively, and in [167], [169] reported it but they did not indicate the value.

The alignment effect was tested during walking except on [33] the test was done during the standing (static alignment). Walking was done overground and on treadmills. The treadmill was primarily utilized for controlling the gait speed [36], [167], [193], [199]. Most of the papers used walkways lengths between 10 m and 15 m. Papers [185]–[187] adopted the number of steps instead of distance to describe the walking length, for instance, 6, 8, and 15 steps.

The use of footwear affects gait performance [201]–[203]. Only 36.8% of papers supplied information on footwear, of which in 85.7% participants wore shoes and in 14.3% were barefoot. However, articles did not analyze the effect of wearing shoes in the alignment procedure. The 86.8% of papers revealed information about the type of prosthetic foot, knee joint, suspension, or the socket shape used. In some articles the alignment was tested with patients wearing the same type of prosthesis [33], [160], [177], [179], [180], [183],

[185], [186], [188], [191], [197], [198], [167]–[170], [172], [173], [175], [176], and in papers [36], [171], [194], [195], [200], [178], [181], [182], [184], [187], [189], [190], [192] the prosthetic element was different between patients; however, none described the relationship between the prosthetic component differences and the alignment variations on the patients' performance.

During the prosthesis alignment, one of the most critical concerns is the comfort of the patient; however, the subjective perception of prosthetic performance and comfort was considered only in the minority of studies [36], [160], [167], [168], [174], [178], [181], [184], [186], [187] using instruments such as the prosthetic socket fit comfort score, questionnaire PLUS-M, the Prosthesis Alignment Perception Instrument (PAPI), and some other custom surveys.

3.4.2.2. The typical alignment variations during the prosthetic fit.

Alignment variation was considered as any positional or angular change of prosthetic elements for the fitting of lower limb prostheses. Alignment changes included angulations (51.1%), translations (40.0%), and rotations (11.1%). Nearly half of all papers (44.7%) performed at least three alignment changes, 28.9% between four and ten changes, and 13.2% more than ten alignment changes.

The alignment changes were mainly tested in random order [36], [160], [175]–[178], [181], [182], [184], [186], [188], [189], [167], [192], [194], [195], [197], [198], [168]–[174], but in [157], [183], [185], [187], [191] were predefined, and study [36] used both. Papers [160], [167], [192], [168], [174], [175], [177], [185]–[188] additionally blinded the test, making the amputees unaware of the alignment change. The randomness and

blinding of the alignment tests were considered as a quality indicator and a means of avoiding bias in comfort survey responses as well as the potential for voluntary adjustments of gait.

The movement of socket and foot was performed about the socket / (knee or shank) and the shank/foot pyramidal adaptor, respectively. Only one paper [170] informed changes in both locations at the same time, which led to longer testing times for each participant.

Translations of the socket and foot in anterior or posterior directions were studied in 47.4% of articles, for lateral or medial in 34.2%, and in 5.3% performed shortening or lengthening of the prosthesis. Typical abduction/adduction socket angulation of TF prostheses was 4.5(±2.1) ° and around 1.8(±0.4) cm for anterior/posterior translation movements. Paper [182] tested 6° in flexion/extension and 1.5 cm in lateral/medial. The prosthetic foot of TF was shifted mainly 1.7(±0.6)cm in anterior/posterior direction, but in studies [36] and [179] included a 0.5 cm lateral/medial movement and an angulation of 10° in dorsiflexion/plantarflexion, respectively.

The alignment of the socket in TT prostheses included angulations of 5.3(±2.9)° in flexion/extension and 4.4(±2.2)° in abduction/adduction. Additionally, paper [189] reported 2.0(±1.4) cm lengthening and shortening of the TT prosthesis. The prosthetic foot of TT prosthesis was angulated 6.4(±3.5)° in dorsiflexion/plantarflexion, rotated internally and externally in 13.5(±12.0)°, translations of 1.3(±1.2) cm in anterior/posterior and 2.5(±1.4) cm in lateral/medial, and [170] reported a 6.0° movement in inversion/eversion.

3.4.3. Amputee performance alteration by prosthetic alignment variations.

Variations in the prosthetic alignment produced changes of socket reaction moment (SRM) of TT amputees. Angulation of 2.0° socket extensions produced changes of maximums SRM [195], a similar result happens in [197] for a maximum sagittal moment for 6.0° of flexion compared to 6.0° of extension. Extension movements of 3.0° or 6.0° of the socket have produced variations in 30% of stance phase [172]. In [173] was reported SRM alterations for 3.0° in flexion/extension and abduction/adduction, and 0.5 cm in anterior/posterior and lateral/medial translational movements. Alterations of SRM were observed for angulations of 6.0° in extension and flexion during the alignment tests of TF amputees [182].

Generally, angulations and translational alignment changes of TT prostheses in coronal and sagittal planes resulted in variations of SRM [169], [194], [197], [198]; however, the results for TF amputees were not found to be significant. Movements in the sagittal plane of foot produced changes in horizontal and vertical ground reaction force (GRF) for TT amputees [200]. Authors in [180] showed that foot dorsiflexion and plantarflexion alignment variations increased the GRF, and other external moments on the hip and knee of TTA, affecting the normal movement of the knee during walking and increasing external loads on knee ligaments. Likewise, TF amputees recruited in [167] increased their hip extension moment during the early-stance phase as a strategy for keeping knee joint stability for shifts of 2.0 cm of the socket in an anterior/posterior direction. When the foot was perturbed in varus, valgus, or external rotations, the GRF in the mediolateral direction and the ankle moment in the coronal plane during terminal stance exhibited changes in GRF [189].

The distribution of pressure of the socket-stump interface in TT amputees was commonly affected by 1 cm socket translation alignment changes in coronal and sagittal planes [175], even using different types of socket. An increase of pressure on the anterodistal stump area was found for 6.0° socket flexion, while an extension of 6.0° in socket extension produced a significant reduction in pressure at this site [168].

Different articles reported significant changes in some spatiotemporal parameters such as stance phase duration and single support duration in intact limbs for 5.0°, 6.0°, and 10.0° internal/external foot rotations [178], [184]. Likewise, article [191] found that an excessive external rotation (10.0° and 36.0°) produced variations in stance and swing times and step length. The symmetry of the step length was affected by movements of 2.0° of the foot in plantarflexion [157].

Alignment variations produced a significant decrease in the comfort [176], [191], highlighting changes of 6° in internal foot rotation [184], and alterations of 3.0° and 6.0° of socket abduction/adduction and flexion/extension [186]. Even though the patient's comfort is a meaningful parameter, the articles did not deepen the analysis of participants' satisfaction.

The use of EMG for studying gait during prosthetic alignment was infrequent [177], [180]. The most symbolic effect was produced by movements of 6° in flexion/extension of the socket, supplying a 50% hamstring muscle force increase and 20% more in *rectus femoris* and *vasti* for TT participants.

The balance of TTA was affected by flexion/extension perturbations of socket alignment perturbations [33]; correspondingly on [179], it was revealed a lateral center of pressure

displacement by foot adduction variations. TTA voluntarily decreased the anterior inclination of their body, generating stabilization mechanisms for adapting to alignment changes of the foot in dorsiflexion, plantar flexion, and prosthesis lengthening or shortening [183].

For TT participants, the plantar foot pressure distribution was notably affected by rotations in sagittal and coronal planes of socket and foot simultaneously, producing shifts of the center of pressure [170]. The TFA during coronal translational variations shows an increase in burning calories and average heart rate, and intact/prosthetic limb symmetry [193]. Another article [36] found no significant variations of oxygen consumption for TTA and TFA during anterior/posterior shifts (2.0 cm) of the knee. Authors in [157] showed few gait asymmetry influence due to the alignment variations, finding only a small difference in the step length by making variations of 2.0° in foot plantar-flexion.

3.5. Discussion.

The alignment research outcomes were discussed according to the population characteristics, experimentation procedures, and the amputees' alignment effects reported on papers.

3.5.1. Population attributes.

High prevalence in studies on prosthesis alignment of TTA was clear, having a 5.5 higher occurrence than TFA. The quality A or B of papers were mainly focused on TTA, therefore, more information on the effects in TF prosthetic alignment is still needed. The

preference of TTA researchers is likely due to the higher prevalence of TT amputation compared to the TF as it has been revealed in other studies [204], [205].

The use of a non-amputee control group (NAC) was not frequent and did not influence the quality of the articles. Typically, it was employed as a biomechanical reference; therefore, it does not appear imperative to include a control group. The definition of the sample size of TFA or TTA groups was not uniform because the values varied between 1 and 15 people. For gender, the set of females was considerably low; therefore, further quality research relating to gender and alignment are needed.

Typically, the papers reported that participants had more than six months of acclimation to wearing lower limb prosthesis or since the amputation. Considering that gait skills are related to the duration of prostheses use [206], there exists a potential gap in knowledge about prosthetic alignment for new amputees.

3.5.2. Alignment procedure characteristics.

Articles analyzed in this review preferred the over ground walking compared with the use of treadmills. Considering the ambulation method affects the kinetic or kinematics of the gait [207], [208], it is necessary to research the effects of the ambulation alternatives or the terrain shape, in the alignment studies.

The literature generally did not define the accommodation time to a new alignment condition; however, their definition could be related to the training time for wearing a new prosthesis. According to [206], [209], [210] an amputee takes between 5 and 300 minutes to learn how to use a lower-limb prosthetic device. Considering that the amputees

adopted stabilization mechanisms for adapting to prosthetic alignment changes, a long accommodation time could affect the accuracy of alignment procedures; therefore, a specific study to estimate this time is needed.

The number of trials and the number of alignment variations increase the total duration of the alignment's experiments. Prolonged tests might induce physical and mental fatigue, frustration, and possible rejection to perform the tests, likely resulting in bias on the feeling of comfort for an alignment condition given. Specifically, the fatigue parameter was not included in any alignment study; therefore, future studies should address this question by adding the fatigue as a parameter of interest. Additionally, periods for patient resting should be included to minimize or control for these effects.

The articles reported a preference toward shod gait [160], [170], [178], [183], [184], [188], [192] instead of barefoot walking [171]. The effects of using footwear or wearing different kinds of shoes during alignment procedures is not clear and needs to be further researched. The prosthetic components are fitted based on amputees' requirements and it's not something controllable during alignment tests. The relationship between the prosthetic device capabilities and the gait performance is well-known [115], [211]–[213]; therefore, including different types of prosthetic components in the alignment procedure would allow differentiating between the influence of the prosthetic alignment and the prostheses components on the amputee's performance.

Considering dynamic alignment procedure implies fittings of the socket, knee, and foot positions or angles, it is clear a lack of quality articles assessing alignment procedure including translational, rotational, and angulation movements of all prosthetic elements.

The review evidenced a lack of information in TTA outcomes for variations of the foot in internal/external, inversion/eversion, and translation movements. Likewise, knowledge of the alignment effects for socket movements in anterior/posterior, internal/external rotations, medial/lateral, and length variations are still insufficient. For the TFA, the alignment information is significantly lower; thus, more research in patient outcomes is needed in this kind of prostheses.

Prosthetists typically define nominal or optimal alignment through gait observations and patients' feedback. The analytical skills of the prosthetist were not included or assessed during any alignment testing, so studies are needed to identify the relation between optimal alignment, amputees' comfort perception, and the expertise level of prosthetists for performing prosthetic alignment procedures.

The review showed the TTA could regulate their gait speed, cadence, and body inclination during changes of the prosthetic alignment; however, more quality information for TTA, especially for TFA and other amputation levels is still missing. The review revealed a knowledge gap about patients' outcomes by socket alignment in internal and external rotations, valgus, and varus angulations, as well as lengthening and shortening of the prosthesis. In terms of prosthetic foot alignment, there is a lack of research for eversion and inversion, as well as medial and lateral translational movements.

The clinically accepted protocol to perform prosthetic alignment includes the fitting of socket and foot; therefore, and notably, not enough evidence was observed about the changes of amputees' performance when these prosthetic elements were aligned simultaneously; especially for kinetic parameters such as SRM and GRF, kinematic and

spatiotemporal parameters, energy expenditure, comfort evaluation, and plantar foot pressure measures.

3.5.3. General considerations for performing the prosthetic alignment.

The alignment procedure places the prosthetic elements in positions relative to the biomechanical lines of the amputee; nevertheless, the quality of the alignment in clinical practice and research should consider individuals characteristics and their functional capabilities, the prosthetist's skill, and the alignment procedure features.

Clinicians and researchers must consider rotations, angulations, and translations of both prosthetic elements socket and foot, in sagittal, coronal, and transverse planes. The magnitude of alignment movements is related to anatomical characteristics of the residual limb and natural body lines. The number of alignment variations during testing in research projects is strongly associated with the participants' fatigue; thus, the comfort surveys should ask about the mood and physical state of the volunteer.

To evaluate the amputee's performance for walking, the ambulation methods during the alignment procedure should include diverse terrain relief and assess the use of footwear or barefoot. The prosthetist's knowledge in the prosthetic alignment procedure influences the alignment accuracy and contributes to the successful prosthetic adaptation of the patient; however, researchers also should consider the amputee's skills for walking because it could mask the alignment effect.

3.6. Conclusion.

This paper review reveals a baseline for prosthetic alignment studies, showing the primary metrics used to analyze the prosthetic amputees' performance such as spatiotemporal and kinematic gait data, ground reaction force, socket-stump interface pressure, body balance, and muscular activity.

Alignment studies must consider angulations, rotations, and translation movements in the sagittal, coronal, and transverse axis. For a better understanding of gait performance outcomes, influenced by alignment variations, alignment modifications in socket and foot must be performed.

Considering that the alignment is a process with a high subjectivity associated with the characteristics of the amputee, the definition of "optimal" alignment of TT and TF prosthesis is nearly a concept for both amputees and prosthetists, therefore it is strictly necessary to use a questionnaire to measure the comfort or satisfaction of the amputee, this being the most essential instrument. The dynamic prosthetic alignment should be further researched to achieve a more objective definition.

Chapter 4.

The effect of prosthetic alignment on the stump's temperature and the ground reaction force

Contribution to Ph.D. research: This chapter helped in the fulfillment of the fourth objective of the thesis: "*To propose and evaluate a computational model based on the biomechanical variables recorded during the static and dynamic analysis of the transfemoral mechanical prostheses".* The analysis of the parameters recorded during the alignment procedure are discussed in Chapter 4. and Chapter 5. This chapter shows the statistical analysis of the vertical and anteroposterior components of the Ground Reaction Force (GRF) and the temperature of the residual limb to identify the effects of prosthetic alignment on transfemoral amputees during gait.

The intra-subject analysis showed the stump temperature is affected by the prosthetic alignment for more than 70.0% of trials; however, results were not generalized to the population of amputees. The between subject analysis showed changes in the GRF parameters between nominal and misalignments. Therefore, this chapter demonstrates the effectiveness of GRF in describing the effects of prosthetic misalignment.

The findings described in this chapter were analyzed in cooperation with Dr. Josep M. Font-Llagunes, professor at the Biomechanical Engineering Laboratory of the Universitat Politècnica de Catalunya, Barcelona, Spain

This chapter has one supporting appendix. Refers to **Appendix PA** for information about the amputee volunteers and control group.

Title of research paper: The Effect of Prosthetic Alignment on the Stump Temperature and Ground Reaction Forces during Gait in Transfemoral Amputees.

Published in: Gait & Posture

Cited as: Andres M. Cárdenas, Juliana Uribe, Josep M. Font-Llagunes, Alher M. Hernández, Jesús A. Plata, "The Effect of Prosthetic Alignment on the Stump Temperature and Ground Reaction Forces during Gait in Transfemoral Amputees," Volume 95, 2022, Pages 76-83, ISSN 0966-6362,

DOI: https://doi.org/10.1016/j.gaitpost.2022.04.003

4.1. Abstract.

Background: Lower limb prosthetic alignment is a procedure mostly subjective. A prosthetic misaligned induces gait deviations and long-term joint diseases. The alignment effects for each lower limb and the stump stays uncertain.

Research objective: To identify the effect of the transfemoral alignment prosthesis on ground reaction forces and thermal images of the residual limb.

Methods: The effect of misalignment and nominal alignment was evaluated in sixteen transfemoral amputees. The nominal alignment was considered as the optimal alignment for each subject. Misalignment included random variations in the anterior-posterior and medial-lateral translation of the prosthetic foot and the angle of flexion-extension, abduction-adduction, and internal-external rotation of the socket and prosthetic foot. The control group consisted of fifteen non-amputee individuals. The ground reaction force parameters and stump temperature were analyzed for each alignment condition. The statistical analysis included the Kruskal-Wallis and multiple comparison tests.

Results: The prosthesis did not produce statistically significant changes in the average temperature of residual limbs. However, the temperature distribution on the stump skin was different ($P<0.05$). The transfemoral prosthesis misalignment produced an irregular heat diffusion on the anterior, posterior, and lateral sides of the stump contour compared to the nominal alignment ($P<0.05$). The sound limb did not show differences between nominal alignments and misalignments for most ground reaction force parameters. For almost all GRF parameters, significant differences were observed for the prosthetic limb between misalignment and nominal alignment ($P<0.001$). The symmetry indices of

ground reaction force parameters of transfemoral amputees did not show any kind of significant improvements after aligning the prosthesis nominally.

Significance: The findings in the analysis of the stump's temperature distribution and the ground reaction force of the prosthetic limb provide a better understanding of the alignment procedure of the transfemoral prosthesis.

4.2. Introduction.

The alignment is an iterative procedure of prosthesis adjustment to provide static balance and dynamic function of amputees according to their biomechanical characteristics. The prosthetist's skills are crucial for a successful alignment; therefore, the optimum prosthetic alignment is achieved mainly by subjective judgments. A proper prosthesis fitting increases the adaptation of amputees to daily activities. Conversely, an inadequate prosthetic alignment is a common cause of an abnormal prosthetic gait. In addition, gait deviations lead to secondary musculoskeletal disorders such as stump pain, osteoarthritis, and low back pain [214].

Kinetic parameters such as the ground reaction force (GRF) and joint moments have been used to find the effects of misalignment on prosthetic gait. Van Velzen et al. [189] identified systematic effects in the medial-lateral GRF during terminal stance for varus and valgus or exo-rotation foot alignments. The effect of the translational alignment of prosthetic feet has also been evaluated for the standing and sitting trials [215]. The braking impulse was smaller on the prosthetic side and greater on the sound limb for anterior alignment compared to the posterior alignment. Pinzur et al. [216] evaluated the

vertical ground reaction forces of transtibial amputees during gait trials. Authors suggested that prosthetic misalignments increase the loading on the contralateral limb and, in the same way, the stance phase time and vertical GRF peak were different between misalignments and nominal alignments. Zhang et al. [217] identified for transfemoral amputees an effect of the prosthetic misalignment in the intact hip and knee joint moments by following a within-subject analysis. In general, earlier studies have found a significant relationship between GRF parameters and prosthetic alignment conditions.

Thermography has been used as a tool to evaluate the interactions of the stump-socket interface. Raggi et al. [218] proposed a protocol that integrated thermal imaging for the evaluation of the whole prosthetic setup, finding hot spot temperature differences according to the socket type. The temperature assessment of the interface between residual limb and liners of below-knee amputees was proposed in [98]. The thermography of the stump showed the presence of hot spots at the liner-stump interface during gait and standing trials. The hot spots increased 20% after walking with good inter-subject repeatability. On the same line, Živčák et al. [99] informed that the use of thermography is an appropriate method for a rapid diagnosis during design, manufacture, and application of the socket for transtibial amputees.

Thermal images have been used in the adaptation of lower limb prostheses and their effectiveness during prosthetic manufacturing has been confirmed; however, to the best of the authors' knowledge, thermography has not been used to assist the prosthetic alignment procedure. An incorrect prosthetic alignment produces an improper distribution of the socket-stump interface loads [93], [194], leading to increased friction and stress on the interface, and later surface damage to the soft tissue [219]. As well as

the change of the skin pressures produced by misalignments could affect muscles' blood perfusion [220], therefore, the use of thermal photos could help to find prosthetic alignment problems.

Although earlier studies have supplied useful information to aid prosthetists during prosthetic alignment, the alignment procedure uncertainty and the amputees' gait compensation skill are still being challenged for qualitative gait assessment [176]. Therefore, new quantitative strategies for helping prosthetists during prosthetic alignment are needed. Considering the effectiveness of the ground reaction force to find issues associated with prosthetic misalignments and that the residual limb temperature changes while wearing the prosthesis, it is hypothesized that the quality of the prosthetic alignment can produce changes in the skin temperature of the residual limb, the ground reaction force, and the symmetry of the gait pattern. Therefore, this article evaluates the effectiveness of the ground reaction force parameters and thermal images of the residual limb to describe the effect of misalignments and nominal alignment on the prosthetic gait of transfemoral amputees.

4.3. Methods.

4.3.1. Subjects and experimental equipment.

The Ethics Committee of the Institute of Medical Research of the Universidad de Antioquia (Medellín, Colombia) approved this research study. The inclusion criteria of amputees were (1) unilateral transfemoral amputees, (2) a functional level higher than 2

[14], and the control group included (3) ages over 18 years old, and (4) not report other diseases. Table 3 details the information of the registered subjects. Mahavir Kmina artificial limb center in Medellín, Colombia, assembled all prostheses. Prosthetic devices included an ischial containment socket, a suction suspension system, a ReMotion prosthetic knee (D-Rev V3, USA), and a Jaipur foot (BMVSS, Jaipur, India). Subjects did not use any interface like socks or liners.

The ground reaction force was recorded using the force platform P6000 (BTS Bioengineering, Italy) and the Smart Clinic and Smart Analyzer software (BTS Bioengineering, Italy). The camera Gobi 640 (Xenics, Belgium) and software Xeneth 2.6. (Xenics, Belgium) were used to capture thermography. Matlab (MathWorks, USA) and Statgraphics Centurion (Statgraphics Tech., USA) were used to analyze signals.

ID	Volunteer	Gender	Age (years)	Weight (kg)	Height (cm)	BMI	Amputation etiology	Amputation Side
1	Transfemoral Amputee	Male	34	72.0	175.2	23.5	Road accident	Left
2	Transfemoral Amputee	Male	44	68.0	165.0	25.0	Vascular	Right
3	Transfemoral Amputee	Male	50	70.0	169.0	24.5	Gunshot wound	Right
4	Transfemoral Amputee	Male	53	80.0	170.0	27.7	Road accident	Left
5	Transfemoral Amputee	Male	29	56.5	174.0	18.7	Gunshot wound	Left
6	Transfemoral Amputee	Male	33	63.0	171.0	21.5	Road accident	Left
7	Transfemoral Amputee	Male	45	68.8	166.0	25.0	Road accident	Left
8	Transfemoral Amputee	Female	45	68.8	166.0	25.0	Road accident	Right
9	Transfemoral Amputee	Male	51	62.2	145.0	29.6	Road accident	Left
10	Transfemoral Amputee	Male	25	70.3	173.0	23.5	Road accident	Left
11	Transfemoral Amputee	Male	35	52.8	178.0	16.7	Road accident	Left
12	Transfemoral Amputee	Male	29	85.5	182.0	25.8	Road accident	Right
13	Transfemoral Amputee	Male	34	79.0	168.0	28.0	Road accident	Left
14	Transfemoral Amputee	Female	33	71.0	166.0	25.8	Cancer	Right
15	Transfemoral Amputee	Male	30	57.7	161.0	22.3	Workplace injury	Right
16	Transfemoral Amputee	Male	35	62.0	161.0	23.9	Gunshot wound	Right
17	Control	Female	21	58.5	166.0	21.2	-	-
18	Control	Female	21	54.0	158.0	21.6	-	-
19	Control	Female	46	58.0	159.0	22.9	-	-
20	Control	Female	27	70.1	158.0	28.1	-	-
21	Control	Male	28	72.3	170.0	25.0	-	-
22	Control	Male	49	77.2	175.0	25.2	-	-
23	Control	Female	24	57.3	162.0	21.8	-	-
24	Control	Female	27	53.0	162.0	20.2	-	-
25	Control	Female	19	53.4	160.0	20.9	-	-
26	Control	Male	31	80.5	171.0	27.5	-	-
27	Control	Female	51	58.7	163.0	22.1	-	-
28	Control	Male	31	58.7	163.0	22.1	-	-
29	Control	Male	39	64.0	168.0	22.7	-	-
30	Control	Female	19	48.0	160.0	18.8	-	-
31	Control	Male	59	88.0	181.0	26.9	-	-

Table 3. Information about recruited volunteers: the main characteristics of the thirty-one volunteers recruited are described.

4.3.2. Experimental protocol.

The temperature reference was recorded by using thermal photographs from the anterior, posterior, and lateral views of the stump. The following steps were performed for five trials: (1) the socket and foot angle were randomly changed (Figure 22); (2) the subjects walked for ten minutes on a ten meters hallway using a self-selected walking speed; (3) the ground reaction force was recorded for each lower limb; (4) the prosthesis was removed, and thermal photos were taken from anterior, posterior, and lateral sides; (5) the amputee rested for twenty minutes without the socket. For one trial, randomly chosen, the prosthesis was optimally aligned, and this condition was named the nominal alignment. The prosthetist was blind for the alignment order. The control group did not perform steps (4) and (5). The alignment variations included socket rotations in flexion-extension (-6.0° to 7.0°), adduction-abduction (-8.0° to 6.0°), and internal-external rotation (-18.0° to 28.0°). The prosthetic foot included dorsi-plantar flexion (-7.0° to 6.0°), eversion-inversion (-4.0° to 6.0°), and internal-external rotation (-13.0° to 11.0°).

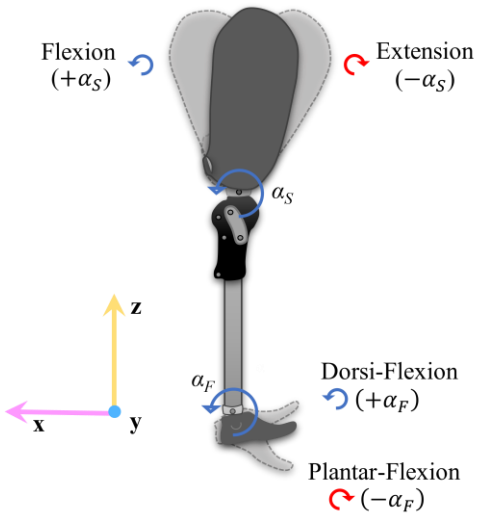

(a). Lateral view of prosthetic limb.

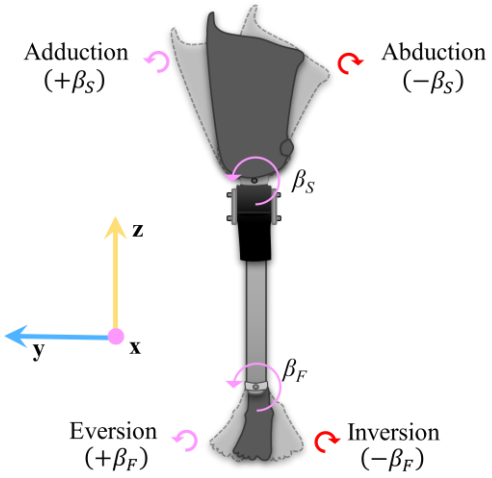

(b). Anterior view of prosthetic limb.

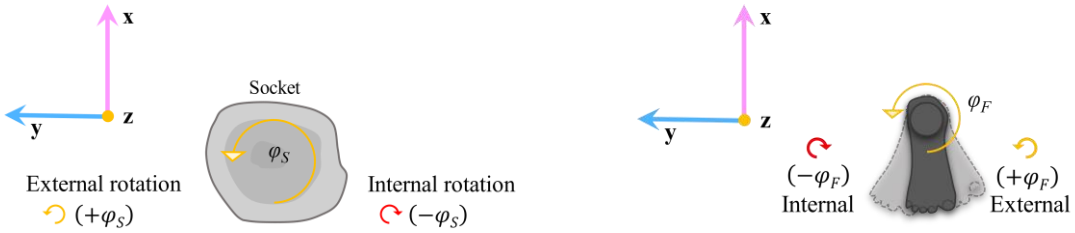

(c). Socket top view.

(d). Foot lateral view.

Figure 22. Movements of the socket and prosthetic foot to produce misalignments.

4.3.3. Data capturing and analysis.

4.3.3.1. Temperature of the residual limb.

Temperature measurements were made directly on the skin of the stump. Eighteen photos were excluded because their quality was not proper. Finally, 222 thermographic photos were analyzed. The stump thermal images were analyzed using the K-means method [221] for temperature clustering. Figure 23 shows an example of clustering for misalignments and nominal alignments. The appropriate number of clusters was calculated using Calinski-Harabasz [122] and Davies-Bouldin [123] methods.

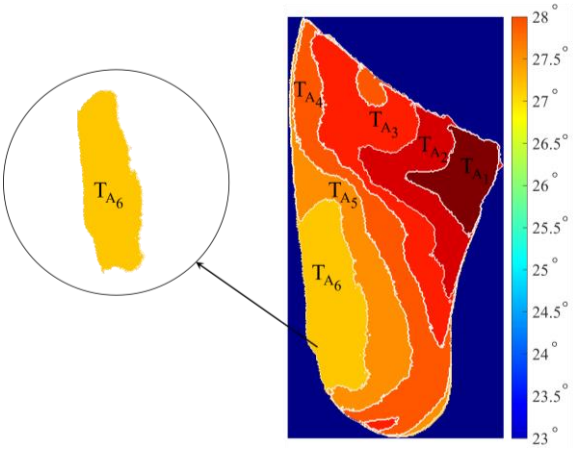

(a). Temperature clustering of the stump after walking using a nominally aligned prosthesis for the amputee number six (posterior side).

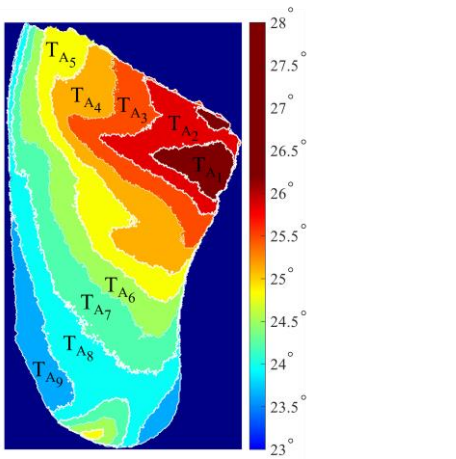

(b). Temperature clustering of the stump after walking using a misaligned prosthesis for the amputee number six (posterior side).

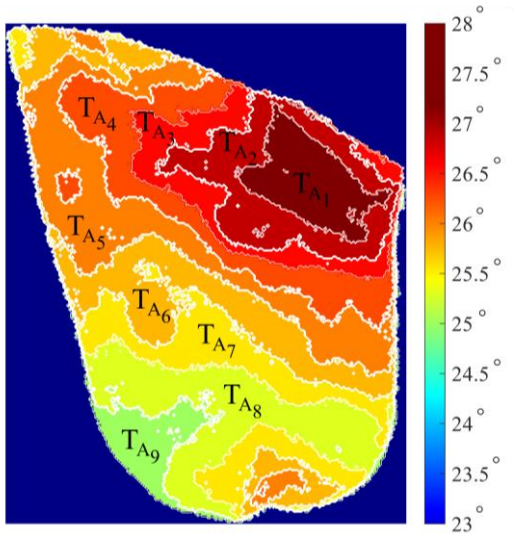

(c). Nominal aligned prosthesis in the anterior side. Third volunteer.

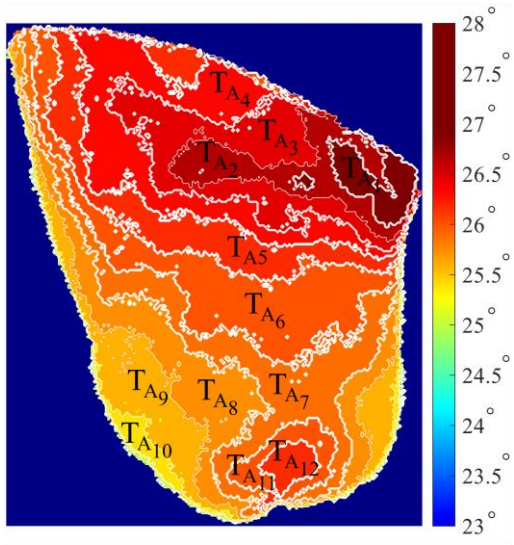

(d). Misaligned prosthesis in the anterior side. Third volunteer.

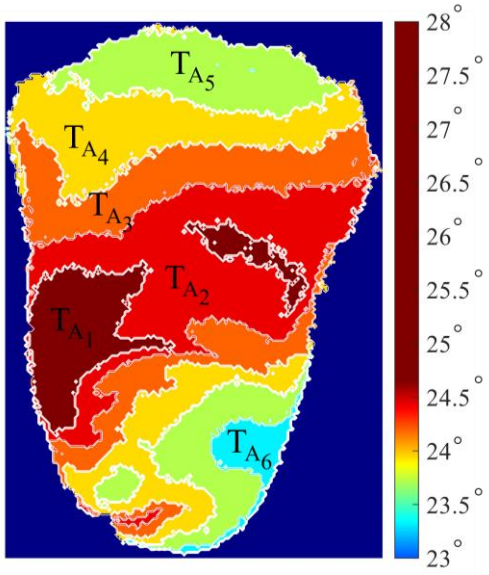

(e). Nominal aligned prosthesis in the lateral side. Second volunteer.

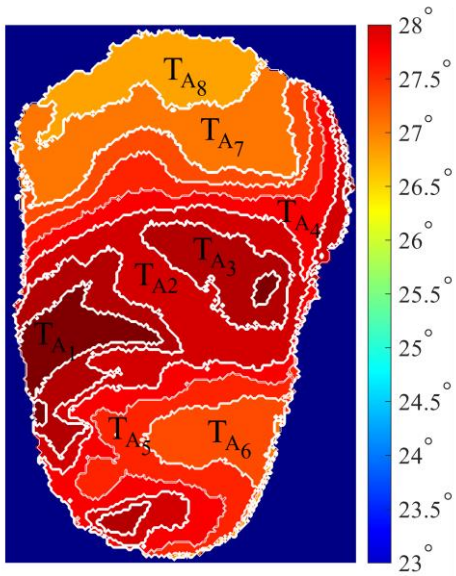

(f). Misaligned prosthesis in the lateral side. Second volunteer.

Figure 23. Clustering of heat regions of the residual limb from the posterior side.

Clustering of the residual limb heat regions for the posterior side: Each thermal photo has a set of identified clusters. The cluster has an associated mean temperature $\{T_{P_1} \cdots T_n\}$ and an area $\{CA_{P_1} \cdots CA_{P_n}\}$.

Each thermal photo has a total number of hot spots named clusters and labeled such as $[C_A \quad C_P \quad C_L]$. The subscripts A, P, and L were used to name the anterior, posterior, and

lateral sides. The temperature average for each cluster was named by $[T_A \quad T_P \quad T_L]$; likewise, the clusters' area was identified as $[CA_A \quad CA_P \quad CA_L]$. The variability was calculated using the ratio between the standard deviation and the mean. The variation coefficient was calculated for the temperature ($[CV_{T_A} \quad CV_{T_P} \quad CV_{T_L}]$) and the clusters' area ($[CV_{CA_A} \quad CV_{CA_P} \quad CV_{CA_L}]$) from each view, and for the number of clusters between sides (CV_C). Finally, the factor analysis method [222] was used to parametrically adjust the variation coefficient of temperature (eq. 4.1), clusters' areas (eq. 4.2), and a total number of clusters (eq. 4.3).

$$CV_T = 0.075CV_{T_A} + 0.017CV_{T_P} + 0.011CV_{T_L} \tag{4.1}$$

$$CV_{CA} = 0.142CV_{CA_A} + 0.131CV_{CA_P} - 0.177CV_{CA_L} \tag{4.2}$$

$$C = 0.142C_A + 0.131C_P - 0.177C_L \tag{4.3}$$

4.3.3.2. Ground Reaction Force (GRF).

Vertical and anterior-posterior ground reaction forces were normalized to the body weight. The medial-lateral component was not considered because of its lower reliability [223]. The following parameters were calculated according to [61]. The anterior-posterior components: breaking peak (F_3), propulsion peak (F_4), braking force impulse (I_3), propulsion force impulse (I_4), duration of stance phase (t_1), duration of the braking phase (t_4), duration of the propulsion phase (t_5), time to braking peak (t_6), time to propulsion peak (t_7), and total impulse ($TI_{AP} = I_3 + I_4$). From vertical component: loading response peak (F_5), terminal stance peak (F_6), midstance valley (F_7), time to loading response peak (t_8), time to midstance valley (t_9), time to terminal stance peak (t_{10}), time from midstance valley to toe-off (t_{11}), the impulse of loading response and midstance (I_5), the impulse of terminal stance

and pre-swing (I_6), and the total impulse of the vertical component $TI_V = (I_5 + I_6)$. Finally, the loading rate (LR), unloading rate (UR), and the braking (BI_V) and propulsion impulse (PI_V) were calculated according to [224], [225]. The limb symmetry index (eq. 4.4) is used to identify the asynchronous movement of the lower limbs [226]. The correspondences between the duration of braking and propulsion phases $(CI_1 = t_4/t_5)$, for the peak values $(CI_2 = F_3/F_4)$, for the impulses $CI_3 = I_3/I_4$, and for the loading and unloading rate $(CI_4 = LR/UR)$ were calculated as well.

$$SI_{\{p\}} = {(X_L - X_R)}\Big/{0.5(X_L + X_R)} * 100\% \quad (4.4)$$

4.3.4. Statistical analysis.

The Kurtosis-bias analysis and Kolmogorov-Smirnov tests confirmed the normal data distribution. The Kruskal-Wallis method [227] evaluated the statistical significance of the differences of groups with a statistical significance of $P<0.05$. The multiple comparison test used the Bonferroni method [228]. The statistical analysis included between-subjects and within-subjects.

4.4.Results.

The following subsections illustrate the statistical analysis of the stump's temperature and the ground reaction force.

4.4.1. The temperature of the stump.

4.4.1.1. Subjects wearing prosthesis vs the reference.

The temperature of the stump was compared after walking using the prosthesis with the temperature of the residual limb while the amputee was resting, namely without socket wearing. For volunteers in the control group, thermal photographs were not taken because it is not possible to simulate the effect of alignment on a non-amputated limb. During the whole study, the ambient temperature was 23.4 ± 1.6 °C. Subjects reported increased stump sweating during warm days; however, it did not significantly affect our outcomes.

The prosthetic wearing did not produce statistically significant changes for the average temperature of residual limbs compared to the reference temperature. However, the number of clusters on the anterior side (C_A), the total number of clusters (C), and the variability of temperature on the lateral side (CV_{T_L}) were 16.2% higher in the reference than thermal photos during the prosthetic wearing for at least 80.0% of trials ($P<0.05$). By contrast, the number of clusters of the anterior side (C_A), the variation coefficient of clusters' area (CV_{CA_A}), the variation coefficient of temperature on the anterior side (CV_{T_A}), the total variation coefficient (CV_T) were at least 11.0% higher during prosthetic wearing than reference for nearly 70.0% of trials ($P<0.05$).

4.4.1.2. Subjects wearing misaligned vs nominally aligned prosthesis.

The results of the temperature variables are presented in Table 4. The between-subjects analysis did not show significant differences, however, the analysis for within-subject shows that the variation coefficient of temperature on the anterior CV_{T_A}, posterior CV_{T_P}, and lateral

CV_{T_L} sides, as well as total CV_T were at least 3.5% higher in misaligned than nominally aligned prosthesis for above 70.0% of trials. The gait trials for misaligned prostheses had more than 10.0% more clusters on the anterior side (C_A) than nominal alignments for above 70.0% of thermal images (P<0.05). Furthermore, the total variation coefficient of clusters (CV_C) was 21.0% higher for misaligned than nominally aligned prosthesis for nearly 70.0% of trials (P<0.05). Likewise, the variation coefficient of the cluster' area on lateral sides (CV_{CA_L}) was 9.0% higher for 70.0% of trials.

4.4.2. Ground Reaction Force – GRF.

The difference between the ground reaction force of the control and amputee groups was inspected. Likewise, an analysis of the gait symmetry indices was performed for the amputees and control groups. The GRF outcomes of transfemoral amputees were analyzed to find the effect of misalignments and nominal alignments. The data normality was verified, and different statistical tests were conducted.

4.4.2.1. Subjects wearing prosthesis vs the reference.

The Figure 24 shows the symmetry index between lower limbs for the control group and the transfemoral amputees considering both alignment conditions. The within-subjects and between-subjects analysis did not show significant differences between GRF outcomes for the control group, which is an expected result because volunteers did not report gait disorders. The amputees' group had more asymmetric gait than the control regardless of the type of alignment. The vertical GRF components: loading response peak (F_5) and midstance valley (F_7), the time from midstance valley to toe-off (t_{11}), and the impulse of loading response and midstance (I_5) were the most symmetric parameters and like those of the control group.

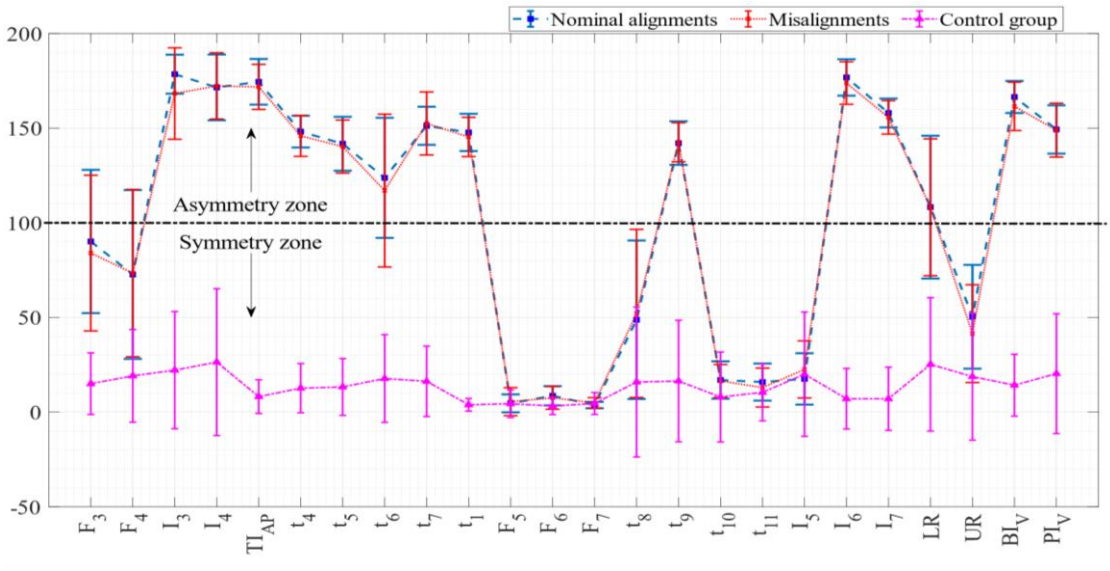

Figure 24. Symmetry index of GRF parameters between lower limbs.

Values greater than one hundred indicate asymmetry and values less than or equal to 100 indicate symmetry between lower limbs.

Parameters F_3, F_4, I_3, t_6, F_5, t_8, t_{10}, t_{11}, and SI_2 of amputee's intact sides during nominal alignments did not show significant differences with control group limbs. Variables such as F_6, UR, SI_1, and SI_3 were at least 104% higher for control group limbs than for 88.2% of nominal alignments. The rest of the anteroposterior forces (I_4, TI_{AP}, t_1, t_4, t_5, t_7), and vertical forces (F_7, t_9, I_5, I_6, I_7, LR, BI_V, and PI_V), and the symmetry index (SI_4) were at least 115% larger in the intact limbs for 98% of nominal alignments than nonamputees.

GRF parameters of the intact limb during misalignments compared to lower limbs of the control group had an almost identical behavior to the above result. The time to braking peak (t_6) was at least 101% larger for control group legs than in 83.8% of the amputee's intact side during misalignments.

The prosthetic side had the same significant differences with the lower limbs of the control group, regardless of the alignment type. Parameters F_5, SI_2, SI_3, and SI_4, did not show significant differences. Values of F_7, t_8, I_5, LR, and UR were 111% higher in the prosthetic side regardless of alignment type than average of control group both limbs. The remaining values were at least 108% higher on the prosthetic side during any kind of alignment than the lower legs of the control group.

4.4.2.2. Subjects wearing misaligned vs nominally aligned prosthesis.

Table 4 shows the comparison of GRF parameters for intact and prosthetic limbs during nominal alignments and misalignments of the prosthesis. The sound limb did not show differences between nominal alignments and misalignments for most ground reaction force parameters, excluding three variables (P<0.01). The time to midstance valley (t_9), the loading rate (LR), and the time from the midstance valley to toe-off (t_{11}) had representatively different values for nearly 70.0% of trials.

Parameter	Acronym	Prosthetic limb			Sound limb		
		Nominal	Misalignment	Repeatability (%)	Nominal	Misalignment	Repeatability (%)
Antero-posterior Ground Reaction Force	F_3 *	12.92 ± (5.13)	8.62 ± (2.70)	92.6 %	12.92 ± (5.13)	13.00 ± (5.57)	52.9%
	F_4 *	15.88 ± (4.54)	8.95 ± (2.87)	94.1 %	15.88 ± (4.54)	15.91 ± (5.45)	55.9%
	I_3 *†	2.81 ± (0.99)	0.25 ± (0.17)	100 %	2.81 ± (0.99)	3.01 ± (1.13)	51.5%
	I_4 *†	4.34 ± (0.85)	0.32 ± (0.22)	100 %	4.34 ± (0.85)	4.31 ± (0.96)	51.5%
	TI_{AP} *†	7.23 ± (1.53)	0.56 ± (0.30)	100 %	7.23 ± (1.53)	7.39 ± (1.65)	51.5%
	t_4 *†	0.55 ± (0.06)	0.09 ± (0.02)	100 %	0.55 ± (0.06)	0.56 ± (0.05)	45.6%
	t_5 *†	0.59 ± (0.09)	0.10 ± (0.03)	97.1 %	0.59 ± (0.09)	0.58 ± (0.08)	47.1%
	t_6 *	0.11 ± (0.02)	0.03 ± (0.02)	92.6 %	0.11 ± (0.02)	0.12 ± (0.04)	45.6%
	t_7 *†	0.44 ± (0.06)	0.06 ± (0.02)	95.6 %	0.44 ± (0.06)	0.44 ± (0.08)	48.5%
Vertical Ground Reaction Force	F_5	104.24 ± (9.55)	102.86 ± (6.37)	55.8 %	104.24 ± (9.55)	105.32 ± (9.92)	52.9%
	F_6 *	103.25 ± (5.75)	96.51 ± (5.92)	86.8 %	103.25 ± (5.75)	103.39 ± (5.55)	51.5%
	F_7 *	90.16 ± (4.42)	88.17 ± (3.38)	69.2 %	90.16 ± (4.42)	91.21 ± (5.01)	48.5%
	t_8 *	22.64 ± (8.76)	36.70 ± (4.27)	92.6 %	22.64 ± (8.76)	24.20 ± (10.44)	47.1%
	t_9 *†‡	0.53 ± (0.05)	0.09 ± (0.02)	97.1 %	0.53 ± (0.05)	0.56 ± (0.06)	69.1%
	t_{10} *	77.06 ± (6.57)	63.94 ± (4.20)	94.1 %	77.06 ± (6.57)	76.13 ± (5.77)	57.4%
	t_{11} *‡	52.13 ± (6.26)	48.17 ± (4.11)	76.5 %	53.13 ± (6.26)	50.72 ± (5.04)	68.2%

	I_5 *	6.07 ± (1.61)	5.47 ± (0.56)	68.3 %	6.07 ± (1.61)	6.43 ± (1.67)	47.1%
	I_6 *†	88.91 ± (11.39)	6.69 ± (3.59)	100 %	88.91 ± (11.39)	90.61 ± (10.58)	47.1%
	TI_V *†	94.98 ± (11.33)	12.28 ± (3.60)	100 %	94.98 ± (11.33)	97.11 ± (10.56)	50.0%
	LR *†‡	0.01 ± (0.00)	0.04 ± (0.01)	98.5 %	0.01 ± (0.004)	0.012 ± (0.007)	68.8%
	UR *	0.02 ± (0.01)	0.03 ± (0.01)	76.5 %	0.02 ± (0.01)	0.02 ± (0.01)	44.1%
	BI_V *†	46.37 ± (6.15)	5.17 ± (1.99)	98.5 %	46.37 ± (6.15)	48.27 ± (5.12)	47.1%
	PI_V *†	48.71 ± (7.76)	7.20 ± (2.43)	100 %	48.71 ± (7.76)	48.93 ± (9.09)	52.9%
Impulse Rates	CI_1 *	0.26 ± (0.06)	0.51 ± (0.32)	82.4 %	0.26 ± (0.06)	0.27 ± (0.10)	48.5%
	CI_2	0.89 ± (0.36)	0.91 ± (1.03)	57.4 %	0.80 ± (0.36)	0.92 ± (0.37)	49.7%
	CI_3 *	1.66 ± (0.22)	2.39 ± (4.76)	63.2 %	0.66 ± (0.22)	0.75 ± (0.24)	47.1%
	CI_4 *†	2.73 ± (1.18)	0.90 ± (0.37)	100 %	2.73 ± (1.18)	2.72 ± (1.37)	51.5%
Stance time	t_1 *†	1.13 ± (0.12)	0.18 ± (0.05)	100 %	1.13 ± (0.12)	1.15 ± (0.12)	44.1%
The temperature of the residual limb	T_A	26.42 ± (1.45)	25.81 ± (1.33)	59.6%	-	-	-
	T_P	26.19 ± (1.40)	25.61 ± (1.35)	59.6%	-	-	-
	T_L	26.01 ± (1.49)	25.40 ± (1.34)	61.7%	-	-	-
	CV_{T_A} *	0.40 ± (0.06)	0.46 ± (0.06)	74.5%	-	-	-
	CV_{T_P} *	0.44 ± (0.04)	0.48 ± (0.04)	73.8%	-	-	-
	CV_{T_L} *	0.43 ± (0.06)	0.49 ± (0.03)	76.0%	-	-	-
	CV_T *	0.007 ± (0.005)	0.011 ± (0.005)	70.1%	-	-	-
	CA_A	2951.3 ± (866.6)	3001.9 ± (1288.8)	61.7%	-	-	-
	CA_P	3786.3 ± (2343.2)	2912.5 ± (1208.2)	51.1%	-	-	-
	CA_L	1045.8 ± (831.9)	897.8 ± (357.8)	61.7%	-	-	-
	CV_{CA_A}	0.65 ± (0.05)	0.67 ± (0.08)	51.1%	-	-	-
	CV_{CA_P}	0.63 ± (0.11)	0.64 ± (0.07)	55.3%	-	-	-
	CV_{CA_L} *	0.67 ± (0.13)	0.64 ± (0.13)	70.2%	-	-	-
	CV_{CA}	0.65 ± (0.37)	0.65 ± (0.26)	57.4%	-	-	-
	C_A *	11.17 ± (1.55)	12.18 ± (2.69)	74.5%	-	-	-
	C_P	8.92 ± (3.46)	8.86 ± (2.68)	48.9%	-	-	-
	C_L	7.41 ± (3.53)	7.16 ± (2.69)	48.9%	-	-	-
	CV_C *	0.43 ± (0.21)	0.34 ± (0.16)	69.0%	-	-	-

Table 4. Ground reaction force and stump temperature parameters.

Results are shown for each lower extremity for the alignment conditions evaluated. Percent repeatability indicates the percentage of comparisons that showed significant differences. * Parameter that showed significant within-subject differences for the prosthetic limb. † Parameters that showed significant differences between subjects for the prosthetic limb. ‡ Parameters that showed significant differences within-subjects for the intact limb.

The following parameters show the most significative differences within-subjects, and it was depicted in Figure 25. However, the following parameters additionally met the between-group comparison for 100% of the population. The braking impulse (I_3), propulsion impulse (I_4), the impulse of terminal stance and pre-swing (I_6), the total anteroposterior impulse (TI_{AP}), the total impulse of the vertical component (TI_V), braking impulse (BI_V), and

propulsion impulse (PI_V) were at least 88.0% higher during nominal alignments than misalignments for almost 99.0% of patients. Similarly, the duration of stance phases (t_1), braking phase duration (t_4), duration of the propulsion phase (t_5), time to propulsion peak (t_7), and the time to midstance valley (t_9) were at least 76.0% slower for above 95.0% of trials. The loading and unloading rates were at least 66.0% greater for all trials. Particularly, the loading (LR) was 70.0% higher in misaligned than nominal aligned prosthetic limb for at least 98.5% of trials.

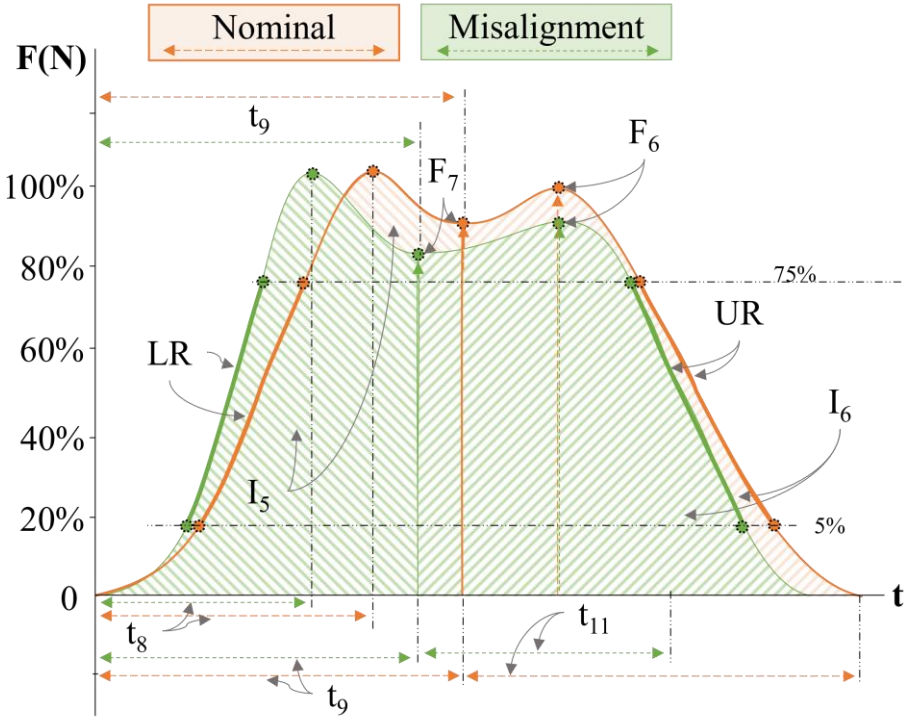

(a). Vertical component.

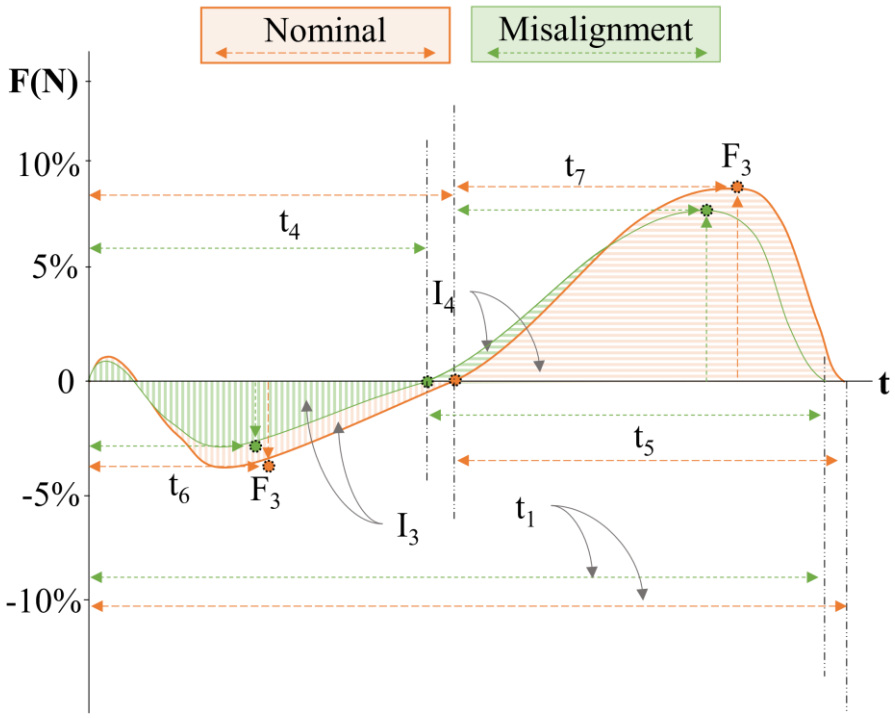

(b). Anterior-posterior component.

Figure 25. Average ground reaction force for the prosthetic limb for the amputees' group during nominal alignments and misalignments.

4.5. Discussion.

The hypothesis proposed in this work was focused on finding changes produced by the quality of the prosthetic alignment on the skin temperature of the residual limb, the ground reaction forces, and the symmetry of the gait pattern. In this regard, the ground reaction forces during walking of transfemoral amputees and the control group were recorded. Furthermore, thermal photographs of the residual limb were taken for the group of amputees. The information collected was processed and statistically analyzed to confirm our hypothesis. The findings suggested significant differences for the ground reaction forces of the prosthetic limb and the heat distribution on the stump's skin between nominal alignment and

misalignment of the prosthesis. On the other hand, the alignment did not affect the GRF symmetry between the intact and prosthetic limbs.

The ambient temperature showed a positive correlation with the stump's temperature and the increased perspiration reported by amputees. Earlier research has reported relations between the skin blood perfusion rate and changes in ambient temperature [229], [230]. Hence, the stump's skin heating and perspiration could be related to the thermo-regulation process of each subject, and not necessarily to the use of sockets.

Previous research has shown the effectiveness of thermography in the design and alignment of transtibial prostheses and to assess the socket-stump interface [98], [99], [218]. Our outcomes showed a slight increase in the mean temperature of the stump during nominal alignments compared to misalignments for near 60% of amputees. Despite this result, we hypothesize that the misalignments could have increased the number of local pressure points in the stump, which affected the microvasculature in the stump’s distal region and possibly long-term vasoconstriction. This produced stump regions cooler than others, increasing the dispersion of temperature during misalignment and resulting in higher temperature variation coefficients for nearly 76.0% of transfemoral amputees. The unbalance of the stump load line over the socket caused by the misalignments could have affected the pressure distribution at the stump-socket interface, affecting the blood capillaries, the blood supply distribution, and the temperature dissipation. The local pressure or friction increase could induce ulcers caused by ischemia, which could affect the amputees' compliance to the prosthesis.

Our socket design has two weight-bearing zones: one over the ischial notch region and the other on the scarp triangle. Figure 23(a) shows a better temperature distribution over the ischial region during nominal alignment compared to Figure 23(b) which shows the hot spots

observed during prosthetic misalignment. Likewise, Figure 23(c) shows the nominal alignment produced a better temperature distribution on the scarp triangle contour compared to the thermal results for the misaligned prosthesis (Figure 23(d)). It is expected that the regions of the residual limb with larger contact with the socket walls have greater mechanical stress, friction, and localized pressure, affecting the microvasculature of the skin. For this reason, it is suggested that prosthetic misalignment did not affect the mean temperature of the stump, since the blood perfusion of the skin was focally disturbed, producing small hot spots that did not change the average temperature [231]. The non-generalization of the results for a greater number of amputees could be due to the amputee's metabolic characteristics, prosthesis' mechanical factors, and the blood perfusion of the residual limb; however, thermography can assist clinicians and prosthetists during the fitting and alignment of transfemoral prosthesis components.

The muscle tissue loss caused by the lower limb amputation induces an impulsive force decrease of the prosthetic limb in vertical and anteroposterior curves ($PI_V, TI_V, I_4, I_6, CI_4$) [182]. The prosthetic misalignment altered the force transfer to the ground on the prosthetic side; therefore, the impulsive force (F_6) decreased and the unloading rate increased. It is well known that amputees shift the center of mass towards the intact limb to achieve a more comfortable and stable gait [232]. Prosthetic misalignment increased this shifting to the contralateral side producing a shorter stance phase (t_1) in the prosthetic side compared to nominal alignment. As well as the instability of a misaligned prosthesis produced decreased braking forces and decreased temporal parameters during misalignments ($I_3, t_4, t_5, t_9, BI_V, LR$). Likewise, the single-support phase of the vertical ground reaction force curves of the intact limbs was flatter than on prosthetic limbs, which has been

associated with slow gait speed [233]. The GRF outcomes suggest that nominal alignment improves the stability of the amputee on the prosthetic side during the stance phase; therefore, the measurement of GRF parameters on the prosthetic side could help the prosthetist to identify the nominal alignment to increase the amputee's compliance to the prosthesis.

The symmetry indices of transfemoral amputees did not show significant improvements after nominally aligning the prosthesis, which can be explained by the gait compensations of amputees to adapt to alignment changes [171], [176], [234]. Therefore, symmetry might not be a proper indicator to assess the quality of the alignment.

Prosthetic misalignment induced a shift between the anatomical line of amputees and the load line of the prosthesis, causing the shifting of the amputee's center of mass. Amputees adopt gait compensation mechanisms to keep a suitable gait performance, however, our results proved that the analysis of the residual limb's GRF could be useful to detect prosthetic misalignments. The use of GRF parameters such as I_3, I_4, TI_{AP}, t_1, t_4, t_5, t_7, t_9, I_6, TI_V, LR, BI_V, PI_V, and CI_4 provides useful indicators to aid in the alignment procedure of transfemoral amputees. This finding helps to find computational models for classification or prosthetic alignment assessment.

The results found in this study could be limited by the number of patients, the use of a single type of socket and a prosthetic foot, the non-inclusion of liners or stockings for the stump, and the condition of walking barefoot. Future work should quantify the magnitude of misalignment to identify the individual and collective effects of flexion-extension, abduction-adduction, and internal-external rotations of the socket and prosthetic foot. Finally, automatic alignment procedures supported by computational models are necessary to improve the adaptation of the transfemoral amputee to the prosthesis.

4.6. Conclusion.

The stump temperature did not show a direct relationship with changes in prosthetic alignment and their variation may be related to different exogenous factors. The intersubject observations show that several parameters of the Ground Reaction Force (GRF) could be considered as descriptors of the dynamic prosthesis alignment procedure. This information is useful to propose computational models of the prosthetic alignment.

Chapter 5.

Evaluation of the prosthesis alignment effects on spatiotemporal, comfort, balance, and muscle activity information of transfemoral amputees during gait and standing

Contribution to Ph.D. research: This chapter helped in the fulfillment of the fourth objective of the thesis: "*To propose and evaluate a computational model based on the biomechanical variables recorded during the static and dynamic analysis of the transfemoral mechanical prostheses".* The analysis of the parameters recorded during the alignment procedure are discussed in in Chapter 4. and Chapter 5. This chapter statistically analyzed the effects of prosthetic alignment on standing and gait in transfemoral amputees to define the descriptors set of the static and dynamic alignment. During standing and walking, the statistical tests did not show significant differences between the alignment conditions for the amputee's balance, comfort, and muscle activity of the intact limb. The ground reaction force (GRF) during walking tests showed significant differences between alignment conditions. Therefore, this chapter proves that the prosthetic limb GRF is a descriptive variable of the

dynamic alignment procedure. Likewise, the chapter shows the unreliability of recorded parameters to propose a computational model for static alignment.

Refers to **Appendix CS** for more information on the comfort survey.

Title of research paper: Evaluation of the prosthesis alignment effects on spatiotemporal, comfort, balance, and muscle activity information of transfemoral amputees during gait and standing.

Published in: (Not published yet)

Impact factor: NA

Cited as: Andres M. Cárdenas, Juliana Uribe, Alher M. Hernández, Jesús A. Plata, "Evaluation of the prosthesis alignment effects on spatiotemporal, comfort, balance, and muscle activity information of transfemoral amputees during gait and standing.,", pp. 1–10.

DOI: NA

5.1 Abstract.

Background: Lower limb prosthetic alignment is a procedure mostly subjective, and a misaligned prosthesis induces gait deviations and long-term joint diseases. The prosthetic misalignment effects on muscular activity, comfort, kinematics, and kinetics must be studied.

Research objective: To identify the effect of prosthetic misalignment in muscular activity, comfort, kinematics, and kinetics during the standing and walking of transfemoral amputees.

Methods: The effect of misalignment and nominal alignment was evaluated in sixteen transfemoral amputees. The optimal alignment made by the prosthetist was named nominal alignment. Misalignments included random variations in the flexion-extension, abduction-adduction, and internal-external rotation of the prosthetic socket and foot. The ground reaction force, electromyography, spatiotemporal parameters, and comfort were analyzed for each alignment condition. The statistical analysis included Friedman, Kruskal-Wallis, and multiple tests. The study included a control group of fifteen healthy volunteers for comparing results.

Results: Misalignments and nominal alignments did not produce significant differences on the sound limb of the spatiotemporal parameters. The stance phase in the prosthetic side for amputees wearing a misaligned prosthesis was 80.0% faster than nominally aligned prosthesis ($P<0.05$). The nominal alignment and prosthetic misalignment during gait trials showed significant differences for the tibialis anterior and rectus femoris in the mean frequency and median frequency parameters ($P=0.001$). During standing, significant differences were observed in the total power parameter of the tibialis anterior ($P<0.01$). Statistically significant differences between misalignments and nominal alignments based on

a comfort survey were not found in the standing and walking test. The ground reaction force was not different between nominal alignments and misalignments during standing. The prosthetic gait of the transfemoral amputees was faster, more unstable, and fatiguing than the normal gait of the control group.

Significance: The results of this study allow to identify the most informative parameters for prosthetists to evaluate the optimal alignment of transfemoral prostheses.

5.2 Introduction.

The prosthetic alignment is an iterative procedure to provide static balance and dynamic function to amputees by following the biomechanical characteristics of amputees and a gait analysis. Continuous communication between the amputee and the prosthetist, the attitude of the amputee, and the prosthetist knowledge in the alignment procedure are decisive factors to ensure the success of prosthetic alignment; therefore, prosthetic alignment is mainly a subjective judgment.

A poorly performed prosthetic alignment leads to prosthetic gait deviations, which produce secondary musculoskeletal disorders [214]. Gait deviations are related to perturbations of plantar foot pressures [156], step length asymmetries [157], changes of the stump pressure [158], [166], standing balance deviations [159], perturbations of spatiotemporal parameters [160], [161], and increased energy consumption [36]. Additionally, misalignment increases user dissatisfaction [162] and results in continuous visitations to prosthetics centers for prosthesis adjustments [16, p. 2].

The procedures to analyze prosthetic gait have been described in diverse articles. Sagawa et. al. [235] and Soares et. al. on [236] identified the parameters most commonly registered for prosthetic gait analysis. Authors in [164], [165] present the influence of rotational and translational movements of the transtibial prosthesis during the alignment procedure. Factors such as spatiotemporal parameters, muscle activity, satisfaction, falls, among others, were highlighted as elements for the evaluation of alignment and prosthetic adaptation of transtibial amputees.

Previous research has proven that movements of the foot in the sagittal plane produces changes in both horizontal and vertical ground reaction force (GRF) for transtibial amputees [200]. As well as variations of foot dorsiflexion and plantarflexion alignment increase the GRF, affecting the normal movement of the knee during walking and increasing external loads on knee ligaments [180]. Anterior-posterior translations of a prosthetic foot in transfemoral amputees result in an increase of the hip extension moment during the early-stance phase [167]. Perturbations in the foot alignment in varus-valgus and external rotations produce changes in the mediolateral component of GRF for transtibial amputees [189]. In a within-subject analysis, Zhang et al. [217] found that misalignment has an effect on moments at hip and knee of the intact limb in transfemoral amputees.

Internal foot rotations of transtibial prosthesis [176], [184], [191] and socket abduction-adduction and flexion-extension [186] produced a significant reduction in comfort; however, a deeper analysis of volunteers' satisfaction was not performed.

Flexion and extension perturbations of the socket alignment and foot adduction variations. [33], [179] produced a displacement of the lateral center of pressure of transtibial amputees.

The stance phase duration and single support duration in intact limbs for internal/external foot rotations of transtibial amputees [178], [184]. Likewise, excessive external rotations produced changes in the stance time, swing time, and step length [191].

The use of surface electromyography (sEMG) to assess the prosthetic alignment in transtibial prosthesis was proposed in [177], [180]. Mainly results showed that flexion-extension of the socket of transtibial amputees produce 50% muscle force increasing on hamstring and 20% in *rectus femoris* and *vasti* for transtibial amputees

Previous studies have recognized the effects of prosthetic alignment in gait biomechanics, mainly in transtibial amputees. The study of the prosthetic alignment in transfemoral amputees remains incomplete. Likewise, the knowledge of the effects of misalignment and nominal alignment of transfemoral prostheses is also uncertain. Therefore, new quantitative strategies for helping prosthetists during prosthetic alignment are needed.

This study aims to analyze the standing and gait of transfemoral amputees to identify the effect of the nominal and misalignments of the prosthesis in the spatiotemporal, electromyographic, ground reaction force, and comfort parameters. This is a complementary work of [237]. A progressive study of prosthetic alignment will allow the identification of useful descriptors to quantitatively assess the prosthetic alignment procedure and propose novel strategies for prosthetist assistance.

5.3 Methods.

The next section explains the methods, tools, and statistical strategies used to assess the alignment of transfemoral amputees.

5.3.1. Subjects and experimental equipment.

The Ethics Committee of the Institute of Medical Research of the Universidad de Antioquia (Medellín, Colombia) approved this research study. The inclusion criteria of amputees were (1) unilateral transfemoral amputees, (2) a functional level higher than 2 [14], and the control group included (3) ages over 18 years old, and (4) not having any other disease. Table 3 details the information of subjects. The Mahavir Kmina Artificial Limb Center in Medellín, Colombia, assembled all prostheses. Prosthetic devices included an ischial containment socket, a suction suspension system, a ReMotion prosthetic knee (D-Rev V3, USA), and a Jaipur foot (BMVSS, Jaipur, India). Subjects did not use any interface like socks or liners.

The kinetics and spatiotemporal data were recorded with a force platform P6000 and the Motion Capture System manufactured by BTS bioengineering, Italy. The six-channel electromyography system MOBI was used to report activity muscle (TMSI, Holland). A Spanish adaptation of the Prosthesis Evaluation Questionnaire (PEQ) was used to measure amputee comfort [42], [43]. The Smart Clinic and Smart Analyzer software (BTS Bioengineering, Italy). The Portilab 2 software (TMS International, The Netherlands) was used to measure electromyography signals. GeoGebra (International Geogebra Institute, Austria) was used to calculate the alignment angles. Matlab (MathWorks, USA) and Statgraphics Centurion (Statgraphics Tech., USA) were used to process and analyze the signals.

5.3.2. Experimental protocol.

The procedure explained here includes the recording of the parameters during standing, thus extending the Experimental protocol explained in the chapter Chapter 4 The Davis protocol [238] was used for the location of reflective markers on the body. The rectus femoris, biceps femoris, medial gastrocnemius, and tibialis anterior muscles were measured to estimate the muscular activity of the lower limb. The temperature reference was recorded at the beginning of gait trials by using thermal photographs from the anterior, posterior, and lateral views of the stump. The alignment testing protocol followed the following structure:

(1). Alignment procedure. The socket and foot angle were randomly changed (Figure 22). The alignment variations included socket rotations in flexion-extension (-6.0° to 7.0°), adduction-abduction (-8.0° to 6.0°), and internal-external rotation (-18.0° to 28.0°). The prosthetic foot included dorsi-plantar flexion (-7.0° to 6.0°), eversion-inversion (-4.0° to 6.0°), and internal-external rotation (-13.0° to 11.0°). The alignment variation was blind for the patients and the prosthetist.

(2). Training stage. The subjects walked for ten minutes on a ten meters hallway using a self-selected walking speed. During this time, the amputee was adapted to the new alignment condition.

(3). The recording of volunteers' standing. The volunteer was positioned over the force platform and the ground reaction force was recorded. The electromyography of the sound limb in amputees and the lateral preference in the control group were recorded.

(4). Walking tests. The volunteer walked for five minutes. Three gait cycles were captured. The electromyography of the sound limb of amputees and the lateral preference for the control group, the motion capture of the volunteers' walking, and the GRF for both lower limbs were recorded.

(5). Resting. The amputee rested for twenty minutes without prosthesis. It is expected that the blood flow of the residual limb will return to normal. During resting time, the amputees evaluated their walking comfort using the prosthesis.

This procedure was repeated five times. In one trial, randomly chosen, the prosthetist performs the optimal alignment, named the nominal alignment. The remaining four repetitions were termed misalignments. The control group did not perform steps (4) and (5).

5.3.3. Gait assessment parameters.

This chapter shows the spatiotemporal, muscle activity, comfort, and ground reaction force parameters used in this research to assess the effects of misalignment in transfemoral amputees.

5.3.3.1. Spatiotemporal parameters.

Smart Clinic software (BTS Bioengineering, Italy) analyzes the data from the motion capture system and produced a clinical reporting the following temporal and kinematics parameters: stride time (sec), stance time (sec), and swing time (sec), mean gait velocity (m/s), cadence (steps/min), the stance phase (%), swing phase (%), single support phase (%), double support phase (%), stride length (m), step length (m), step width (m), and the Gait Deviation Index [239].

5.3.3.2. Muscular activity.

The surface electromyography (sEMG) of the *rectus femoris*, *biceps femoris*, *tibial anterior*, and *gastrocnemius medialis* of the sound limb was used to estimate the muscular activity. Electromyography was not normalized to avoid prolonging the duration of the alignment trials. Therefore, a frequency analysis of the electromyographic signals was performed. To remove the Power Line Interference (PLI) caused by the electromagnetic noise [240], a notch filter was designed. The filter included the 60 Hz frequency and seven harmonics (120 Hz, 180 Hz, 240 Hz, 300 Hz, 360 Hz, and 420 Hz) and 60 dB Notch attenuation.

The baseline wander is caused by perspiration, body movements, and poor electrode contact. The spectral content is low frequency, typically below 2 Hz [241]–[243]; therefore, a high-pass infinite impulse response (IIR) filter of twenty order and 2 Hz cut frequency was designed to remove baseline noise. The significant power spectrum of EMG signals ranges is about 10 Hz and 500 Hz [244], [245], therefore, a twenty-order pass band IIR filter was applied to the sEMG signals. Finally, the signals were full-wave rectified, smoothed and the DC offset was removed. The root-mean-square [246] envelopes with twenty samples sliding window length were used for the smoothing.

Time and frequency domain techniques were used for the sEMG feature extraction [247]. Temporal parameters such as the root mean square (eq. 5.1) and mean absolute value (eq. 5.2) are indices related to the fatigue, the force exerted, and contraction force of muscles [248], [249].

$$RMS = \sqrt{\frac{1}{N}\sum_{i=1}^{N} x[n]^2} \tag{5.1}$$

$$MAV = \frac{1}{N}\sum_{n=1}^{N} x[n] \tag{5.2}$$

, N is the signal length and $x[n]$ is the sEMG sampled signal.

Variations in muscle force cause changes of frequential content of the sEMG; therefore, spectral information was extracted from signals [247]. The muscle fatigue presence is commonly related to a downward shift of the sEMG frequency spectrum. Hence, the frequency at which the spectrum is divided into two regions with equal amplitude was found (eq. 5.3). The average frequency was found by calculating the mean frequency of the power spectral density estimate (eq. 5.4). The total power spectrum for frequencies between 10 Hz to 500 Hz (eq. 5.5).

$$MDF = \frac{1}{2}\sum_{j=1}^{N} P_j \tag{5.3}$$

$$MNF = \sum_{j=1}^{N} f_j P_j \Big/ \sum_{j=1}^{N} P_j \tag{5.4}$$

$$TTP = \sum_{j=1}^{N} P_j \tag{5.5}$$

, N is the signal length, P_j is the power spectral density for bin j, and f_j is the frequency of the spectrum at frequency bin j.

Prosthetic alignment involves fitting the prosthetic load lines and the anatomical lines of the amputee; therefore, any decompensation could produce a greater load for the residual limb or the sound limb [24]. The muscular fatigue of the sound limb is then a fact that can occur. It was hypothesized that prosthetic misalignment produces fatigue in the sound limb muscles; therefore, there should see a shift of the frequency spectrum towards the low frequencies. Hence, the high-low frequencies ratio (eq. 5.6) could provide information about the alignment quality [55], [250]. The high-frequency bands for the lower limb muscles are between 105 Hz and 220 Hz in consideration of the results observed in [74], [251]–[253] for biceps femoris, rectus femoris, tibialis anterior, gastrocnemius, and vastus muscles. The low-frequency band used was 25 Hz to 60 Hz, as suggested [254]–[257] considering motor unit synchronization in beta and low gamma bands.

$$LHR = \sum_{j=LHC}^{UHC} P_j \Big/ \sum_{j=LLC}^{ULC} P_j \tag{5.6}$$

, LHC and UHC are the lower and upper cutoff frequencies of the high-frequency band.

5.3.3.3. Amputee's comfort assessment.

A translation and adaptation of the Prosthesis Evaluation Questionnaire (PEQ) survey was used [42], [43]. Seventeen questions focused on identifying information about the alignment trials, as it is shown in the following:

Group 1. Ask for the amputees' motivation: physical exhaustion and motivation of the amputee. Questions: (1). Rate how physically exhausted you are now. (2). Rate how motivated you are to take this survey.

Group 2. Ask for the prosthetic fit: the mechanical adjustment of the prosthesis. Questions: (3). During the last trial, rate the fitting of your prosthesis. (4). During the last trial, rate your comfort while standing when using your prosthesis. (5). During the last test, rate how often you felt off balance while using your prosthesis. (6). During the last test, rate how much energy it took to use your prosthesis for as long as you needed it (making him feel tired).

Group 3. Ask for the pain level: the pain of residual limb caused by misalignments. Questions: (7). During the last test, rate the feel pressure or heating on your stump. (8). If you had any pain in your stump during the last test, rate how intense it was on average. (9). During the last test, how bothersome was the pain in your stump? (10). Did you feel pain in your sound limb during the last test, how painful was it? (11). During the last test, how bothersome was the pain in your sound limb? (12). During the last test, had you felt back pain, how painful was it? (13). During the last test, how bothersome was your back pain? bothersome was your back pain?

Group 4. Ask for the frustration: social and emotional aspects of prosthetic use. Question: (14). During the last test, estimate how often you felt frustrated with your prosthesis.

Group 5. Ask for the walking skill: the effect of misalignment on the ability to walk. Question: (15). During the last test, rate your ability to walk using your prosthesis.

Group 6. Ask for the satisfaction level: satisfaction of the amputee with the prosthesis. Questions: (16). During the last test, rate how satisfied you were with the prosthesis. (17). During the last test, rate how satisfied you have been with how you are walking.

Survey responses were averaged according to each group and hypothesis tests were applied to find significant differences between nominal alignments and misalignments.

5.3.3.4. Ground Reaction Force.

The parameters of the ground reaction force (GRF) during gait trials were calculated according to Methods in Chapter 4 The ground reaction force parameters during the standing to assess the static alignment are presented in Figure 26. The magnitude of GRF components F_x, F_y, and F_z were normalized to the body weight. The cartesian coordinates of the GRF vector were recorded (P_x, P_y, and P_z). The variability of resultant force and position parameters was calculated using their standard deviation and the mean ratio; therefore, the variation coefficients were named as CV_F and CV_P, respectively. The spanned area (A) by the force vector was calculated while the volunteer was standing.

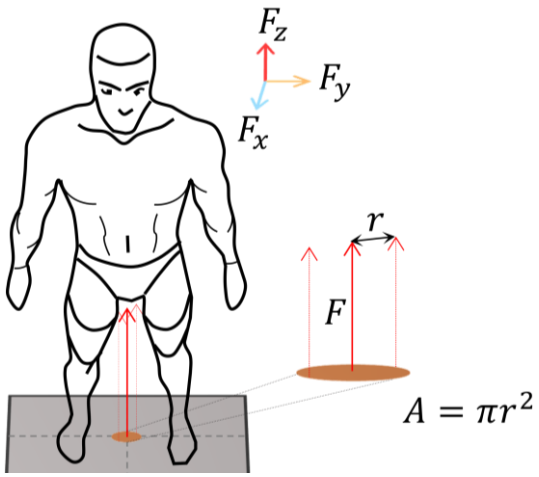

Figure 26. Ground reaction force during the standing.

5.3.4. Statistical analysis.

The Kurtosis-bias analysis and Kolmogorov-Smirnov tests confirmed the normal data distribution. The Friedman [258] and Kruskal-Wallis [227] non-parametric statistical tests were used to find statistically significant differences between groups with a statistical significance of $P<0.05$. Furthermore, multiple comparison tests using the Bonferroni method [228] were used. The statistical analysis included between-subjects and within-subjects.

5.4. Results.

This chapter summarizes the statistical analysis of the recorded parameters for volunteers during walking and standing.

5.4.1. Spatiotemporal parameters.

Spatiotemporal data were not recorded during the volunteers' standing. The statistical evaluation of the parameters is presented from different approaches:

5.4.1.1. Comparison between control group vs amputees' group.

(1). Between the control group and the amputees: statistical tests did not show significant differences for the stance phase and swing phase between the control group and transfemoral amputees; however, the stance phase was slightly higher in amputees than control and the opposite for the swing phase. The remaining spatiotemporal parameters were statistically different between groups ($P<0.03$). The single support phase was 3.1% higher in amputees than in the control group. The double support phase was 48.2% higher in the control group.

The amputees' gait was 12.5% faster than in the control group, as was the cadence (15.3%). The stride length was 22.3% longer in the non-amputees, as well as the step length (10.0%) and the step width (64.1%). The gait deviation index was 22.7% higher in the amputees than in the control group.

5.4.1.2. Comparison between nominal alignment and misalignments.

Between nominal alignments and misalignments: parameters of the prosthetic limb and the sound limb were averaged, and values were compared between the nominal alignments and the misalignments. There were no statistically significant differences between nominal alignments and misalignments for the spatiotemporal parameters.

The results for the intact and prosthetic limbs were analyzed separately during nominal alignments and misalignments. The sound limb did not show significant differences during nominal alignments and misalignments. Prosthetic limb did show a difference in the mean velocity (m/s) ($P < 0.05$) between alignment conditions. The stance phase in the prosthetic side for amputees wearing a misaligned prosthesis was 80.0% faster than nominally aligned prosthesis ($P<0.05$). Although not significant, the cadence was slightly higher during the misalignments trials. No more significant differences were observed.

5.4.2. Muscular activity.

The frequency content of the electromyography was analyzed to find the signal power distribution in the frequency spectrum. Changes in the power density of electromyography is associated with muscle fatigue [259]; therefore, the frequency analysis was used to identify the effect of prosthetic alignment on the muscle fatigue. The temporal and frequency

parameters of the electromyography were compared to find significant differences between the control and amputees' groups during walking trials and standing. In this same line, the amputees' group included comparison between nominal alignments and misalignments.

5.4.2.1. Results for the control group and the amputee group.

During the walking tests, the control and amputee groups showed statistically significant differences ($p < 0.05$) in almost all the parameters calculated for the tibial anterior muscle, excepting the total spectrum (TTP). The temporal and frequency parameters of the tibialis anterior were greater for the amputee's group than the control group. Values of MNF, MDF, LHR were higher in transfemoral amputees than the control group. The standing tests showed significant differences between the control group and amputees on the rectus femoris for the RMS, MAV, MDF, MNF, TTP, and LHR parameters ($p < 0.01$). Furthermore, these parameters were higher in the amputee group than compared to the control group.

5.4.2.2. Results for nominal alignment and misalignments.

Comparison between nominal alignment and prosthetic misalignment in transfemoral amputees during gait trials showed statistically significant differences for the tibialis anterior and rectus femoris in the *MDF* and *LHR* parameters ($P=0.001$), respectively; however, our results were achieved for 69.0% of alignment trials. Although the results were replicated in a large portion of the population, they were not conclusive for the generality of amputees. During standing, significant differences were only observed in the tibialis anterior *TTP* parameter ($P<0.01$).

5.4.3. Comfort assessment.

No comfort assessment was made to the control group, so no comparative results were obtained between amputee and non-amputee volunteers. Hypothesis tests did not show statistically significant differences between misalignments and nominal alignments based on the questions about motivation, prosthetic fit, residual limb pain, frustration, walking skills, and level of satisfaction; however, some slight differences could be observed in Figure 27. The motivation level was always good, even though the alignment trials took more than six hours. Although not significant, the boxplot graph shows a slight decrease in the prosthetic fitting sensation during misalignments. The amputees did not advertise pain caused by the alignment variations. The level of frustration during nominal alignment was more variable than misalignments. The ability to walk decreased slightly during misalignments. The satisfaction level of the prosthesis was more variable during misalignments than nominal alignments.

In sixteen trials, amputees rated a misalignment with a level of satisfaction close to or higher than the nominal alignment score. Since the trials were blinded and randomized, this phenomenon could suggest that the nominal alignment perceived by the amputee is not necessarily the same as that suggested by the prosthetist. It is normal for this to occur, for example, when the prosthetist adjusts the prosthesis to correct gait deviations adopted by the amputee, which undoubtedly increases the feeling of discomfort even if the gait improves biomechanically.

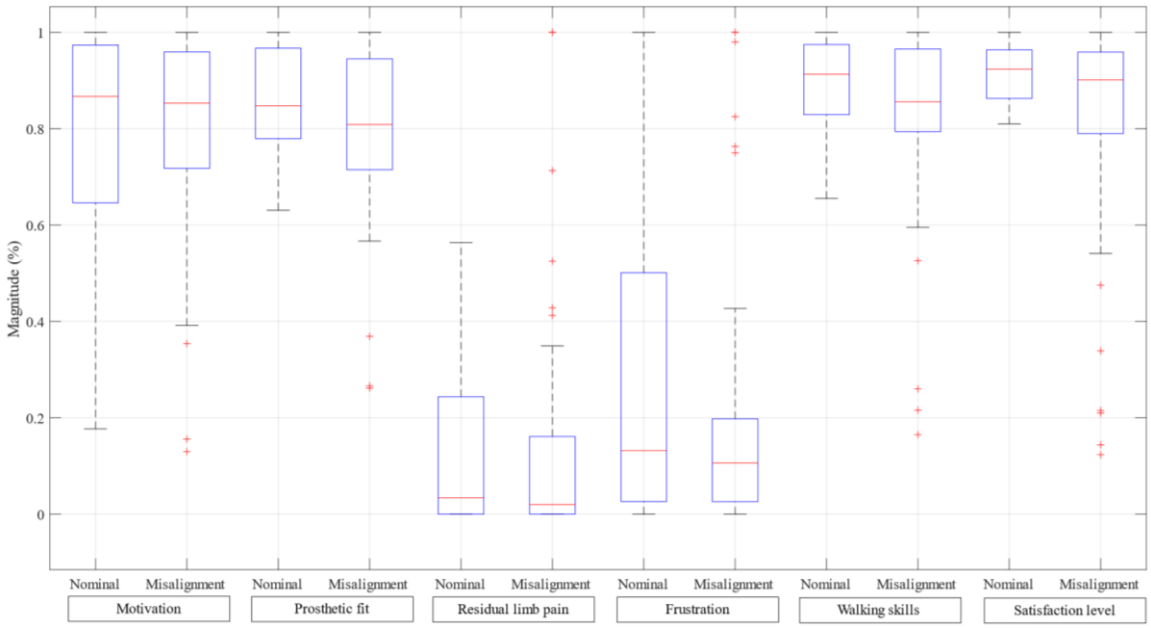

Figure 27. Boxplot of comfort assessment.

5.4.4. Ground Reaction Force GRF.

The difference between the ground reaction force of the control and amputee groups during standing and gait trials was inspected. Additionally, the GRF outcomes of transfemoral amputees were analyzed to find the effect of misalignments and nominal alignments.

5.4.4.1. Comparison of GRF between control and amputee groups.

The control and amputees groups did show statistically significant differences (P<0.01) during gait trials in most of the GRF parameters, excepting F_5, F_6, F_7, t_8, t_{10}, t_{11}, I_5, and UR.

5.4.4.2. Comparison of GRF between nominal alignments and misalignments.

The comparison between the control and amputee groups during standing showed statistically significant differences (P<0.01) for the variation coefficient of the total force

(CV_F) and position (CV_P). The GRF parameters during gait showed significant differences between nominal alignment and prosthetic misalignment; those results were presented in 0 of Chapter 4. The evaluation of the alignment effects during standing did not show statistically significant differences between nominal alignments and misalignments for all the parameters recorded.

5.5. Discussion.

This article aimed to evaluate the effect of prosthetic misalignment on the gait biomechanics of transfemoral amputees. It was hypothesized that perturbations of the nominal alignment of a transfemoral prosthesis would cause significant changes in the spatiotemporal parameters, muscular activity, comfort, and ground reaction force during standing trials. The information collected was processed and statistically analyzed to confirm our hypothesis.

The results for spatiotemporal data were different between the prosthetic gait of transfemoral amputees and the normal gait. The gait speed was faster and the cadence greater on amputees than the control group, which produced step and stride lengths shorter in amputees. A smaller step width in amputees was observed; therefore, this could be related to an imbalance feeling [260], [261]. Effects on the step length of the prosthetic limb for transtibial amputees have been reported during changes in prosthetic alignment [167]. Significant changes in the stance phase duration and single support duration in intact limbs during foot internal/external rotations were divulged in [178], [184], and plantarflexion evidenced a bilateral symmetry of the step length [157]. Likewise, authors in [191] found that an excessive external rotation produced variations in stance and swing times and step length. However, we did not find

enough evidence on the effects of misalignment on the spatiotemporal parameters of transfemoral amputees, other than an increase in the stance phase and of the prosthetic limb and mean gait speed during misalignments. Amputees might have found strategies to adapt to a new alignment condition as suggested by [167], [172], [185], however, the change in the stance phase demonstrates a certain degree of mistrust in the prosthesis while it is misaligned. Further research is needed to find the effect of prosthetic alignment on spatiotemporal data.

The prosthetic alignment shifts the load lines of the amputee on the prosthesis; therefore, it is hypothesized that a misaligned prosthesis produces a greater muscle load on the amputees' intact limb than a nominally aligned prosthesis and the control group. For this reason, the sEMG of the intact limb in amputees was compared between suitable and unfitting alignment conditions and with the control group. The RMS value of the sEMG increased in constant-force and fatiguing tasks [248]; therefore, results found in our research could suggest that prosthetic gait is more fatiguing than normal gait. The increasing amplitude of the sEMG signal-induced growth of the MAV in the amputee's group. This event has turned out to be associated with fatigue on the muscle fiber level MAV [262]. Likewise, the MNF and MDF increase in the amputees' group could suggest an increase of the muscle force or load [263]. The sEMG results showed a greater muscle load in the prosthetic limb of the amputees than in the control group. The muscular activity of the sound limb of transfemoral amputees was not affected by prosthetic aligned conditions during walking and standing trials, so our hypothesis could not be confirmed.

Comfort is usually used as a criterion to assess the amputee’s prosthetic adaptation [264], under this consideration, it was hypothesized that prosthetic misalignment would produce negative effects on the amputee’s comfort. Previously, the effect of prosthetic alignment on

transtibial amputees' comfort was studied on [265], finding statistically significant differences in the amputees' comfort between walking trials using prosthesis nominal aligned and misaligned; however, researchers suggested including other prosthetic assessment methods because the comfort had reduced reliability. Our investigation did not reveal illuminating information in the amputee's comfort variations by using misaligned or nominally aligned prostheses during walking trials and standing. The slight influence of prosthetic misalignment on amputee's comfort could have some causes. The prosthesis used during the experiments was donated to each amputee and they knew it. This might explain why amputees did not criticize the prosthesis and even it could influence the comfort assessment, even though they were advised to express their opinion. The alignment trials were lengthy; therefore, this could influence the attention of volunteers during survey answering.

The ground reaction force (GRF) was recorded in amputees and the control group. It was hypothesized that misalignment or nominal alignment produced changes in GRF during standing and gait trials. The standing trials showed high variability in the force vector magnitude and the position of the center of gravity, which could be an indicator of a less balanced posture in amputees than in the control group. This is reinforced by the small step width values seen in the spatiotemporal data. In the present research, no significant differences were observed between the two alignment conditions. Finally, according discussed in 4.5 of Chapter 4, there were multiple significant differences between the amputees and the control group. This was expected, because amputees feel less confident during gait [232]. The most significant effects of misalignment and nominal alignment were

observed in the prosthetic limb, particularly affecting the parameters I_3, I_4, TI_{AP}, t_1, t_4, t_5, t_7, t_9, I_6, TI_V, LR, BI_V, and PI_V on the prosthetic side.

Our results could be biased for the use of a single type of socket (ischial containment) and a prosthetic foot (Jaipur foot). The alignment tests were lengthy and strenuous for amputees, so it could have affected the comfort survey. To improve the generalization of our results, the diversity of prosthetic components should be greater. Future work should quantify the magnitude of misalignment to identify the individual and collective effects of flexion-extension, abduction-adduction, and internal-external rotations of the socket and prosthetic foot.

5.6. Conclusion.

In this research, the effects of prosthetic misalignment on the ground reaction force for the prosthetic limb were confirmed during walking trials; however, did not show differences during the standing. During prosthetic gait and standing the misalignment did not produce significant perturbations on the amputees' balance, comfort, and muscular activity of the sound limb. The strategies used by the amputee to adapt gait during misalignments were sufficient to keep the spatiotemporal parameters without significant modifications. The prosthetic gait of the transfemoral amputees was faster, more unstable, and fatiguing than the normal gait of the control group.

Chapter 6.

Computational protocol to assist the prosthetist during the alignment of transfemoral prosthesis

Contribution to Ph.D. research: This chapter fulfills objectives four and five of the thesis: "*To propose and evaluate a computational model based on the biomechanical variables recorded during the static and dynamic analysis of the transfemoral mechanical prostheses*" and "*To propose an alignment protocol to support the prosthetist during the static and dynamic alignment of transfemoral mechanical prostheses, based on the computational model*". This is the integrating chapter of the accumulated knowledge on the alignment procedure directly of the amputees, prosthetists, the dataset analysis, and from the literature review to propose a protocol for dynamic alignment of transfemoral mechanical prostheses.

The parameters recorded during static alignment were not statistically different between nominal alignment and prosthetic misalignment, so a computational model for static

alignment could not be described. However, during dynamic alignment, the prosthetic limb ground reaction force showed statistically significant differences between nominal alignment and misalignments. This allowed the identification of computational models to support prosthetic alignment.

This chapter shows the design and validation of a protocol for alignment of transfemoral mechanical prostheses supported by computational models.

During the study of the machine learning techniques, two articles were published (See **Appendix MLA** and **Appendix PKM**). The article related to this chapter is being reviewed for submission to an indexed journal.

Title of research paper: Gait parameters identification for the differentiation of neurodegenerative diseases using classifiers.

Published in: IEEE Xplore

Cited as: A. M. Cárdenas, C. Isaza, J. Uribe, and A. M. Hernadez, "Gait parameters identification for the differentiation of neurodegenerative diseases using classifiers," 2018 Global Medical Engineering Physics Exchanges/Pan American Health Care Exchanges (GMEPE/PAHCE), 2018, pp. 1-5, doi: 10.1109/GMEPE-PAHCE.2018.8400751.

DOI: 10.1109/GMEPE-PAHCE.2018.8400751

Title of research paper: Parametric Modeling of Kinetic-Kinematic Polycentric Mechanical Knee

Published in: Springer

Cited as: Cárdenas A.M., Uribe J., Hernández A.M. (2017) Parametric Modeling of Kinetic-Kinematic Polycentric Mechanical Knee. In: Torres I., Bustamante J., Sierra D. (eds) VII Latin American Congress on Biomedical Engineering CLAIB 2016, Bucaramanga, Santander, Colombia, October 26th -28th, 2016. IFMBE Proceedings, vol 60. Springer, Singapore. https://doi.org/10.1007/978-981-10-4086-3_150

DOI: https://doi.org/10.1007/978-981-10-4086-3_150

Title of research paper: 4. Computational protocol to assist the prosthetist during the alignment of transfemoral prosthesis.

Published in: Article in preparation

Cited as: A. M. Cárdenas, J. Uribe, A. M. Hernadez, and Jesús A. Plata " 4. Computational protocol to assist the prosthetist during the alignment of transfemoral prosthesis,", 2021, pp. 1-10

DOI: NA

6.1. Abstract.

Background: Dynamic alignment of transfemoral prostheses is a mostly subjective procedure. Prosthetic misalignments cause gait deviations and long-term illness. The literature does not show the use of computational models to support prosthetists during the alignment of transfemoral prostheses.

Research objective: To propose a novel prosthetic alignment protocol for transfemoral mechanical prostheses supported by computational models to help the prosthetist during dynamic prosthetic alignment.

Methods: The ethics committee of the University of Antioquia approved this study. Sixteen transfemoral amputees were recruited for the trials. Five alignment variations were evaluated, one nominal and four misalignments. The alignment variations consisted of simultaneous angulations of the socket and prosthetic foot in the coronal, sagittal, and transverse planes. Eleven parameters of the ground reaction force were recorded in the vertical and anteroposterior components. A Support Vector Machines model was implemented with a Gaussian kernel radial basis function for the classification between nominal alignment and misalignments. A Bayesian Regularization Neural Networks was implemented with 30 hidden layers to predict the magnitude and angle of the misalignments. The protocol for dynamic alignment of transfemoral prosthesis was confirmed in two transfemoral amputees. A junior and senior prosthetist evaluated the alignment protocol.

Results: The SVM accuracy to classify between nominal alignment and misalignment was 92.6%. The computational model incorrectly classified two misalignments as nominal alignments. The Bayesian Regularization Neural Network correctly retrieved 94.11% of the

dataset with an error of 0.51° for the socket and prosthetic foot alignment angles. The validation of the computational prosthetic alignment protocol was tested in two amputees. For the first amputee, the nominal alignment did not converge throughout the three iterations. For the second amputee, the computational prosthetic alignment protocol aided the prosthetists to achieve the nominal alignment in the second protocol iteration. The learning curve in the use of the protocol by the prosthetists could affect the non-convergence to the nominal alignment for the first amputee; however, prosthetists reported that the computational protocol helped them do a better job. The protocol convergence could be improved by the computational models retraining; however, the accuracy of angular adjustment is perhaps affecting the convergence of the nominal alignment. Therefore, further research should be focused on the development of more precise alignment tools.

Significance: The prosthetic alignment protocol is a computational tool that reduces the subjectivity of classical alignment procedures and decreases the probability of gait deviations and musculoskeletal diseases, improving the quality of life of amputees.

6.2. Introduction.

Prosthetic alignment is a procedure conducted during the adaptation of amputees to lower limb prostheses. The goal of the alignment procedure is to adjust the prosthetic load lines with the amputee's anatomical and biomechanical lines [16], to provide stability and movement functionality [41]. Alignment is typically performed in three stages: assembling and balancing the weight of the prosthesis (bench alignment), appropriately distributing the amputee's weight on the sound and prosthetic sides in the standing position (static alignment),

and finely adjusting the prosthesis during amputees' walking to avoid gait deviations (dynamic alignment) [150].

Alignment is a complex procedure that relies heavily on the process iteration and the amputee's feedback. Optimal prosthetic alignment is judged primarily by gait observations; therefore, the subjectivity of the procedure is highly dependent on the knowledge and skills of the prosthetist in the alignment procedures. A properly prosthetic fitting increases the adaptation of amputees to daily activities; however, prosthetic misalignments lead to amputees developing strategies to compensate for misalignment, which ends in gait deviations. An improperly performed alignment procedure could cause injuries in the musculoskeletal system and affect the amputee’s quality of life [214].

Technological devices such as biaxial tilt sensors [173], [198], [266], goniometers [33], [157], [181], comfort surveys, Europa™ system [267], and the posture device (L.A.S.A.R. [36]) are used as assistance tools during the alignment judgment. However, not all prosthetic adaptation centers have access to technical support to monitor the alignment, so computational modeling becomes a relevant strategy. especially when the efficiency of machine learning in biomechanics has already been proven [268]–[270]. Despite this, the computational models for the assistance of prosthetic alignment procedures have not been widely studied.

Few authors were found in the literature working in computational models to analyze prosthetic alignment. Luengas, et al. proposed a decision rules model to predict the center of pressure (COP) and the hip, knee, and ankle joint angles during variations of the prosthetic alignment in flexion-extension of transtibial prostheses during standing [271]. With the same purpose, Camargo, et al. in [31] used the Neural Networks of Generalized Regression

(GRNN) with 700 hidden layers, reaching a maximum error of 6.25% in the estimation of the COP and the hip, knee, and ankle joint angles.

The classification of the prosthetic gait of transtibial amputees using correctly aligned and misaligned prostheses was studied in [30]. The vertical (VF), horizontal (HF), and a combination of both components (VH) of the Ground Reaction Force (GRF) were used for training a Support Vector Machine (SVM) classifier. The linear, polynomial, and radial basis function (RBF) kernels were evaluated. The better inter-subject accuracy was achieved with an RBF kernel, getting 72.78% for VF, 85.56% for HF, and 88.89% for VH.

Luengas et al. in [32] and [272] presented the use of the Neural Networks (NN), Decision Trees (TD), and the SVM to classify the standing of transtibial amputees during changes in static alignment. The authors use 16 parameters associated with the center of pressure (COP) on the mediolateral and anteroposterior sides. The NN was trained with 16 inputs, one output (nominal or misaligned), and 10 hidden layers. The SVM was trained with a Gaussian kernel, and they used a DT type C4.5 for discrete values with noise. The results were highly satisfactory, achieving 96.22% classification accuracy for the NN and 100% in the case of SVM and DT.

Considering the lag in computational models for prosthetist assistance during prosthetic alignment procedure, particularly in transfemoral prostheses, this paper proposes a novel protocol for assisting prosthetists during the dynamic alignment of mechanical transfemoral prostheses. The alignment protocol is supported in a Vector Support Machines model with a Gaussian radial basis function to classify between nominal alignment and misalignment (classes) using eleven parameters of the vertical and anteroposterior components of the GRF (predictor variables) [237]. Additionally, a Bayesian Regularization Neural Networks

(BRNN) is trained to predict the magnitude and angle of misalignment of the socket and prosthetic foot (Inputs) from the registration of the vertical and anteroposterior components of the GRF (Targets). The following chapters develop the design and validation of the computational models and the novel prosthetic alignment protocol.

6.3. Methods.

6.3.1. Subjects, methods, and measurement devices for training models.

The Ethics Committee of the Institute of Medical Research of the Universidad de Antioquia (Medellín, Colombia) approved this research study.

The computational models were trained using a population of sixteen transfemoral amputees, two women, and fourteen men. The population was 35.4 ($\pm$11.1) years of average age, a weight of 65.8 ($\pm$10.3) kg, an average height of 166.7 ($\pm$7.7) cm, and a body mass index of 23.7 ($\pm$3.0). The prosthetic devices provided to volunteers were assembled by Mahavir Kmina Artificial Limb Center in Medellín, Colombia. A quadrilateral socket, prosthetic knee ReMotion (D-Rev V3, USA), and Jaipur foot (BMVSS, Jaipur, India) were used to assemble the prosthesis.

The prosthetic alignment procedure for modeling purposes followed three stages: (1) the socket angle was randomly changed between -18.0° to 28.0° in flexion-extension, adduction-abduction, and internal-external movements. Furthermore, the prosthetic foot alignments were ranged between -13.0° to 11.0° in dorsi-plantar flexion, eversion-inversion, and internal-external rotation. Alignment changes were recorded in real time with a goniometer. The alignment angle variation of the socket and foot were taken respect to the knee and the

shank, respectively. Furthermore, photographs of the prosthesis were taken in the anterior and sagittal view and the Geogebra software (International Geogebra Institute, Austria) was used to calculate the misalignment angles. The alignment variation limits were bounded to avoid falls due to loss of balance. (2) Amputee walked for fifteen minutes on a ten meters hallway using a self-selected walking speed. During the last five minutes, the Ground Reaction Force of the prosthetic limb was recorded. (3). The amputee rested for twenty minutes with the stump undressed.

The 1, 2, and 3 steps of the procedure were repeated five times. In one of the repetitions, the prosthetist performed the optimal alignment for the amputee, which was termed the nominal alignment. The remaining four repetitions were named misalignments.

The Ground Reaction Force (GRF) was recorded with the force platform P6000 (BTS Bioengineering, Italy) sampling to 120 Hz. Rules and a goniometer were used to measure the prosthetic misalignments. The Smart Clinic and Smart Analyzer software (BTS Bioengineering, Italy) was used to capture force signals. MATLAB (MathWorks, USA) was used to analyze the signals and training models. GeoGebra (Google) was used to digitally measure the prosthetic misalignments.

Three footprints of the prosthetic limb were chosen. The raw data of the vertical and anteroposterior GRF components were pre-processed in MATLAB. A total of 439 signals were filtered using a Butterworth second-order low pass filter with a cutoff frequency of 20 Hz to eliminate the electromagnetic noise of the GRF signals.

The following prosthetic limb ground reaction force showed statistically significant differences between nominal alignment and misalignments (see *The effect of prosthetic*

alignment on the stump's temperature and the ground reaction force. (**Chapter 4.**).): the braking force impulse (I_3), propulsion force impulse (I_4), total anteroposterior force impulse (TI_{AP}), duration of the stance phase (t_1), duration of the braking phase (t_4), duration of the propulsion phase (t_5), time to propulsion peak (t_7), time to midstance valley (t_9), the impulse of terminal stance and pre-swing (I_6), the total impulse of the vertical component (TI_V), the loading rate (LR), the braking (BI_V), and propulsion impulse (PI_V). The set of GRF parameters was selected for its effectiveness in the analysis of prosthetic alignment transfemoral [237] y transtibial [30], [31]. The parameters were calculated in MATLAB for each GRF component. The mean value of the GRF parameter was calculated using three samples for each alignment variation.

6.3.2. Validation procedure of the transfemoral prosthetic alignment protocol.

The validation of the alignment protocol was conducted according to the scheme presented in Figure 28. Protocol validation includes four sub-functions. The *SF1* subfunction describes the data collection and processing procedure. The *SF2* describes the process performed by the classification model and the *SF3* function describes the process of the computational regression model. Finally, the *SF4* describes the prosthetic alignment fitting performed by the prosthetist using the angles suggested by computational alignment protocol.

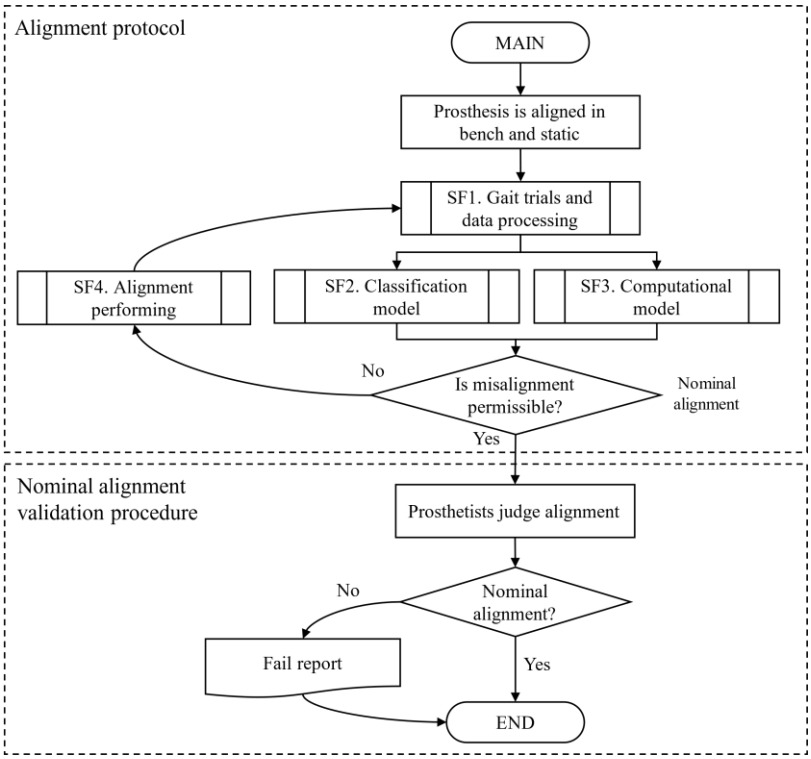

(a). Main algorithm of the prosthetic alignment procedure.

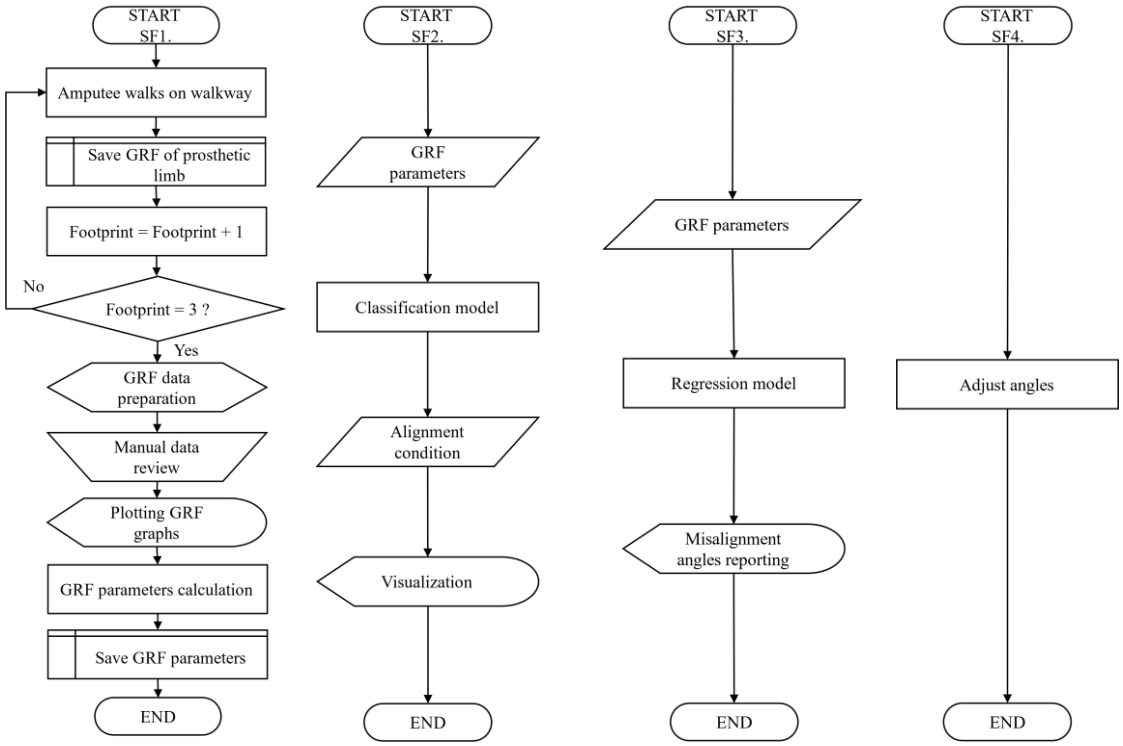

(a). Subfuntion SF1. (b). Subfuntion SF2. (c). Subfuntion SF3. (d). Subfuntion SF4.

Figure 28. Architecture to validate the prosthetic alignment protocol.

The computational alignment protocol is executed three times or until the smallest misalignment tolerance is reached. The minimum tolerance for misalignment was found from the precision of the prosthetist's alignment angulations and the computational models' accuracy. This error is produced by the bias between the angles suggested by the computational alignment protocol and the precision of the angles that could be adjusted on the adapter. The prosthetist's error in the alignment fitting was ± 1.5°. The accuracy error of the computational protocol was ± 0.5° according to the error histogram. Alignment angles less than ± 2.0° suggest that the alignment recorded is close to the nominal alignment; therefore, the alignment procedure is ended when all angles are less than ± 2.0°.

One junior and one senior prosthetist accompany the alignment protocol validation tests. At the testing start, the amputees walk wearing a prosthesis without dynamic alignment. The computational models assess the ground reaction force during the amputee's gait and estimate the recommended angles for nominally aligning the prosthesis. Prosthetists use a goniometer to apply the alignment angles recommended by the computational alignment protocol. The first iteration ends here.

In the second protocol iteration, the amputees walk again wearing the prosthesis aligned by the computational alignment protocol. The amputee walks again in the hallway and the Ground Reaction Force is measured. The junior and senior prosthetists separately evaluate the amputee's gait performance with a score between 1 to 10. The second iteration ends here. The computational alignment protocol analyzes the data and suggests a new adjustment of the alignment angles to achieve nominal alignment. If the alignment angles are within the error margin, the alignment is considered nominal, and the prosthetists are consulted for their

opinion of the alignment. If the prosthetists and the protocol agreed, the procedure is finished, otherwise, the prosthesis is adjusted with the new suggested angles.

The third iteration walking GRF outcomes are analyzed for the computational protocol. The computational protocol assesses gait and shows whether the prosthesis is nominally aligned. If the prosthetist and the computational protocol match in the gait assessment, the protocol is ended. If they do not agree, the protocol is stopped, and fail is informed. This failure shows that the protocol did not converge in the iterations performed, so a fourth iteration should be performed.

During all iterations, both prosthetists assess the gait of the amputees. At the end of the alignment protocol validation, a survey is applied to the prosthetists. The questions were the following: (1). Rate the amputee's gait from 1 to 10 with the alignment suggested by the model. (2). Regardless of the efficiency of this new protocol, do you consider that this type of initiative should continue to be developed? rate the importance from 1 to 10. (3). Did the alignment protocol allow you to do a better job? rate the importance from 1 to 10. (4). Did it take longer to do your job with this new protocol? how long was it (in minutes)? (5). What would you improve on the new alignment protocol?

The Mahavir Kmina Artificial Limb Center provides the prosthetist and the new prostheses for the volunteers participating in the study. Two transfemoral volunteers were recruited for two days to validate the protocol. The population characteristics were as follows: mean age of 37.0 ± 11.3 years, an average weight of 59.9 ± 1.6 kg, an average height of 166 ± 0.0 cm and a body mass index of 25.4 ± 0.6.

6.3.3. Computational models.

The alignment protocol for transfemoral prostheses involved finding two computational models. The Support Vector Machines (SVM) was used to classify the GRF parameters of amputees between gait using a prosthesis nominally aligned or misaligned. A second model using Neural Networks estimated the misalignment angle in the socket and foot from the GRF parameters during prosthetic misalignment.

The neural network (NN) simulates the human brain's behavior. The architecture of an artificial neural network with feedforward multilayer perceptron and backpropagation error uses multiple layers (g_i) to describe the neuron interconnection and a set of weights (w_i) to represent the interconnection strength between neurons (eq. 6.1). Each node uses an activation function (f); usually being the sigmoid function. Neural network learning is achieved when a cost function (eq. 6.2) is minimized. Parameter w denotes weights, b is the bias, N is the training examples, a is the activation output vector produced by each input x, and y is the target output.

$$y(\bar{X}) = f\left(\sum_{i}^{N} w_i g_i(\bar{X})\right) + B \tag{6.1}$$

$$C(w,b) = \frac{1}{2N}\sum\nolimits_{x} \|y(x) - a\|^2 \tag{6.2}$$

The Bayesian Regularization Neural Networks (BRNN) minimizes an objective function (eq. 6.3), considering a mean squared error function (eq. 6.4) and a weight attenuation function (eq. 6.5) to avoid overfitting. The α and β parameters are distribution control hyper-parameters. Value of w_i are the *ith* weight of neural network and m is the number of weights.

N is the total number of the input-output set for training; finally, the *ith* output is named as y_i.

$$F = \beta E_D + \alpha E_W y(\bar{X}) \tag{6.3}$$

$$E_D = \frac{1}{N}\sum_{i}^{N}(y_i - t_i)^2 = \frac{1}{N}\sum_{i}^{N} e_i^2 \tag{6.4}$$

$$E_W = \frac{1}{2}\sum_{i}^{m} w_i^2 \tag{6.5}$$

The weight initialization is randomly set. Iterations of the density function (eq. 2.13) update the weight values, in simple words, this equation describes the rate between likelihood multiplying prior and the evidence. M is the architecture of the neural network. $P(w|\alpha, M)$ is the prior knowledge of the weights. $P(D|w, \beta, M)$ is the likelihood function of the data occurrence given the weight w. $P(D|\alpha, \beta, M)$ is a normalization factor [133], [134].

$$P(w|D, \alpha, \beta, M) = \frac{P(D|w,\beta,M).P(w|\alpha,M)}{P(D|\alpha,\beta,M)} \tag{6.6}$$

The support vector machine (SVM) is a technique based on the statistical learning theory proposed by Cortes & Vapnik [135]. The purpose of SVM is to find a plane to separate a dataset into groups known a priori, maximizing the distance (margin) between the values closest to the plane, called support vectors; however, the groups' separation is becoming increasingly difficult when the dataset size increases; therefore, hyperplanes are used to represent an n-dimensional plane [137].

The SVM proposes that a dataset is linearly separable if there exists a pair w, b such that the inequality (eq. 6.7) is satisfied in (eq. 6.8). The solution is achieved when the objective

function $J(w) = 1/2\,\|w\|^2$ is minimized. Where the training dataset is the vector $x = [x_0, x_1, \dots, x_m]$, the bias is labeled as b, the categories as y_i and the weighted vector is w.

$$f(x) = w^T x + b \tag{6.7}$$

$$\begin{cases} (w \cdot x_i + b) \geq 1 & y_i = 1 \\ (w \cdot x_i + b) \leq -1, & y_i = -1 \end{cases} \quad i = 1, \dots N \tag{6.8}$$

The Lagrangian function is used to minimize or maximize the objective function augmented (eq. 6.9). Parameters w and b are renowned as primal variables, and λ_i are the Lagrange multipliers [138].

$$\mathcal{L}(w, b, \lambda) = \frac{1}{2} w^T w - \sum_{i=1}^{N} \lambda_i [y_i (w^T x_i + b) - 1] \tag{6.9}$$

The Kernel method transforms the input data to a higher-dimensional space, in which data is linearly separable [140]. The kernel satisfied the Mercer's theorem (eq. 6.10), where $\phi(x_i)$ is a function belongs to Hilbert space to project x_i to a high-dimensional space [141].

$$K(x_i, x_j) = \phi(x_i)\phi(x_j) \tag{6.10}$$

The Kernel used was the Gaussian radial basis function (6.11). The solution of equation (6.12) will allow finding the hyperplane of separation between classes subject to $\sum_{i=1}^{K} \lambda_i y_i = 0$ for $0 \leq \alpha_i \leq C$.

$$K(x_i, x_j) = e^{\left(-\frac{\|x-u\|^2}{\sigma^2}\right)} \tag{6.11}$$

$$\max_{\lambda} \sum_{i=1}^{N} \lambda_i - \frac{1}{2} \sum_{i=1}^{N} \sum_{j=1}^{N} \alpha_i \alpha_j y_i y_j K(x_i, x_j) \tag{6.12}$$

6.3.4. Model validation techniques.

The K-Fold cross-validation was used to train and assess the computational models using thirty folds were used ($k = 30$). For the training process, twenty-nine (29) groups of samples were used, and the remaining group was used for validation. This procedure was repeated thirty times and a different validation group was chosen. Finally, the best model was chosen according to estimation error and model performances. Confusion matrices and the receiver operating characteristic curve (ROC) were used to assess the performance of the SVM computational model [142], [143].

6.4. Results.

This chapter divides the results achieved into three topics: the classification model, the regression model, and the prosthetic alignment protocol.

6.4.1. Alignment classification model.

The data was divided into two categories, nominal alignments, and misalignments. A target data matrix was built with GRF parameters for each category. The parameters chosen for the modeling were I_3,I_4, t_1, t_4, t_5, t_7, t_9, I_6, LR, BI_V, and PI_V. Parameters TI_{AP} and TI_V were rejected in the modeling process because they were linearly dependent.

The SMV method with a fine Gaussian Kernel was used to finely detail differences between nominal and misalignments. The dataset was divided into 80% for training and validation,

and 20% for model testing. The cross-validation algorithm used 30 folds for training and validation. The entire modeling procedure was performed in MATLAB.

The resultant model separated the dataset between nominal alignment and misalignment with 95.5% accuracy and a misclassification cost of four data. The confusion matrix of Figure 29(a) shows that three of the prosthetic misalignments (5.5%) were classified as nominal alignments, and one nominal alignment was classified within the misalignments group (1.8%). Figure 29(c) shows the set of parameters that were misclassified for a specific alignment. The misclassified alignments corresponded to volunteers' number two, ten, eleven, and fourteen. In assessing the level of satisfaction with which the volunteers evaluated the alignments that were misclassified by the model, we found some confusing responses, i.e., in some cases the level of satisfaction when walking with a misaligned prosthesis was close to or higher than that of the nominal alignment and vice versa in other cases. This could mean that the nominal alignment was not optimal or that the misalignments were too close to the angles for the nominal alignment.

Figure 29(b) and Figure 29(d) show the receiver operating characteristic curve (ROC) for the classification model performance, relating the information of false positive and true positive rates. The value of the area under the ROC curve (AUC) is 0.98 in Figure 29(b) and Figure 29(d), indicating that the model correctly predicts 98.0% of the misalignments and nominal alignments.

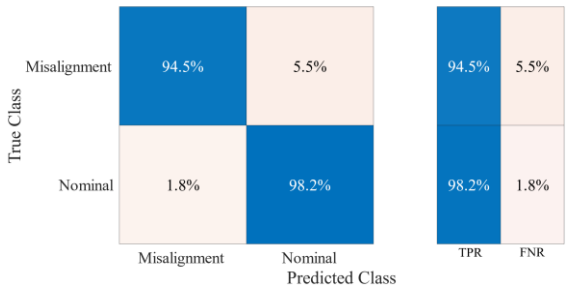

(a). Confusion matrix. TPR: true-positive rate; FNR: False-negative rate.

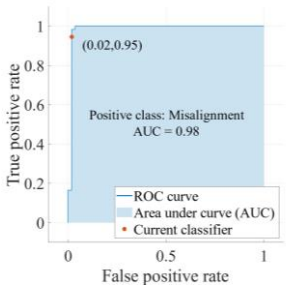

(b). ROC curve for misalignment class.

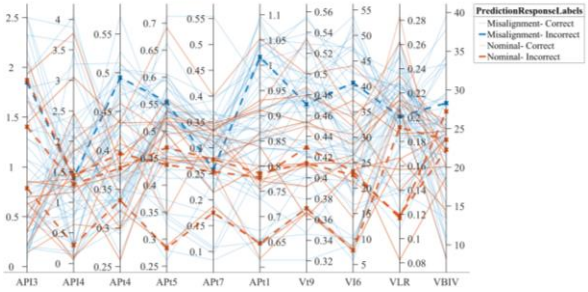

(c). Minimum classification error plot

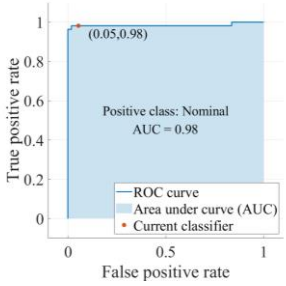

(d). ROC curve for nominal alignment class.

Figure 29. Validation charts of the classification model performance for the support vector machines.

The SVM with a Gaussian kernel was used for classification exercises between nominal alignments and misalignments. The SVM model was computationally validated using the remaining 20% of the dataset (testing data). The testing validation resulted in 92.6% accuracy, reducing by 2.9% of the cross-validation accuracy. Two misalignments were incorrectly classified as nominal alignments.

6.4.2. Prosthetic misalignment model.

The Bayesian regularized artificial neural networks were used to identify a computational model to estimate the misalignment angle of the socket and foot in transfemoral prosthesis using the ground reaction force parameters of the prosthetic limb. The neural network training was performed in MATLAB with the architecture shown in Figure 30.

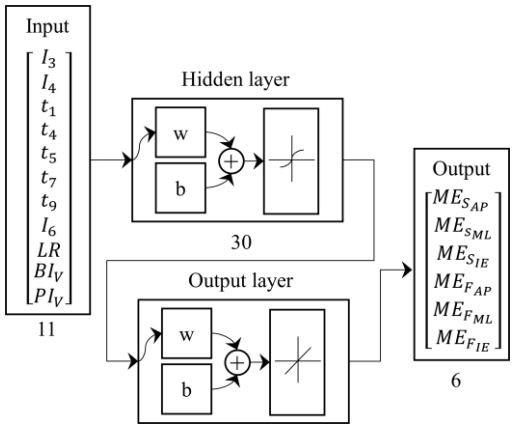

Figure 30. Neural network architecture.

The input vector is composed of eleven GRF parameters, the same used for the classification model. Formulation of the output vector involved calculating the error and the magnitude of the socket and prosthetic foot misalignment respecting the nominal alignment (eq. 6.13).

$$\underbrace{\begin{bmatrix} ME_{S_{AP}} \\ ME_{S_{ML}} \\ ME_{S_{IE}} \\ ME_{F_{AP}} \\ ME_{F_{ML}} \\ ME_{F_{IE}} \end{bmatrix}}_{\text{Misalignment error}} = \underbrace{\begin{bmatrix} S_{M_{AP}} \\ S_{M_{ML}} \\ S_{M_{IE}} \\ F_{M_{AP}} \\ F_{M_{ML}} \\ F_{M_{IE}} \end{bmatrix}}_{\text{Nominal Alignment}} - \underbrace{\begin{bmatrix} S_{N_{AP}} \\ S_{N_{ML}} \\ S_{N_{IE}} \\ F_{N_{AP}} \\ F_{N_{ML}} \\ F_{N_{IE}} \end{bmatrix}}_{\text{Misalignment}} \tag{6.13}$$

For the model identification process, 70.0% of the dataset was used for training, 15.0% for validation, and 15.0% for testing. The best model fitting was achieved for thirty hidden layers and the results achieved are observed in Figure 31. The neural network during training the computational model recovered 100% of the data. Model could recover 94.11% of data, Figure 31(a) shows the validation chart. The model response for testing data (Figure 31(b)) shows a smaller amount of information recovered (77.27%). The error histogram chart (Figure 31(c)) shows that all the error is concentrated in values close to 0.51 ° between the estimated value and the real value.

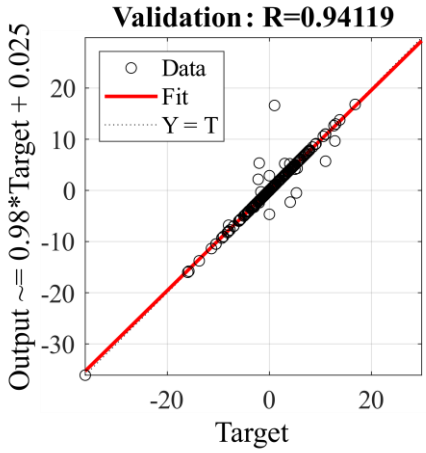

(a). Model regression with validation data.

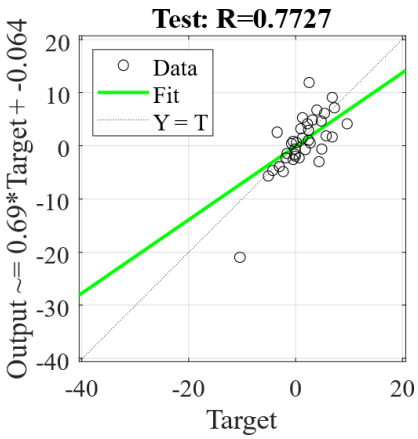

(b). Model regression with testing data.

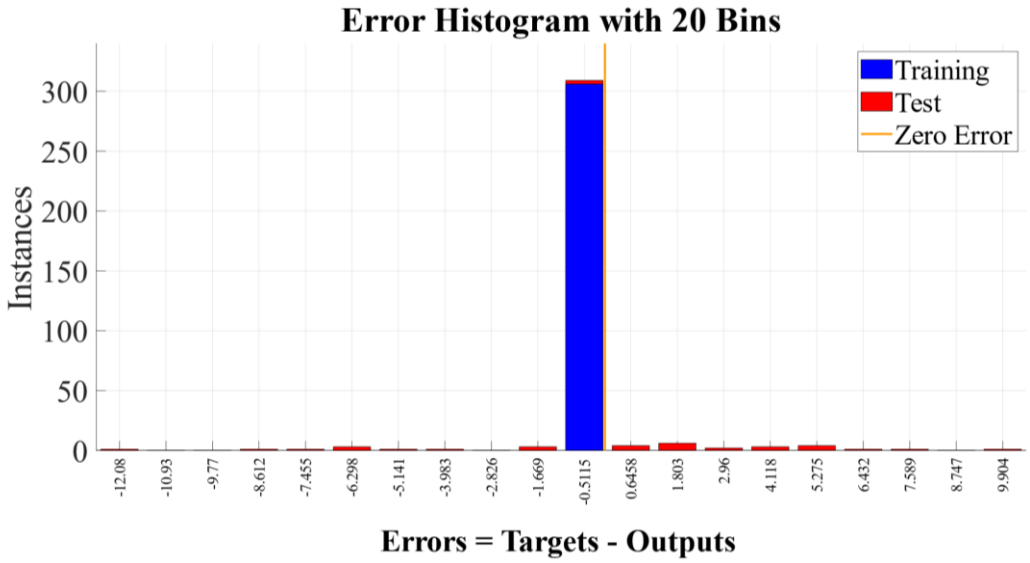

(c). Error histogram.

Figure 31. Results of the neural network trained.

6.4.3. Prosthetic alignment protocol.

The prosthetic alignment protocol explained in 6.3.2 was carried out in the Mahavir Kmina artificial limb center for two days. Validation results are presented for each amputee in Table 5.

No.	Iteration	Angles	Prosthetic alignment score	
			Junior	Senior
1	1	$\begin{bmatrix} S_{AP} = 1.8° \; F & S_{ML} = 8.3° \; Add & S_{IR} = 5.9° \; ER \\ F_{AP} = 4.4° \; PF & F_{ML} = 2.7° \; Ev & F_{IR} = 5.9° \; IR \end{bmatrix}$	4.3	3.4
	2	$\begin{bmatrix} S_{AP} = 2.2° \; F & S_{ML} = 1.3° \; Add & S_{IR} = 1.3° \; ER \\ F_{AP} = 8.1PF° \; PF & F_{ML} = 3.0° \; Ev & F_{IR} = 5.7° \; IR \end{bmatrix}$	5.2	6.2
	3	$\begin{bmatrix} S_{AP} = 2.4° \; F & S_{ML} = 1.4° \; Add & S_{IR} = 0.7° \; IR \\ F_{AP} = 1.2° \; PF & F_{ML} = 3.1° \; Ev & F_{IR} = 1.1° \; IR \end{bmatrix}$	7.6	8.4
2	1	$\begin{bmatrix} S_{AP} = 1.4° \; F & S_{ML} = 0.8° \; Add & S_{IR} = 0.3° \; ER \\ F_{AP} = 0.6° \; PF & F_{ML} = 2.0° \; Ev & F_{IR} = 0.1° \; IR \end{bmatrix}$	5.9	7.5
	2	$\begin{bmatrix} S_{AP} = 0.7° & S_{ML} = 0.7° \; Add & S_{IR} = 0.2° \; IR \\ F_{AP} = 0.1° \; DF & F_{ML} = 2.0° \; Ev & F_{IR} = 0.8° \; IR \end{bmatrix}$	9.8	9.4
	3	-	-	-

Table 5. Performance of prosthetic alignment protocol.

For the socket, the initials F, E, Add, Abd, ER, and IR refer to Flexion, Extension, Adduction, Abduction, External Rotation, and Internal Rotation, respectively. For the foot, the initials PF, DF, Inv, Ev, ER, and IR refer to dorsiflexion, plantar flexion, inversion, eversion, external rotation, and internal rotation, respectively.

For amputee number 1, the protocol iterated three times, not reaching nominal alignment. The patient reported not having ingested alcoholic drinks for 48 hours before the test. The amputee did not inform any difficulty during the protocol execution. The prosthetists had difficulties adjusting the angles in the first iteration; however, they rapidly learned to perform the angulations. The computational protocol indicated a misaligned prosthesis in the first iteration outcome. Prosthetists rated the amputee's initial gait at 3.9. In the second iteration, the prosthetists rated the alignment suggested by the model with 5.7. In the last iteration, the prosthetists scored the gait at 8.0. The prosthetists and computational protocol matched in the prosthetic misalignment for all three iterations, and the computational protocol could not align the prosthesis nominally throughout the iterations.

The second amputee communicated not having consumed alcoholic drinks 48 hours before the test. The amputee did not communicate difficulties during the walking tests. In the first

iteration, the prosthetists rated the initial gait at 6.7. Prosthetists and computational protocol agreed that the prosthesis was misaligned, so the computational protocol suggested a new angulation for the prosthetic components (Table 5 – second amputee – first iteration). The computational alignment protocol reached the nominal alignment in the second iteration and the prosthetists matched with the protocol outcome. The prosthetist ranged the amputee's gait at 9.6.

The alignment protocol validation was assessed by a survey answered by the prosthetists (Figure 32). The prosthetists on average scored 8.18 on the prosthetic gait after applying the computational alignment protocol. The natural amputees' gait patterns affected gait quality; therefore, the correction of gait deviations should be done with a posterior treatment.

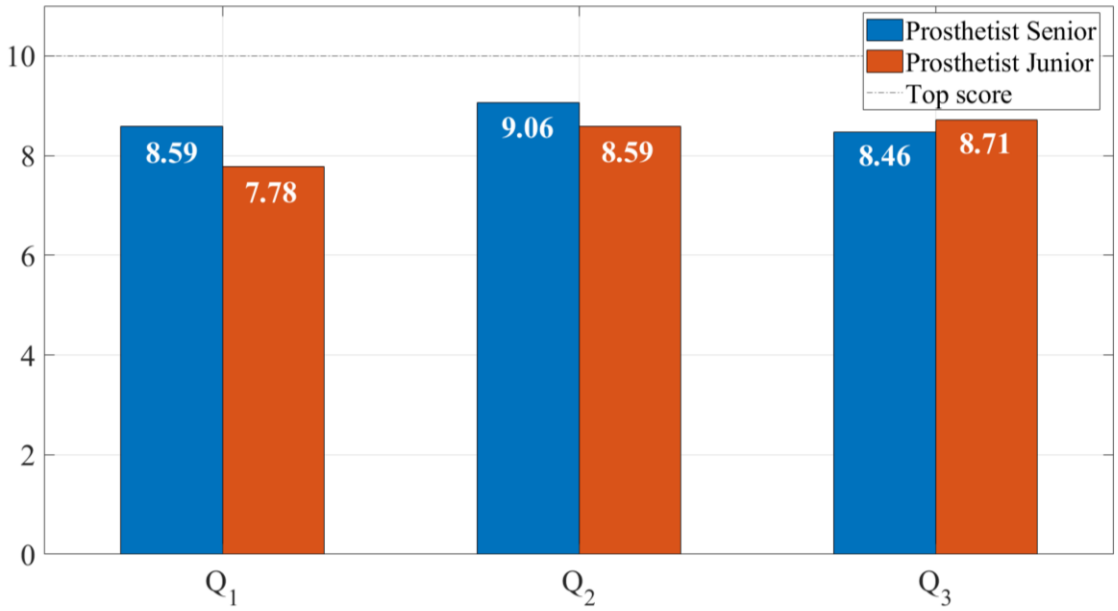

Figure 32. Opinion survey of the prosthetic alignment computational protocol.

The Q_1, Q_2, and Q_3 labels refer to questions of the survey. The scale of Q_1, Q_2, and Q_3 are between zero to ten

Prosthetists scored 8.52 to this kind of computational assistance of the prosthetic alignment and they stated that the alignment protocol allowed them to do a better job, rating it with an

8.58. The senior prosthetist said that the protocol made him take 37 minutes longer than usual and the Junior prosthetist stated that computational protocol did not take him longer.

6.5. Discussion.

The objective of this thesis was to propose an alignment protocol to support the prosthetic alignment assessment of transfemoral amputees. Two computational models were found to identify the nominal alignment and the prosthetic misalignment grade from the ground reaction force of the prosthetic limb of transfemoral amputees. The efficiency of the ground reaction force to evaluate the alignment effects in the gait of amputees was supported in diverse works. For transtibial amputees, effects have been identified in the terminal phase of stance [189], changes in the braking impulse on the prosthetic side and sound limb [215], differences in the loading on the contralateral limb between misalignments and nominal alignments [216]. Few studies focused on transfemoral amputation have been reported in the literature. For instance, Zhang et al. [217] identified alterations in the intact hip and knee joint moments during prosthetic misalignments. In [237] found that socket and foot misalignments mostly affect the performance on the prosthetic side than the intact side, suggesting GRF parameters on which the effects are particularly observed. Despite the lower evidence of GRF effects in transfemoral amputees [273], the results of our classification model confirm that the behavior of the prosthetic limb changes between nominal alignment and misalignments for transfemoral amputees.

The literature shows few references to the prosthetic alignment computational models. The works proposed by Luengas, et al. and Zhang et al. presented classification and regression models of prosthetic alignment in transtibial amputees; however, our information search did

not recover research for the computational models for transfemoral prostheses alignment. Zhang, et al. in [30] proposed a classification model using SVM with a Radial Basis Function (RBF) kernel to detect automatically the misalignment of transtibial prostheses through ground reaction force (GRF), achieving 88.89% accuracy. Luengas, et al. used SVM, neural networks (NN), and decision trees (DT) to detect between nominal alignment and prosthetic misalignments between five transtibial amputees during the standing [32], [272]. The SVM and DT models differentiated between alignments with accuracy 100%. The NN reached 96.2% accuracy. Our classification model using support vector machines (SVM) with a Gaussian kernel reached 95.5% accuracy in the alignment classification of the transfemoral amputees during gait. A false-negative rate of 5.5% was achieved for the misaligned gait classification and 1.8% for the gait with nominally aligned prostheses. The result of our work is comparable with the Zhang, et al. and Luengas, et al. research.

The Bayesian regularized neural networks proposed in our article reached 94.11% accuracy to estimate the magnitude and direction of prosthetic misalignment of transfemoral prostheses in flexion-extension, abduction-adduction, and internal-external rotation of the socket, and dorsiflexion-plantarflexion, inversion- eversion, and medial-lateral rotation of the prosthetic foot. Camargo, et al. and Luengas used Generalized Regression Neural Networks (GRNN) to estimate joint ranges and center of pressure in ipsi and contralateral sides using socket flexion-extension alignment angles in a transtibial prosthesis [31], [271]. The model found had maximum approximation errors of the 6.25% order. Although the model's results are not comparable, due to the type of amputation (transtibial and transfemoral) and the type of alignment (static and dynamic), this research is a great advance

for the adaptation of amputees and minimization of subjectivity in the prosthetic alignment process.

The computational prosthetic alignment protocol worked for all amputees recruited for validation; however, for the first amputee recruited the nominal alignment did not converge during the three iterations. This could be due to the precision of the prosthetists in adjusting the angles suggested by the computational protocol, however, surely the fourth iteration could have adjusted the alignment to achieve nominal gait. As well, the learning curve in the use of the protocol by the prosthetists could affect the non-convergence of the nominal alignment. In the second protocol validation session, prosthetists were more skilled in the alignment's adjustments, so the nominal alignment was achieved in the second iteration. The computational prosthetic alignment protocol assisted the prosthetists during the alignment procedure and allowed them to perform a better job. As prosthetists become more proficient in the alignment protocol, the results should be more satisfactory. The rate of convergence of the protocol could be improved by retraining the computational models with a larger dataset; however, the accuracy of angular adjustment is perhaps affecting the convergence of the nominal alignment. Therefore, further research should be focused on the development of more precise alignment tools.

For validation of the alignment protocol, the same population of amputees used for modeling was called upon, which is a limitation in the evaluation of the model. To minimize the impact of this limitation, a new prosthesis was built for each registered amputee, i.e., a new socket was manufactured, and all prosthetic components were replaced. Considering that the nominal alignment is not unique, as it depends on the characteristics of the amputee and the prosthesis, the models were confronted with different data and situations for which they were

trained. This gives a certain degree of confidence in our results; however, the protocol needs to be validated with more volunteers to be further optimized.

The most important limitations of the alignment protocol consider a few aspects. The judgment of a nominal alignment was decided for only one senior prosthetist, so the protocol generalization could be compromised. The use of specific types of a prosthetic foot (Jaipur foot), a socket (ischial restraint), a polyaxial knee (automatic locking, D-Rev), among other specificities, also limits the protocol scope. All transfemoral prostheses were manufactured by the Mahavir Kmina Artificial Limb Center, so there is a bias in the construction procedure; however, Mahavir Kamina's prosthetists have fitted more than 5,000 amputees, so they have sufficient experience in prosthetic manufacturing. The alignment protocol was evaluated in transfemoral amputees wearing prosthesis with polyaxial knee; however, the protocol could be evaluated in prostheses with monocentric knees with pyramidal adapters. Future studies should evaluate the efficacy of the protocol in other types of prostheses. Finally, the amputees' skill to adapt their gait patterns and to accommodate to misalignments is complex bias [274][275]; however, the walking trials were carried out in short times to minimize the probability of this phenomenon occurring. The results obtained by the alignment classification model and the misalignment estimation model for transfemoral amputees are a significant advance in the state of the art.

6.6. Conclusion.

Regardless of the result of this research, developing computational alternatives to reduce the subjectivity in the prosthetic alignment procedure should be an important study matter in future research. The complexity of the experiments, the intra-individual variability, and the

wide possibility of prosthetic devices present challenges for the scientific community, but the computational power could overcome these restrictions. As computational power increases, the strengthening of alignment protocols such as the one discussed here could solve the complexity of the prosthetic alignment process.

The accuracy of the prosthetic alignment angles is perhaps one of the greatest uncertainty inducers during the nominal alignment convergence; therefore, further research should be focused on the development of more precise alignment tools.

General conclusions.

This thesis presented a novel prosthetic alignment protocol based on a cross-sectional study of sixteen patients with transfemoral amputation. Random variations of alignment were performed between -18.0° and 28.0° flexion-extension, adduction-abduction, and internal-external rotation of the socket. Alignment of the prosthetic foot was varied between -13.0° and 11.0° in dorsal-plantar flexion, eversion-inversion, and internal-external rotation. Twenty-eight Ground Reaction Force parameters, twelve spatiotemporal parameters, six electromyography parameters, nineteen stump temperature parameters, and seventeen comfort questions were recorded. Statistical analysis showed significant differences for the prosthetic limb between correctly and incorrectly performed alignments. Computational models were proposed using the prosthetic alignment descriptor parameters, resulting in an alignment protocol that assisted the prosthetist during alignment with a success factor of 88.0%.

During static alignment, the amputee's recorded standing data were evaluated. No significant differences were observed between nominal alignment and prosthetic misalignment in

transfemoral amputees. As a result, no variables describing the static alignment procedure could be proposed, so it was not possible to include static alignment in the alignment protocol. Previous literature shows a static alignment protocol for transtibial amputees, however, the loss of the knee during transfemoral amputation imposes major mobility restrictions on the amputee.

The orthopedic specialist was a key player in the alignment procedure. This person must evaluate the parameters reported by the gait and standing analysis systems, the anatomical and biomechanical characteristics of the amputee, the prosthetic performance, the amputee's feedback of the prosthesis usefulness, and observation of the entire procedure. The clinical diagnosis of prosthetic alignment depends on the skills and experience of the prosthetist to evaluate this information. The variability and subjectivity of the alignment procedure imply a high probability of error.

The data analysis developed in this thesis showed that transfemoral amputees did not significantly change the behavior of the sound limb during alignment variations, whether standing or walking. The prosthetic limb did not show significant differences between subjects for most of the parameters recorded during standing and walking, except for the ground reaction force during walking exercises with misaligned and nominally aligned prostheses. This showed that despite the amputee's skills for adapting to new alignment conditions, the misalignment produced changes in the force distribution between lower limbs. These gait patterns were complex to detect visually, but computational models were effective tools for detecting this type of misalignment.

Electromyography frequency analysis revealed a degree of prosthetic limb fatigue when the amputee was using a misaligned prosthesis. The results were not representative for the entire

population of transfemoral amputees, so this parameter was not included in the alignment protocol. It is likely that the amputee's skills to compensate for the gait patterns during alignment changes could minimize the effect of alignment on muscle activity. In our research we were restricted in the number of muscles recorded, since our equipment had only four channels. Therefore, normalized electromyography of the sound limb and residual limb should be further studied, considering a larger number of muscles.

In this thesis, a comfort survey instrument based on the Prosthesis Evaluation Questionnaire (PEQ) was used. The analysis of the comfort surveys was not satisfactory, because no significant differences were observed between nominal alignment and misalignments. The alignment trials took an average of 8 hours for each amputee, so rest times were given to avoid volunteer fatigue; however, it was seen that in some cases amputees filled out the comfort survey with a lower degree of commitment, possibly due to the duration of the tests. Fatigue could have biased the results obtained from the comfort surveys.

In some cases, we observed that the amputee's opinion did not match with the diagnosis of optimal prosthetic alignment. This phenomenon was produced because the prosthetist adjusted the prosthesis to correct gait deviations previously adopted by the amputee; however, the variability and subjectivity of the procedure could cause the prosthetist to have failed to achieve nominal alignment. This helped to prove that nominal alignment is not unique and depends on the specific characteristics of each amputee's prosthetic fitting. Preliminary results obtained in this thesis proved that, despite the variability of nominal alignment, computational models broke the between-subject variability to find gait patterns of nominally aligned prostheses and supported the alignment of transfemoral prostheses.

The effect of prosthetic misalignment was masked in most of the spatiotemporal data. This phenomenon has been widely reported in previous research, so the results achieved in this thesis reinforce this argument. However, the gait speed and stance phase of the prosthetic limb tended to be faster during gait with misaligned prostheses, which could signify a lower level of confidence in the prosthetic limb. Future work should contrast comfort with spatiotemporal data to analyze amputee adaptability.

References

[1] U. Basaninyenzi and The World Bank, “Disability Inclusion Overview: Development news, research, data,” *Disability Inclusion Overview: Development news, research, data*, Mar. 19, 2021. https://www.worldbank.org/en/topic/disability#1 (accessed Oct. 07, 2021).

[2] World Health Organization, “World Report on Disability,” Malta, 2011. doi: ISBN 978 92 4 068521 5.

[3] C. Quintero Quiroz, A. Jaramillo Zapata, M. T. De Ossa Jiménez, and P. A. Villegas Bolaños, “Estudio descriptivo de condiciones del muñón en personas usuarias de prótesis de miembros inferiores,” *Rev. Colomb. Médicina Física y Rehabil.*, vol. 25, no. 2, pp. 94–103, 2015, doi: 10.28957/rcmfr.v25n2a1.

[4] Departamento Administrativo Nacional de Estadística, “Panorama general de la discapacidad en Colombia,” Bogotá, Nov. 2020. Accessed: Oct. 07, 2021. [Online]. Available: https://www.dane.gov.co/files/investigaciones/discapacidad/Panorama-general-de-la-discapacidad-en-Colombia.pdf.

[5] World Health Organization, “Standars for Prosthetics and Orthotics. Part 1. Standardss,” France, 2017. Accessed: Oct. 07, 2021. [Online]. Available: http://apps.who.int/bookorders.

[6] C. L. McDonald, S. Westcott-McCoy, M. R. Weaver, J. Haagsma, and D. Kartin, “Global prevalence of traumatic non-fatal limb amputation,” *Prosthet. Orthot. Int.*, Dec. 2020, doi: 10.1177/0309364620972258.

[7] Departamento Administrativo Nacional de Estadística, Dirección de Censos y Demografía, and Grupo de Registros Demográficos, “Información estadística de la discapacidad,” Bogotá, Jul. 2004. Accessed: Oct. 07, 2021. [Online]. Available: https://www.dane.gov.co/files/investigaciones/discapacidad/inform_estad.pdf.

[8] A. S. Sarvestani and A. T. Azam, “Amputation: A Ten-Year Survey,” *Trauma Mon.*, vol. 18, no. 3, p.

129, Oct. 2013, doi: 10.5812/TRAUMAMON.11693.

[9] T. Lääperi, T. Pohjolainen, H. Alaranta, and M. Kärkkäinen, “Lower-limb amputations,” *Ann. Chir. Gynaecol.*, vol. 82, no. 3, pp. 183–187, 1993.

[10] A. Esquenazi and M. Kwasniewski, “Lower Limb Amputations: Epidemiology and Assessment,” *Medical Rehabilitation - PM&R Knowledge*, Jun. 2021. https://now.aapmr.org/lower-limb-amputations-epidemiology-and-assessment/ (accessed Oct. 07, 2021).

[11] G. Bastas, “Lower Limb Amputations,” *Essentials Phys. Med. Rehabil.*, pp. 658–663, Jan. 2020, doi: 10.1016/B978-0-323-54947-9.00120-6.

[12] G. M. Berke *et al.*, *Transfemoral Amputation: the basics and beyond*. Prosthetics Research Study, 2008.

[13] V. N. M. Arelekatti and A. G. Winter, “Design of mechanism and preliminary field validation of low-cost, passive prosthetic knee for users with transfemoral amputation in India,” in *Proceedings of the ASME Design Engineering Technical Conference*, Jan. 2015, vol. 5A-2015, doi: 10.1115/DETC2015-47385.

[14] M. Marino *et al.*, “Access to prosthetic devices in developing countries: Pathways and challenges,” in *2015 IEEE Global Humanitarian Technology Conference (GHTC)*, 2015, pp. 45–51, doi: 10.1109/GHTC.2015.7343953.

[15] J. E. Edelstein and A. Moroz, *Lower-Limb Prosthetics and Orthotics: Clinical Concepts*, vol. 10. 2011.

[16] M. S. Zahedi, W. D. Spence, S. E. Solomonidis, and J. P. Paul, “Alignment of lower-limb prostheses,” *J. Rehabil. Res. Dev.*, vol. 23, no. 2, pp. 2–19, Apr. 1986.

[17] O. Mohamed and H. Appling, “Clinical Assessment of Gait,” *Orthot. Prosthetics Rehabil.*, pp. 102–143, Jan. 2020, doi: 10.1016/B978-0-323-60913-5.00005-2.

[18] International Committee of the Red Cross, “Manufacturing Guidelines: Trans-Femoral Prosthesis,” Geneva, Sep. 2006. Accessed: May 07, 2021. [Online]. Available: https://www.icrc.org/en/doc/assets/files/other/eng-transfemoral.pdf.

[19] N. Berger, “Analysis of Amputee Gait,” in *Atlas of Limb Prosthetics: Surgical, Prosthetic, and Rehabilitation Principles.*, 2nd ed., American Academy of Orthopedic Surgeons, 2002.

[20] R. Seymour, *Prosthetics and Orthotics: Lower Limb and Spinal*. Baltimore: Lippincott Williams & Wilkins, 2002.

[21] S. Blumentritt, “A new biomechanical method for determination of static prosthetic alignment,” *Prosthet. Orthot. Int.*, vol. 21, no. 2, pp. 107–113, 1997, doi: 10.3109/03093649709164538.

[22] J. Howcroft, E. D. Lemaire, J. Kofman, and C. Kendell, “Understanding responses to gait instability from plantar pressure measurement and the relationship to balance and mobility in lower-limb amputees,” *Clin. Biomech.*, vol. 32, pp. 241–248, Feb. 2016, doi: 10.1016/j.clinbiomech.2015.11.004.

[23] X. Drevelle, C. Villa, X. Bonnet, I. Loiret, P. Fodé, and H. Pillet, “Vaulting quantification during level walking of transfemoral amputees,” *Clin. Biomech.*, vol. 29, no. 6, pp. 679–683, 2014, doi: 10.1016/j.clinbiomech.2014.04.006.

[24] V. Rajťúková, M. Michalíková, L. Bednarčíková, A. Balogová, and J. Živčák, “Biomechanics of Lower Limb Prostheses,” *Procedia Eng.*, vol. 96, pp. 382–391, 2014, doi: https://doi.org/10.1016/j.proeng.2014.12.107.

[25] G. J, “Amputation and prosthesis fitting in paediatric patients,” *Orthop. Traumatol. Surg. Res.*, vol. 102, no. 1 Suppl, pp. S161–S175, Feb. 2016, doi: 10.1016/J.OTSR.2015.03.020.

[26] Fillauer, “ALP-ALU 4-Hole Adapter,” *Orthotics and Prosthetics Manufacturer*, 2021. https://fillauer.com/products/alp-alu-4-hole-adapter/ (accessed Oct. 20, 2021).

[27] Ottobock, “4R101 Aluminum Sliding Adapter - Instructions for Use,” *Sliding Adapter Aluminum*, 2014.
.

[28] T. Gujarathi and K. Bhole, “Gait Analysis using IMU Sensor,” *2019 10th Int. Conf. Comput. Commun. Netw. Technol. ICCCNT 2019*, pp. 1–5, Jul. 2019, doi: 10.1109/ICCCNT45670.2019.8944545.

[29] T. B. Rodrigues, D. P. Salgado, C. Ó. Catháin, N. O’Connor, and N. Murray, “Human gait assessment using a 3D marker-less multimodal motion capture system,” *Multimed. Tools Appl. 2019 793*, vol. 79,

no. 3, pp. 2629–2651, Nov. 2019, doi: 10.1007/S11042-019-08275-9.

[30] X. Zhang, G. Fiedler, Z. Cao, and Z. Liu, “A support vector machine approach to detect trans-Tibial prosthetic misalignment using 3-Dimensional ground reaction force features: A proof of concept,” *Technol. Heal. Care*, vol. 26, no. 4, pp. 715–721, Jan. 2018, doi: 10.3233/THC-181338.

[31] E. Camargo, L. A. Luengas-C, and E. Garzón, “Computational Method to Verify Static Alignment of Transtibial Prosthesis,” *Biomed. J. Sci. Tech. Res.*, vol. 31, no. 2, pp. 24058–24062, Oct. 2020, doi: 10.26717/BJSTR.2020.31.005074.

[32] L. A. Luengas Contreras, G. Sánchez Prieto, and P. R. Vizcaya Guarín, “Alineación Estática de Prótesis a través de Variables Cinéticas y Métodos de Aprendizaje de Máquina,” *Rev. Cuba. Informática Médica*, vol. 9, no. 1, pp. 3–17, 2017, Accessed: Oct. 08, 2021. [Online]. Available: http://scielo.sld.cu/scielo.php?script=sci_arttext&pid=S1684-18592017000100002.

[33] L. A. Luengas, G. Sanchez, and K. Novoa, “Prosthetic alignment and biomechanical parameters in transtibial amputees due landmines,” in *IFMBE Proceedings*, 2017, vol. 60, pp. 765–768, doi: 10.1007/978-981-10-4086-3_192.

[34] M. P. Chagas, F. R. Castro, M. A. A. Sanches, J. H. Agostinho, C. A. Alves, and A. A. Carvalho, “Instrumental platform for the static alignment of lower limb prostheses,” *https://doi.org/10.1080/10739149.2019.1691586*, vol. 48, no. 3, pp. 231–241, May 2019, doi: 10.1080/10739149.2019.1691586.

[35] R. Gailey, K. Allen, J. Castles, J. Kucharik, and M. Roeder, “Review of secondary physical conditions associated with lower-limb amputation and long-term prosthesis use,” *J. Rehabil. Res. Dev.*, vol. 45, no. 1, pp. 15–30, 2008, doi: 10.1682/JRRD.2006.11.0147.

[36] T. Schmalz, S. Blumentritt, and R. Jarasch, “Energy expenditure and biomechanical characteristics of lower limb amputee gait: The influence of prosthetic alignment and different prosthetic components,” *Gait Posture*, vol. 16, no. 3, pp. 255–263, 2002, doi: https://doi.org/10.1016/S0966-6362(02)00008-5.

[37] A. I. Vásquez and J. U. Pérez, “Conceptual design of an alignment device for transfemoral prosthesis,”

Rev. Fac. Ing. Univ. Antioquia, no. 102, pp. 108–114, 2022, doi: 10.17533/UDEA.REDIN.20200805.

[38] D. Moher, A. Liberati, J. Tetzlaff, D. G. Altman, and T. P. Group, "Preferred Reporting Items for Systematic Reviews and Meta-Analyses: The PRISMA Statement," *PLOS Med.*, vol. 6, no. 7, p. e1000097, Jul. 2009, [Online]. Available: https://doi.org/10.1371/journal.pmed.1000097.

[39] S. H. Downs and N. Black, "The feasibility of creating a checklist for the assessment of the methodological quality both of randomised and non-randomised studies of health care interventions," *J. Epidemiol. Community Health*, vol. 52, no. 6, pp. 377–384, Jun. 1998, [Online]. Available: http://www.ncbi.nlm.nih.gov/pmc/articles/PMC1756728/.

[40] H. Van der Linde, C. J. Hofstad, A. C. H. Geurts, K. Postema, J. H. B. Geertzen, and J. van Limbeek, "A systematic literature review of the effect of different prosthetic components on human functioning with a lower-limb prosthesis.," *J. Rehabil. Res. Dev.*, vol. 41, no. 4, pp. 555–570, Jul. 2004.

[41] J. E. Edelstein, "Amputations and Prostheses," in *Physical Rehabilitation*, W.B. Saunders, 2007, pp. 267–299.

[42] P. Ferrand-Ferri, M. Rodríguez-Piñero Durán, C. Echevarría-Ruiz de Vargas, and M. J. Zarco-Periñán, "Versión española del Prosthesis Evaluation Questionnaire (PEQ): parte inicial de su adaptación transcultural," *Rehabilitación*, vol. 41, no. 3, pp. 101–107, Feb. 2007, doi: 10.1016/S0048-7120(07)75496-8.

[43] M. W. Legro, G. D. Reiber, D. G. Smith, M. del Aguila, J. Larsen, and D. Boone, "Prosthesis evaluation questionnaire for persons with lower limb amputations: Assessing prosthesis-related quality of life," *Arch. Phys. Med. Rehabil.*, vol. 79, no. 8, pp. 931–938, Aug. 1998, doi: 10.1016/S0003-9993(98)90090-9.

[44] A. Kallner, "Formulas," in *Laboratory Statistics*, Elsevier, 2018, pp. 1–140.

[45] A. Justel, D. Peña, and R. Zamar, "A multivariate Kolmogorov-Smirnov test of goodness of fit," *Stat. Probab. Lett.*, vol. 35, no. 3, pp. 251–259, Oct. 1997, doi: 10.1016/S0167-7152(97)00020-5.

[46] R. Christensen, "Analysis of Variance and Generalized Linear Models," *Int. Encycl. Soc. Behav. Sci.*,

pp. 473–480, Jan. 2001, doi: 10.1016/B0-08-043076-7/00452-6.

[47] R. N. Forthofer, E. S. Lee, and M. Hernandez, “Nonparametric Tests,” in *Biostatistics*, 2nd ed., Academic Press, 2007, pp. 249–268.

[48] R. J. Freund, W. J. Wilson, and D. L. Mohr, “Inferences for Two or More Means,” in *Statistical Methods*, Academic Press, 2010, pp. 245–320.

[49] D. A. Pisner and D. M. Schnyer, “Support vector machine,” in *Machine Learning: Methods and Applications to Brain Disorders*, A. Mechelli and S. Vieira, Eds. Academic Press, 2020, pp. 101–121.

[50] M. A. Nielsen, “Neural Networks and Deep Learning.” Determination Press, 2015, Accessed: Oct. 09, 2021. [Online]. Available: http://neuralnetworksanddeeplearning.com.

[51] C. C. Aggarwal, *Neural Networks and Deep Learning: A Textbook*. Ney York: Springer International Publishing, 2018.

[52] K. L. Moore, A. F. Dalley, and A. M. R. Agur, *Moore. Fundamentos de anatomía con orientación clínica Ed.6º por Moore, Keith L. - 9788417602512 - Journal*, 6th ed. Wolters Kluwer, 2020.

[53] Chummy S. Sinnatamby, *Anatomía de Last: Regional y Aplicada*. Barcelona: Editorial Paidotribo, 2003.

[54] A. Halim, *Human Anatomy:Volume Ii Abdomen And Lower Limb - A. Halim - Google Libros*, vol. 2th. New Delhi: I.K. International Publishing House Pvt. Ltd., 2008.

[55] R. Merletti and P. Parker, *Electromyography: Physiology, Engineering, and Noninvasive Applications*. Hoboken, NJ, USA: John Wiley & Sons, Inc., 2004.

[56] J. A. Ruiz Caballero, R. Navarro García, Brito Ojeda. Estrella María, M. Navarro Validivieso, R. Navarro Navarro, and J. M. García Mansa, *Análisis del movimiento en el deporte*. Editorial Wanceulen, 2011.

[57] C. Osorio, J. Henry, ; Valencia, and M. Hernando, “Bases for undertanding the human gait process,” *Arch. Med.*, vol. 13, pp. 88–96, Jan. 2013, Accessed: Oct. 01, 2021. [Online]. Available:

http://www.redalyc.org/articulo.oa?id=273828094009.

[58] R. B. Davis, P. A. DeLuca, and S. Ounpuu, “Analysis of Gait,” in *Biomechanics : principles and practices*, London: CRC Press, 2015.

[59] S. I. Yusuf, S. Adeshina, and M. M. Boukar, “Parameters for human gait analysis: A review,” *2019 15th Int. Conf. Electron. Comput. Comput. ICECCO 2019*, pp. 1–4, Dec. 2019, doi: 10.1109/ICECCO48375.2019.9043216.

[60] P. B. Shull, W. Jirattigalachote, M. A. Hunt, M. R. Cutkosky, and S. L. Delp, “Quantified self and human movement: A review on the clinical impact of wearable sensing and feedback for gait analysis and intervention,” *Gait Posture*, vol. 40, no. 1, pp. 11–19, May 2014, doi: 10.1016/J.GAITPOST.2014.03.189.

[61] F. Vaverka, M. Elfmark, Z. Svoboda, and M. Janura, “System of gait analysis based on ground reaction force assessment,” *Acta Gymnica*, vol. 45, no. 4, pp. 187–193, 2015, doi: 10.5507/ag.2015.022.

[62] D. R. Peterson and J. D. Bronzino, *Biomechanics Principles and Applications*, Second. Boca Raton: CRC Press, 2008.

[63] E. W. Broström, A. C. Esbjörnsson, J. Von Heideken, and M. D. Iversen, “Gait deviations in individuals with inflammatory joint diseases and osteoarthritis and the usage of three-dimensional gait analysis,” *Best Pract. Res. Clin. Rheumatol.*, vol. 26, no. 3, pp. 409–422, Jun. 2012, doi: 10.1016/J.BERH.2012.05.007.

[64] L. I. Broche-Vázquez, R. I. Sagaró-Zamora, C. I. Ochoa-Díaz, A. I. Padilha-Lanari-Bó, and F. A. Martinez-Nariño III, “Análisis cinemático y dinámico de las prótesis transfemorales. Implicaciones clínicas Kinematic and dynamic analysis of transfemoral prosthesis. Clinical implications,” *Ing. Mecánica*, vol. 19, no. 3, pp. 150–157, 2016, Accessed: Oct. 01, 2021. [Online]. Available: http://www.ingenieriamecanica.cujae.edu.cu.

[65] R. B. Davis, S. Õunpuu, D. Tyburski, and J. R. Gage, “A gait analysis data collection and reduction technique,” *Hum. Mov. Sci.*, vol. 10, no. 5, pp. 575–587, Oct. 1991, doi: 10.1016/0167-9457(91)90046-

Z.

[66] A. Bonnefoy-Mazure and S. Armand, “Chapter 16 - Normal Gait,” in *Orthopedic Management of Children with Cerebral Palsy*, F. Canavese and J. Deslandes, Eds. Nova Science Publishers, Inc., 2015, pp. 200–213.

[67] J. B. Webster and B. J. Darter, “Principles of Normal and Pathologic Gait,” in *Atlas of Orthoses and Assistive Devices*, J. B. Webster and D. P. Murphy, Eds. Elsevier, 2019, pp. 49-62.e1.

[68] S. Winiarski and A. Rutkowska-Kucharska, “Estimated ground reaction force in normal and pathological gait,” *Acta Bioeng. Biomech.*, vol. 11, no. 1, 2009.

[69] S. Lauzière, M. Betschart, R. Aissaoui, and S. Nadeau, “Understanding Spatial and Temporal Gait Asymmetries in Individuals Post Stroke,” 2014, doi: 10.4172/2329-9096.1000201.

[70] C. T. John, A. Seth, M. H. Schwartz, and S. L. Delp, “Contributions of muscles to mediolateral ground reaction force over a range of walking speeds,” *J. Biomech.*, vol. 45, no. 14, p. 2438, Sep. 2012, doi: 10.1016/J.JBIOMECH.2012.06.037.

[71] D. Levine, J. Richards, and M. W. Whittle, *Whittle’s Gait Analysis*, Fourth edition. London: Elsevier, 2012.

[72] D. A. Winter, *The biomechanics and motor control of human gait : normal, elderly and pathological*, 2nd edition. University of Waterloo Press, 1991.

[73] L. R. Sheffler and J. Chae, “Hemiparetic Gait,” *Phys. Med. Rehabil. Clin. N. Am.*, vol. 26, no. 4, pp. 611–623, Nov. 2015, doi: 10.1016/j.pmr.2015.06.006.

[74] A. Fidalgo-Herrera, J. Miangolarra-Page, and M. Carratalá-Tejada, “Traces of muscular fatigue in the rectus femoris identified with surface electromyography and wavelets on normal gait,” *https://doi.org/10.1080/09593985.2020.1725945*, 2020, doi: 10.1080/09593985.2020.1725945.

[75] M. Singh and M. Singh, “Neuro-Degenerative Disease Diagnosis using Human Gait: A Review,” 2013. Accessed: Oct. 28, 2018. [Online]. Available: http://www.csjournals.com/IJITKM/PDF 7-1/4.pdf.

[76] J. M. Adams and K. Cerny, *Observational Gait Analysis: A Visual Guide*. SLACK Incorporated, 2017.

[77] V. Agostini, M. Ghislieri, S. Rosati, G. Balestra, and M. Knaflitz, "Surface Electromyography Applied to Gait Analysis: How to Improve Its Impact in Clinics?," *Front. Neurol.*, vol. 11, p. 994, Sep. 2020, doi: 10.3389/FNEUR.2020.00994.

[78] A. Esquenazi, "Gait analysis in lower-limb amputation and prosthetic rehabilitation," *Phys. Med. Rehabil. Clin. N. Am.*, vol. 25, no. 1, pp. 153–167, 2014, doi: 10.1016/j.pmr.2013.09.006.

[79] T. Varrecchia *et al.*, "Common and specific gait patterns in people with varying anatomical levels of lower limb amputation and different prosthetic components," *Hum. Mov. Sci.*, vol. 66, pp. 9–21, Aug. 2019, doi: 10.1016/J.HUMOV.2019.03.008.

[80] V. Gil Chang, *Fundamentos de Medicina de Rehabilitación*. Costar Rica: Editorial UCR, 2006.

[81] M. A. Arcas-Patricio, *Manual de Fisioterapia: Traumatología, afecciones cardiovasculares y otros campos de actuación*. Sevilla: Mad, S.L., 2009.

[82] F. García Pérez, "Amputación de extremidad inferior y discapacidad. Prótesis y rehabilitación," *Rehabilitación*, vol. 40, no. 1, p. 64, Jan. 2006, doi: 10.1016/S0048-7120(06)74861-7.

[83] D. Yuseima Govantes Bacallao, D. Carmen Julio Alba Gelabert, A. Arias Cantalapiedra Centro Nacional de Rehabilitación, J. Díaz González, and L. Habana, "Protocolo de actuación en la rehabilitación de pacientes amputados de miembro inferior Protocol of action in rehabilitation of patients with lower limbs amputees," *Rev. Cuba. Med. Física y Rehabil.*, vol. 8, no. 1, pp. 33–43, 2016.

[84] F. Salinas-Durán, L. H. Lugo-Agudelo, and R. Restrepo-Arbeláez, *Rehabilitación en salud*, 2da edición. Medellín: Universidad de Antioquia, 2008.

[85] S. W. Levy, "Chapter 26: Skin Problems of the Amputee," in *Atlas of Limb Prosthetics: Surgical, Prosthetic, and Rehabilitation Principles.*, American Academy of…., Rosemont: American Academy of Orthopedic Surgeons, 2002.

[86] R. H. Meier and D. Melton, "Ideal functional outcomes for amputation levels," *Physical Medicine and Rehabilitation Clinics of North America*, vol. 25, no. 1. Phys Med Rehabil Clin N Am, pp. 199–212,

Feb. 2014, doi: 10.1016/j.pmr.2013.09.011.

[87] J. Andrysek, “Lower-limb prosthetic technologies in the developing world: A review of literature from 1994-2010,” *Prosthet. Orthot. Int.*, vol. 34, no. 4, pp. 378–398, 2010, doi: 10.3109/03093646.2010.520060.

[88] M. D. Muller, “Transfemoral Amputation: Prosthetic Management,” in *Atlas of Amputations and Limb Defi ciencies*, Fourth Edition., American Academy of Orthopaedic Surgeons, 2016, pp. 537–554.

[89] C. M. Schuch and C. H. Pritham, “Current Transfemoral Sockets,” *Clin. Orthop. Relat. Res.*, vol. 361, 1999, [Online]. Available: https://journals.lww.com/clinorthop/Fulltext/1999/04000/Current_Transfemoral_Sockets.7.aspx.

[90] J. Tang *et al.*, “Characterisation of dynamic couplings at lower limb residuum/socket interface using 3D motion capture,” *Med. Eng. Phys.*, vol. 37, no. 12, pp. 1162–1168, Dec. 2015, doi: 10.1016/J.MEDENGPHY.2015.10.004.

[91] S. Arun and S. Kanagaraj, “Performance enhancement of epoxy based sandwich composites using multiwalled carbon nanotubes for the application of sockets in trans-femoral amputees,” *J. Mech. Behav. Biomed. Mater.*, vol. 59, pp. 1–10, Jun. 2016, doi: 10.1016/J.JMBBM.2015.12.013.

[92] R. S. Hanspal, K. Fisher, and R. Nieveen, “Prosthetic socket fit comfort score.,” *Disabil. Rehabil.*, vol. 25, no. 22, pp. 1278–1280, Nov. 2003, doi: 10.1080/09638280310001603983.

[93] L. Paternò, M. Ibrahimi, E. Gruppioni, A. Menciassi, and L. Ricotti, “Sockets for Limb Prostheses: A Review of Existing Technologies and Open Challenges,” *IEEE Trans. Biomed. Eng.*, vol. 65, no. 9, pp. 1996–2010, 2018, doi: 10.1109/TBME.2017.2775100.

[94] X. Jia, X. Li, R. Wang, and D. Jin, “Optimal design of prosthetic alignment angle for monolithic prosthetics,” *Qinghua Daxue Xuebao/Journal Tsinghua Univ.*, vol. 47, no. 5, pp. 647–650, 2007.

[95] N. L. Dudek, M. B. Marks, S. C. Marshall, and J. P. Chardon, “Dermatologic conditions associated with use of a lower-extremity prosthesis,” *Arch. Phys. Med. Rehabil.*, vol. 86, no. 4, pp. 659–663, 2005, doi: 10.1016/j.apmr.2004.09.003.

[96] A. Salawu, C. Middleton, A. Gilbertson, K. Kodavali, and V. Neumann, “Stump ulcers and continued prosthetic limb use,” *Prosthet. Orthot. Int.*, vol. 30, no. 3, pp. 279–285, Dec. 2006, doi: 10.1080/03093640600836139.

[97] J. H. Hong and M. S. Mun, “Relationship between socket pressure and EMG of two muscles in trans-femoral stumps during gait:,” *http://dx.doi.org/10.1080/03093640500116764*, vol. 29, no. 1, pp. 59–72, Jun. 2016, doi: 10.1080/03093640500116764.

[98] A. G. Cutti, P. Perego, M. C. Fusca, R. Sacchetti, and G. Andreoni, “Assessment of lower limb prosthesis through wearable sensors and thermography.,” *Sensors (Basel).*, vol. 14, no. 3, pp. 5041–55, Mar. 2014, doi: 10.3390/s140305041.

[99] J. Živčák, R. Hudák, and V. Rajťúková, “Biomechanical and Thermographic Analysis in the Transtibial Prosthesis Socket - Stump Interface,” *Acta Mech. Slovaca*, vol. 19, no. 2, pp. 18–26, 2015, doi: 10.21496/ams.2015.011.

[100] J. C. Cagle, P. G. Reinhall, B. J. Hafner, and J. E. Sanders, “Development of Standardized Material Testing Protocols for Prosthetic Liners,” *J. Biomech. Eng.*, vol. 139, no. 4, p. 0450011, Apr. 2017, doi: 10.1115/1.4035917.

[101] B. Dupes, “Prosthetic knee systems,” 2014. Accessed: Oct. 05, 2021. [Online]. Available: https://3w568y1pmc7umeynn2o6c1my-wpengine.netdna-ssl.com/wp-content/uploads/2015/05/knees.pdf.

[102] T. M. Köhler, M. Bellmann, and S. Blumentritt, “Polycentric exoprosthetic knee joints – extent of shortening during swing phase,” *Can. Prosthetics Orthot. J.*, vol. 3, no. 1, pp. 1–10, Jul. 2020, doi: 10.33137/cpoj.v3i1.33768.

[103] X. Zhang *et al.*, “On Design and Implementation of Neural-Machine Interface for Artificial Legs,” *IEEE transactions on industrial informatics / a publication of the IEEE Industrial Electronics Society*, vol. 2011, no. 99. p. 1, Sep. 2011, doi: 10.1109/TII.2011.2166770.

[104] N. Palastanga, *Anatomía y movimiento humano : estructura y funcionamiento*, 1a. ed. Barcelona:

Paidotribo, 2000.

[105] P. M. Stevens, J. Rheinstein, and S. R. Wurdeman, “Prosthetic Foot Selection for Individuals with Lower-Limb Amputation: A Clinical Practice Guideline,” *J. Prosthetics Orthot.*, vol. 30, no. 4, p. 180, Oct. 2018, doi: 10.1097/JPO.0000000000000181.

[106] M. S. Zahedi, W. D. Spence, S. E. Solomonidis, and J. P. Paul, “Alignment of lower-limb prostheses,” *J. Rehabil. Res. Dev.*, vol. 23, no. 2, pp. 2–19, 1986.

[107] R. Gailey, K. Allen, J. Castles, J. Kucharik, and M. Roeder, *Review of secondary physical conditions associated with lower-limb amputation and long-term prosthesis use.*, Third., vol. 45, no. 1. United States: Elsevier, 2013.

[108] M. Hekmatfard, F. Farahmand, and I. Ebrahimi, “Effects of prosthetic mass distribution on the spatiotemporal characteristics and knee kinematics of transfemoral amputee locomotion,” *Gait Posture*, vol. 37, no. 1, pp. 78–81, Jan. 2013, doi: 10.1016/J.GAITPOST.2012.06.010.

[109] T. Seel, J. Raisch, and T. Schauer, “IMU-Based Joint Angle Measurement for Gait Analysis,” *Sensors 2014, Vol. 14, Pages 6891-6909*, vol. 14, no. 4, pp. 6891–6909, Apr. 2014, doi: 10.3390/S140406891.

[110] E. C. Wentink, S. I. Beijen, H. J. Hermens, J. S. Rietman, and P. H. Veltink, “Intention detection of gait initiation using EMG and kinematic data,” *Gait Posture*, vol. 37, no. 2, pp. 223–228, Feb. 2013, doi: 10.1016/J.GAITPOST.2012.07.013.

[111] F. Leurs, A. Bengoetxea, A. M. Cebolla, C. De Saedeleer, B. Dan, and G. Cheron, “Planar covariation of elevation angles in prosthetic gait,” *Gait Posture*, vol. 35, no. 4, pp. 647–652, Apr. 2012, doi: 10.1016/J.GAITPOST.2011.12.017.

[112] M. RK, L. P, E. A, and K. R, “Comparison of energy cost in transtibial amputees using ‘prosthesis’ and ‘crutches without prosthesis’ for walking activities,” *Ann. Phys. Rehabil. Med.*, vol. 55, no. 4, pp. 252–262, May 2012, doi: 10.1016/J.REHAB.2012.02.006.

[113] M. Thomas-Pohl *et al.*, “Analyse couplée en IRM fonctionnelle et analyse de marche chez l’amputé : à propos d’un cas de plasticité cérébrale dans l’acquisition tardive de la marche chez une patiente

agénésique," *Ann. Phys. Rehabil. Med.*, vol. 56, p. e27, Oct. 2013, doi: 10.1016/J.REHAB.2013.07.177.

[114] M. W. Whittle, *Gait Analysis: An Introduction*, 3th ed. Oxford: Butterworth-Heinemann, 2001.

[115] J. S. Rietman, K. Postema, and J. H. B. Geertzen, "Gait analysis in prosthetics: Opinions, ideas and conclusions," *Prosthet. Orthot. Int.*, vol. 26, no. 1, pp. 50–57, Apr. 2002, doi: 10.1080/03093640208726621.

[116] N. Berger, "Analysis of Amputee," in *Atlas of Limb Prosthetics: Surgical, Prosthetic, and Rehabilitation Principle*, 2nd edition., B. HK and M. JW, Eds. 2002.

[117] B. P. Zeigler, T. Gon Kim, and H. Praehofer, *Theory of Modeling and Simulation*, 2nd edition. San Diego: Academic Press, 2000.

[118] L. Ljung, C. Andersson, K. Tiels, and T. B. Schön, "Deep Learning and System Identification," *IFAC-PapersOnLine*, vol. 53, no. 2, pp. 1175–1181, Jan. 2020, doi: 10.1016/J.IFACOL.2020.12.1329.

[119] G. Bonaccorso, *Machine Learning Algorithms*. Birmingham: Packt>, 2017.

[120] C. Tuena, M. Chiappini, C. Repetto, and G. Riva, "Artificial Intelligence in Clinical Psychology," *Ref. Modul. Neurosci. Biobehav. Psychol.*, Jan. 2020, doi: 10.1016/B978-0-12-818697-8.00001-7.

[121] T. Jo, "Unsupervised Learning," in *Machine Learning Foundations: Supervised, Unsupervised, and Advanced Learning*, Switzerland: Springer Nature, 2021, pp. 191–215.

[122] T. Caliński and J. Harabasz, "A dendrite method for cluster analysis," *Commun. Stat.*, vol. 3, no. 1, pp. 1–27, Jan. 1974, doi: 10.1080/03610927408827101.

[123] D. L. Davies and D. W. Bouldin, "A Cluster Separation Measure," *IEEE Trans. Pattern Anal. Mach. Intell.*, vol. PAMI-1, no. 2, pp. 224–227, 1979, doi: 10.1109/TPAMI.1979.4766909.

[124] A. F. M. Alkarkhi and W. A. A. Alqaraghuli, "Factor Analysis," in *Easy Statistics for Food Science with R*, Academic Press, 2019, pp. 143–159.

[125] H. Honda and T. Kobayashi, "Fuzzy Control of Bioprocess," in *Comprehensive Biotechnology*, 2th ed., vol. 2, Academic Press, 2011, pp. 863–873.

[126] F. Gabbiani and S. J. Cox, “Neuronal Networks,” in *Mathematics for Neuroscientists*, Elsevier, 2017, pp. 489–527.

[127] A. K. Jain, J. Mao, and K. M. Mohiuddin, *Artificial neural networks: A tutorial*, vol. 29, no. 3. New Zealand: Springer, 1996.

[128] L. O and N. U, “Novel maximum-margin training algorithms for supervised neural networks,” *IEEE Trans. neural networks*, vol. 21, no. 6, pp. 972–984, Jun. 2010, doi: 10.1109/TNN.2010.2046423.

[129] A. Anuse and V. Vyas, “A novel training algorithm for convolutional neural network,” *Complex Intell. Syst. 2016 23*, vol. 2, no. 3, pp. 221–234, Sep. 2016, doi: 10.1007/S40747-016-0024-6.

[130] J. G. Lenard, M. Pietrzyk, and L. Cser, “Knowledge Based Modeling,” in *Mathematical and Physical Simulation of the Properties of Hot Rolled Products*, Elsevier Science Ltd, 1999, pp. 279–318.

[131] N. Nehra, P. Sangwan, and D. Kumar, “Aritificial Neural Networks: A Comprehensive Review,” in *Handbook of Machine Learning for Computational Optimization: Applications and Case Studies*, V. Jain, S. Juneja, A. Juneja, and R. Kannan, Eds. CRC Press, 2000, pp. 1–20.

[132] H. Okut, “Bayesian Regularized Neural Networks for Small n Big p Data,” *Artif. Neural Networks - Model. Appl.*, pp. 1–20, Oct. 2016, doi: 10.5772/63256.

[133] D. J. C. MacKay, “Bayesian Interpolation,” in *Neural Computation*, vol. 4, no. 3, MIT Press - Journals, 1992, pp. 415–447.

[134] J. Shi, Y. Zhu, F. Khan, and G. Chen, “Application of Bayesian Regularization Artificial Neural Network in explosion risk analysis of fixed offshore platform,” *J. Loss Prev. Process Ind.*, vol. 57, pp. 131–141, Jan. 2019, doi: 10.1016/J.JLP.2018.10.009.

[135] C. Cortes and V. Vapnik, “Support-vector networks,” *Mach. Learn. 1995 203*, vol. 20, no. 3, pp. 273–297, Sep. 1995, doi: 10.1007/BF00994018.

[136] M. Awad and R. Khanna, “Support Vector Regression,” *Effic. Learn. Mach.*, pp. 67–80, 2015, doi: 10.1007/978-1-4302-5990-9_4.

[137] C. Cortes, V. Vapnik, and L. Saitta, “Support-Vector Networks Editor,” *Mach. Leaming*, vol. 20, pp. 273–297, 1995.

[138] G. A. Betancourt, “Las Máquinas de Soporte Vectorial (SVMs),” *Sci. Tech.*, vol. 11, no. 27, pp. 67–72, Apr. 2005, Accessed: Oct. 28, 2021. [Online]. Available: https://www.redalyc.org/pdf/849/84911698014.pdf.

[139] T. Hastie, R. Tibshirani, and J. Friedman, “Support Vector Machines and Flexible Discriminants,” in *The Elements of Statistical Learning*, T. Hastie, R. Tibshirani, and J. Friedman, Eds. New York: Springer, New York, NY, 2009, pp. 417–458.

[140] M. Awad and R. Khanna, “Support Vector Machines for Classification,” in *Efficient Learning Machines*, M. Awad and R. Khanna, Eds. Apress, 2015, pp. 39–66.

[141] S. Hongmao, “Quantitative Structure–Activity Relationships: Promise, Validations, and Pitfalls,” in *A Practical Guide to Rational Drug Design*, S. Hongmao, Ed. Woodhead Publishing, 2016, pp. 163–192.

[142] D. Berrar, “Cross-Validation,” *Encycl. Bioinforma. Comput. Biol. ABC Bioinforma.*, vol. 1–3, pp. 542–545, Jan. 2019, doi: 10.1016/B978-0-12-809633-8.20349-X.

[143] R. Jain, M. K. Camarillo, and W. T. Stringfellow, “Detection,” in *Drinking Water Security for Engineers, Planners, and Managers*, Butterworth-Heinemann, 2014, pp. 83–123.

[144] J. H. Bowker, “Chapter 25 – Organization and Operation of an Education - and Research - Based Diabetic Foot Clinic,” in *Levin and O’Neal’s The Diabetic Foot (Seventh Edition)*, Seventh Ed., J. H. Bowker and M. A. Pfeifer, Eds. Philadelphia: Mosby, 2008, pp. 497–504.

[145] J. Parvizi and G. K. Kim, “Chapter 9 - Amputation of the Lower Limb,” in *High Yield Orthopaedics*, J. Parvizi, G. K. Kim, and A. Editor, Eds. Philadelphia: W.B. Saunders, 2010, pp. 17–19.

[146] J. H. Bowker, B. Goldberg, and P. D. Poonekar, “Chapter 18A - Transtibial Amputation: Surgical Procedures and Immediate Postsurgical Management,” in *Atlas of Limb Prosthetics: Surgical, Prosthetic, and Rehabilitation Principles*, 2nd ed., St Louis, 1992, pp. 429–452.

[147] C. A. Miller, “Chapter 23 - Prosthetic management for the older adult with lower limb amputation,” in

Geriatric Physical Therapy (THIRD EDITION), THIRD EDIT., A. A. GUCCIONE, R. A. WONG, and D. AVERS, Eds. Saint Louis: Mosby, 2012, pp. 426–445.

[148] A. Livdans-Forret, "Management of a low back pain patient with a prosthesis and a foot drop orthotic," *The Journal of the Canadian Chiropractic Association*, vol. 49, no. 4. pp. 297–300, Dec. 2005.

[149] A. Eshraghi, Z. Safaeepour, M. D. Geil, and J. Andrysek, "Walking and balance in children and adolescents with lower-limb amputation: A review of literature," *Clin. Biomech.*, vol. 59, pp. 181–198, 2018, doi: https://doi.org/10.1016/j.clinbiomech.2018.09.017.

[150] M. M. Lusardi, M. Jorge, and C. C. Nielsen, *Orthotics and Prosthetics in Rehabilitation*, 3rd ed. Missouri: el Sevier, 2013.

[151] D. Sakaguchi, "Orthotics and Prosthetics in Rehabilitation," *Physiotherapy Canada*, vol. 65, no. 4. p. 399, 2013, doi: 10.3138/ptc.65.4.rev01.

[152] N. Berme, C. R. Purdey, and S. E. Solomonidis, "Measurement of prosthetic alignment," *Prosthet. Orthot. Int.*, vol. 2, no. 2, pp. 73–75, Aug. 1978, doi: 10.1080/03093647809177771.

[153] K. D. Reisinger, H. Casanova, Y. Wu, and C. Moorer, "Comparison of á priori alignment techniques for transtibial prostheses in the developing world - Pilot study," *Disabil. Rehabil.*, vol. 29, no. 11–12, pp. 863–872, 2007, doi: 10.1080/09638280701240243.

[154] J. Mizrahi, Z. Susak, R. Seliktar, and T. Najenson, "Alignment procedure for the optimal fitting of lower limb prostheses," *J. Biomed. Eng.*, vol. 8, no. 3, pp. 229–234, 1986, doi: https://doi.org/10.1016/0141-5425(86)90089-0.

[155] J. A. DeLisa, B. M. Gans, and N. E. Walsh, *Physical Medicine and Rehabilitation: Principles and Practice*, Fourth., no. v. 1. Philadelphia: Lippincott Williams & Wilkins, 2005.

[156] M. D. Geil and A. Lay, "Plantar foot pressure responses to changes during dynamic trans-tibial prosthetic alignment in a clinical setting.," *Prosthet. Orthot. Int.*, vol. 28, no. 2, pp. 105–114, Aug. 2004, doi: 10.1080/03093640408726695.

[157] G. Fiedler, B. A. Slavens, K. M. O'Connor, R. O. Smith, and B. J. Hafner, "Effects of physical exertion

on trans-tibial prosthesis users' ability to accommodate alignment perturbations.," *Prosthet. Orthot. Int.*, vol. 40, no. 1, pp. 75–82, Feb. 2016, doi: 10.1177/0309364614545419.

[158] J. E. Sanders, D. M. Bell, R. M. Okumura, and A. J. Dralle, "Effects of alignment changes on stance phase pressures and shear stresses on transtibial amputees: Measurements from 13 transducer sites," *IEEE Trans. Rehabil. Eng.*, vol. 6, no. 1, pp. 21–31, 1998, doi: 10.1109/86.662617.

[159] E. Isakov, J. Mizrahi, Z. Susak, I. Ona, and N. Hakim, "Influence of prosthesis alignment on the standing balance of below-knee amputees.," *Clin. Biomech. (Bristol, Avon)*, vol. 9, no. 4, pp. 258–262, Jul. 1994, doi: 10.1016/0268-0033(94)90008-6.

[160] D. H. K. Chow, A. D. Holmes, C. K. L. Lee, and S. W. Sin, "The Effect of Prosthesis Alignment on the Symmetry of Gait in Subjects with Unilateral Transtibial Amputation," *Prosthet. Orthot. Int.*, vol. 30, no. 2, pp. 114–128, Aug. 2006, doi: 10.1080/03093640600568617.

[161] A. Wouter, V. Creylman, J. S. Vander, and I. Jonkers, "Extension and anterior alignment of the prosthetic foot normalizes hip and knee loading symmetry in unilateral trans-tibial amputees," *Gait Posture*, vol. 49, p. 127, 2016, doi: https://doi.org/10.1016/j.gaitpost.2016.07.187.

[162] H. A. M. Seelen, S. Anemaat, H. M. H. Janssen, and J. H. M. Deckers, "Effects of prosthesis alignment on pressure distribution at the stump/socket interface in transtibial amputees during unsupported stance and gait.," *Clin. Rehabil.*, vol. 17, no. 7, pp. 787–796, Nov. 2003, doi: 10.1191/0269215503cr678oa.

[163] N. Tafti *et al.*, "A systematic review of variables used to assess clinically acceptable alignment of unilateral transtibial amputees in the literature," *Proc. Inst. Mech. Eng. Part H J. Eng. Med.*, vol. 232, no. 8, pp. 826–840, 2018, doi: 10.1177/0954411918789450.

[164] N. Jonkergouw, M. R. Prins, A. W. P. Buis, and P. van der Wurff, "The Effect of Alignment Changes on Unilateral Transtibial Amputee's Gait: A Systematic Review," *PLoS One*, vol. 11, no. 12, p. e0167466, Dec. 2016, [Online]. Available: https://doi.org/10.1371/journal.pone.0167466.

[165] E. S. Neumann, "State-of-the-Science Review of Transtibial Prosthesis Alignment Perturbation," *JPO J. Prosthetics Orthot.*, vol. 21, no. 4, 2009, [Online]. Available:

https://journals.lww.com/jpojournal/Fulltext/2009/10000/State_of_the_Science_Review_of_Transtibial.3.aspx.

[166] P. Davenport, S. Noroozi, P. Sewell, and S. Zahedi, "Systematic Review of Studies Examining Transtibial Prosthetic Socket Pressures with Changes in Device Alignment," *J. Med. Biol. Eng.*, vol. 37, no. 1, pp. 1–17, 2017, doi: 10.1007/s40846-017-0217-5.

[167] S. R. S. R. Koehler-McNicholas, R. D. R. D. Lipschutz, and S. A. S. A. Gard, "The biomechanical response of persons with transfemoral amputation to variations in prosthetic knee alignment during level walking," *J. Rehabil. Res. Dev.*, vol. 53, no. 6, pp. 1089–1106, 2016, doi: 10.1682/JRRD.2014.12.0311.

[168] X. Jia, S. Suo, F. Meng, and R. Wang, "Effects of alignment on interface pressure for transtibial amputee during walking," *Disabil. Rehabil. Assist. Technol.*, vol. 3, no. 6, pp. 339–343, 2008, doi: 10.1080/17483100802044634.

[169] T. Kobayashi, M. S. Orendurff, and D. A. Boone, "Dynamic alignment of transtibial prostheses through visualization of socket reaction moments," *Prosthet. Orthot. Int.*, vol. 39, no. 6, pp. 512–516, Dec. 2015, doi: 10.1177/0309364614545421.

[170] J. Xiaohong, L. Xiaobing, D. Peng, and M. Zhang, "The Influence of Dynamic Trans-tibial Prosthetic Alignment on Standing Plantar Foot Pressure," *Conf. Proc. IEEE Eng. Med. Biol. Soc.*, vol. 7, pp. 6916–8, 2005, doi: 10.1109/IEMBS.2005.1616096.

[171] H. Hashimoto, T. Kobayashi, F. Gao, M. Kataoka, M. S. Orendurff, and K. Okuda, "The effect of transverse prosthetic alignment changes on socket reaction moments during gait in individuals with transtibial amputation," *Gait Posture*, vol. 65, pp. 8–14, 2018, doi: 10.1016/j.gaitpost.2018.06.119.

[172] T. Kobayashi, M. S. Orendurff, M. Zhang, and D. A. Boone, "Effect of transtibial prosthesis alignment changes on out-of-plane socket reaction moments during walking in amputees," *J. Biomech.*, vol. 45, no. 15, pp. 2603–2609, 2012, doi: 10.1016/j.jbiomech.2012.08.014.

[173] D. A. Boone *et al.*, "Influence of malalignment on socket reaction moments during gait in amputees

with transtibial prostheses," *Gait Posture*, vol. 37, no. 4, pp. 620–626, 2013, doi: 10.1016/j.gaitpost.2012.10.002.

[174] G. Fiedler and M. S. Johnson, "Correlation of transtibial prosthetic alignment quality and step-by-step variance of gait," *J. Prosthetics Orthot.*, vol. 29, no. 1, pp. 19–25, 2017, doi: 10.1097/JPO.0000000000000113.

[175] A. Courtney, M. S. Orendurff, and A. Buis, "Effect of alignment perturbations in a trans-tibial prosthesis user: A pilot study," *J. Rehabil. Med.*, vol. 48, no. 4, pp. 396–401, 2016, doi: 10.2340/16501977-2075.

[176] J. Xiaohong, L. Xiaobing, D. Peng, and M. Zhang, "Influence of Prosthetic Sagittal Alignment on Trans-Tibial Amputee Gait and Compensating Pattern: A Case Study," *Tsinghua Sci. Technol.*, vol. 13, no. 5, pp. 581–586, 2008, doi: 10.1016/S1007-0214(08)70092-0.

[177] L. Fang, X. Jia, and R. Wang, "Modeling and simulation of muscle forces of trans-tibial amputee to study effect of prosthetic alignment," *Clin. Biomech.*, vol. 22, no. 10, pp. 1125–1131, 2007, doi: https://doi.org/10.1016/j.clinbiomech.2007.07.017.

[178] C. Beyaert, C. Grumillier, N. Martinet, J. Paysant, J.-M. André, and C. Beyaert, "Compensatory mechanism involving the knee joint of the intact limb during gait in unilateral below-knee amputees," *Gait Posture*, vol. 28, no. 2, pp. 278–284, 2008, doi: https://doi.org/10.1016/j.gaitpost.2007.12.073.

[179] T. Nomura, K. Watanabe, T. Nosaka, H. Matsubara, M. Akiyama, and K. Inui, "The relationship between trans-femoral prosthesis alignment and the center trajectory of plantar pressure in the frontal plane," *J. Phys. Ther. Sci.*, vol. 28, no. 2, pp. 576–579, Jan. 2016, doi: 10.1589/jpts.28.576.

[180] L. D. Fang, X. H. Jia, R. Wang, and S. Suo, "Simulation of the ligament forces affected by prosthetic alignment in a trans-tibial amputee case study," *Med. Eng. Phys.*, vol. 31, no. 7, pp. 793–798, 2009, doi: https://doi.org/10.1016/j.medengphy.2009.02.010.

[181] C. W. J. Chen *et al.*, "Evaluation of an instrument-assisted dynamic prosthetic alignment technique for individuals with transtibial amputation," *Prosthet. Orthot. Int.*, vol. 40, no. 4, pp. 475–483, 2016, doi:

10.1177/0309364615574161.

[182] T. Kobayashi, M. S. Orendurff, and D. A. Boone, “Effect of alignment changes on socket reaction moments during gait in transfemoral and knee-disarticulation prostheses: Case series,” *J. Biomech.*, vol. 46, no. 14, pp. 2539–2545, 2013, doi: 10.1016/j.jbiomech.2013.07.012.

[183] B. Kolarova, M. Janura, Z. Svoboda, and M. Elfmark, “Limits of Stability in Persons With Transtibial Amputation With Respect to Prosthetic Alignment Alterations,” *Arch. Phys. Med. Rehabil.*, vol. 94, no. 11, pp. 2234–2240, 2013, doi: https://doi.org/10.1016/j.apmr.2013.05.019.

[184] C. Grumillier, N. Martinet, J. Paysant, J.-M. André, and C. Beyaert, “Compensatory mechanism involving the hip joint of the intact limb during gait in unilateral trans-tibial amputees,” *J. Biomech.*, vol. 41, no. 14, pp. 2926–2931, 2008, doi: https://doi.org/10.1016/j.jbiomech.2008.07.018.

[185] E. S. Neumann, J. Brink, K. Yalamanchili, and J. S. Lee, “Regression estimates of pressure on transtibial residual limbs using load cell measurements of the forces and moments occurring at the base of the socket,” *J. Prosthetics Orthot.*, vol. 25, no. 1, pp. 1–12, 2013, doi: 10.1097/JPO.0b013e31827b360c.

[186] D. A. Boone *et al.*, “Perception of socket alignment perturbations in amputees with transtibial prostheses,” *J. Rehabil. Res. Dev.*, vol. 49, no. 6, pp. 843–854, 2012, doi: 10.1682/JRRD.2011.08.0143.

[187] E. S. Neumann, J. Brink, K. Yalamanchili, and J. S. Lee, “Use of a load cell and force-moment analysis to examine transtibial prosthesis foot rollover kinetics for anterior-posterior alignment perturbations,” *J. Prosthetics Orthot.*, vol. 24, no. 4, pp. 160–174, 2012, doi: 10.1097/JPO.0b013e31826f66f0.

[188] A. J. Ikeda, K. D. Reisinger, M. Malkush, Y. Wu, M. L. Edwards, and R. S. Kistenberg, “Á priori alignment of transtibial prostheses: A comparison and evaluation of three methods,” *Disabil. Rehabil. Assist. Technol.*, vol. 7, no. 5, pp. 381–388, 2012, doi: 10.3109/17483107.2011.637284.

[189] J. M. van Velzen, H. Houdijk, W. Polomski, and C. A. M. van Bennekom, “Usability of gait analysis in the alignment of trans-tibial prostheses: A clinical study,” *Prosthet. Orthot. Int.*, vol. 29, no. 3, pp. 255–267, 2005, doi: 10.1080/03093640500238857.

[190] B. Burkett, J. Smeathers, and T. M. Barker, “A Computer Model to Simulate the Swing Phase of a Transfemoral Prosthesis,” *J. Appl. Biomech.*, vol. 20, no. 1, pp. 25–37, 2004, doi: 10.1123/jab.20.1.25.

[191] A. Fridman, I. Ona, and E. Isakov, “The influence of prosthetic foot alignment on trans-tibial amputee gait,” *Prosthet. Orthot. Int.*, vol. 27, no. 1, pp. 17–22, 2003.

[192] A. H. Hansen, M. R. Meier, M. Sam, D. S. Childress, and M. L. Edwards, “Alignment of trans-tibial prostheses based on roll-over shape principles,” *Prosthet. Orthot. Int.*, vol. 27, no. 2, pp. 89–99, 2003, doi: 10.1080/03093640308726664.

[193] S. S. Salgado and A. T. Velásquez, “Analysis of the frontal plane alignment in AK prosthesis,” *Pan Am. Heal. Care Exch.*, pp. 1–5, 2013.

[194] T. Kobayashi, M. S. Orendurff, A. K. Arabian, T. G. Rosenbaum-Chou, and D. A. Boone, “Effect of prosthetic alignment changes on socket reaction moment impulse during walking in transtibial amputees,” *J. Biomech.*, vol. 47, no. 6, pp. 1315–1323, 2014, doi: https://doi.org/10.1016/j.jbiomech.2014.02.012.

[195] T. Kobayashi, A. K. Arabian, M. S. Orendurff, T. G. Rosenbaum-Chou, and D. A. Boone, “Effect of alignment changes on socket reaction moments while walking in transtibial prostheses with energy storage and return feet,” *Clin. Biomech.*, vol. 29, no. 1, pp. 47–56, 2014, doi: 10.1016/j.clinbiomech.2013.11.005.

[196] G. Pirouzi, N. A. Abu Osman, S. Ali, and M. Davoodi Makinejad, “A new prosthetic alignment device to read and record prosthesis alignment data,” *Proc. Inst. Mech. Eng. Part H J. Eng. Med.*, vol. 231, no. 12, pp. 1127–1132, 2017, doi: 10.1177/0954411917735082.

[197] T. Kobayashi, M. S. Orendurff, M. Zhang, and D. A. Boone, “Individual responses to alignment perturbations in socket reaction moments while walking in transtibial prostheses,” *Clin. Biomech.*, vol. 29, no. 5, pp. 590–594, 2014, doi: https://doi.org/10.1016/j.clinbiomech.2014.04.002.

[198] T. Kobayashi, M. S. Orendurff, M. Zhang, and D. A. Boone, “Effect of alignment changes on sagittal and coronal socket reaction moment interactions in transtibial prostheses,” *J. Biomech.*, vol. 46, no. 7,

pp. 1343–1350, 2013, doi: 10.1016/j.jbiomech.2013.01.026.

[199] J. B. J. Bussmann, K. M. Culhane, H. L. D. Horemans, G. M. Lyons, and H. J. Stam, "Validity of the prosthetic activity monitor to assess the duration and spatio-temporal characteristics of prosthetic walking," *IEEE Trans. Neural Syst. Rehabil. Eng.*, vol. 12, no. 4, pp. 379–386, 2004, doi: 10.1109/TNSRE.2004.840495.

[200] S. Tominaga, K. Sakuraba, and F. Usui, "The effects of changes in the sagittal plane alignment of running-specific transtibial prostheses on ground reaction forces," *J. Phys. Ther. Sci.*, vol. 27, no. 5, pp. 1347–1351, May 2015, doi: 10.1589/jpts.27.1347.

[201] X. Zhang, M. R. Paquette, and S. Zhang, "A comparison of gait biomechanics of flip-flops, sandals, barefoot and shoes," *J. Foot Ankle Res.*, vol. 6, no. 1, p. 45, Dec. 2013, doi: 10.1186/1757-1146-6-45.

[202] S. Franklin, M. J. Grey, N. Heneghan, L. Bowen, and F.-X. Li, "Barefoot vs common footwear: A systematic review of the kinematic, kinetic and muscle activity differences during walking," *Gait Posture*, vol. 42, no. 3, pp. 230–239, 2015, doi: https://doi.org/10.1016/j.gaitpost.2015.05.019.

[203] S. M. Kung, P. W. Fink, P. Hume, and S. P. Shultz, "Kinematic and kinetic differences between barefoot and shod walking in children," *Footwear Sci.*, vol. 7, no. 2, pp. 95–105, May 2015, doi: 10.1080/19424280.2015.1014066.

[204] M. Spoden, U. Nimptsch, and T. Mansky, "Amputation rates of the lower limb by amputation level-observational study using German national hospital discharge data from 2005 to 2015," *BMC Heal. Serv Res.*, vol. 16, no. 1, pp. 1–8, 2019, doi: 10.1186/s12913-018-3759-5.

[205] B. Imam, W. C. Miller, H. C. Finlayson, J. J. Eng, and T. Jarus, "Incidence of lower limb amputation in Canada," *Can J Public Heal.*, vol. 108, no. 4, pp. 374–380, 2017, doi: 10.17269/CJPH.108.6093.

[206] G. Fiedler and X. Zhang, "Quantifying accommodation to prosthesis interventions in persons with lower limb loss," *Gait Posture*, vol. 50, pp. 14–16, 2016, doi: https://doi.org/10.1016/j.gaitpost.2016.08.016.

[207] F. Yang and G. A. King, "Dynamic gait stability of treadmill versus overground walking in young

adults," *J. Electromyogr. Kinesiol.*, vol. 31, pp. 81–87, 2016, doi: https://doi.org/10.1016/j.jelekin.2016.09.004.

[208] H. Stolze *et al.*, "Gait analysis during treadmill and overground locomotion in children and adults," *Electroencephalogr. Clin. Neurophysiol. Mot. Control*, vol. 105, no. 6, pp. 490–497, 1997, doi: https://doi.org/10.1016/S0924-980X(97)00055-6.

[209] T. Schmalz, M. Bellmann, E. Proebsting, and S. Blumentritt, "Effects of Adaptation to a Functionally New Prosthetic Lower-Limb Component: Results of Biomechanical Tests Immediately after Fitting and after 3 Months of Use," *JPO J. Prosthetics Orthot.*, vol. 26, no. 3, 2014, [Online]. Available: https://journals.lww.com/jpojournal/Fulltext/2014/07000/Effects_of_Adaptation_to_a_Functionally_New.4.aspx.

[210] A. B. Wanamaker, R. R. Andridge, and A. M. W. Chaudhari, "When to biomechanically examine a lower-limb amputee: A systematic review of accommodation times," *Prosthet. Orthot. Int.*, vol. 41, no. 5, pp. 431–445, Dec. 2016, doi: 10.1177/0309364616682385.

[211] H. Bateni and S. J. Olney, "Effect of the Weight of Prosthetic Components on the Gait of Transtibial Amputees," *JPO J. Prosthetics Orthot.*, vol. 16, no. 4, pp. 113–120, Oct. 2004, doi: 10.1097/00008526-200410000-00004.

[212] A. Eshraghi, N. A. Abu Osman, M. Karimi, H. Gholizadeh, E. Soodmand, and W. A. B. Wan Abas, "Gait biomechanics of individuals with transtibial amputation: effect of suspension system," *PLoS One*, vol. 9, no. 5, pp. e96988–e96988, May 2014, doi: 10.1371/journal.pone.0096988.

[213] J. Andrysek and A. Eshraghi, "Influence of Prosthetic Socket Design and Fitting on Gait BT - Handbook of Human Motion," B. Müller, S. I. Wolf, G.-P. Brueggemann, Z. Deng, A. McIntosh, F. Miller, and W. S. Selbie, Eds. Cham: Springer International Publishing, 2017, pp. 1–25.

[214] C. A. Rábago and J. M. Wilken, "The Prevalence of Gait Deviations in Individuals With Transtibial Amputation.," *Mil. Med.*, vol. 181, no. S4, pp. 30–37, Nov. 2016, doi: 10.7205/MILMED-D-15-00505.

[215] L. A. Nolasco, D. C. Morgenroth, A. K. Silverman, and D. H. Gates, "Effects of anterior-posterior shifts

in prosthetic alignment on the sit-to-stand movement in people with a unilateral transtibial amputation," *J. Biomech.*, vol. 109, Aug. 2020, doi: 10.1016/j.jbiomech.2020.109926.

[216] M. S. Pinzur, W. Cox, J. Kaiser, T. Morris, A. Patwardhan, and L. Vrbos, "The effect of prosthetic alignment on relative limb loading in persons with trans-tibial amputation: a preliminary report.," *J. Rehabil. Res. Dev.*, vol. 32, no. 4, pp. 373–377, Nov. 1995.

[217] T. Zhang, X. Bai, F. Liu, R. Ji, and Y. Fan, "The effect of prosthetic alignment on hip and knee joint kinetics in individuals with transfemoral amputation," *Gait Posture*, vol. 76, pp. 85–91, Feb. 2020, doi: 10.1016/j.gaitpost.2019.11.006.

[218] M. Raggi, D. Monari, A. G. Cutti, G. Gregori, and G. Verni, "A novel protocol to evaluate the human-prosthesis interaction fusing kinematics, kinetics and infrared thermography." Accessed: May 05, 2021. [Online]. Available: www.inail-ricerca.it.

[219] A. F. Mak, M. Zhang, and D. A. Boone, "State-of-the-art research in lower-limb prosthetic biomechanics-socket interface: a review.," *J. Rehabil. Res. Dev.*, vol. 38, no. 2, pp. 161–174, 2001.

[220] J. E. Sanders, "Thermal response of skin to cyclic pressure and pressure with shear: a technical note.," *J. Rehabil. Res. Dev.*, vol. 37, no. 5, pp. 511–515, 2000.

[221] D. Arthur and S. Vassilvitskii, "K-Means++: The Advantages of Careful Seeding," in *Proceedings of the Eighteenth Annual ACM-SIAM Symposium on Discrete Algorithms*, 2007, pp. 1027–1035.

[222] R. A. Johnson and Dean W. Wichern, "Factor Analysis and Inference for Structured Covariance Matrices," in *Applied Multivariate Statistical Analysis*, 6th ed., New Jersey, USA, 2008, p. 767.

[223] C. Fortin, S. Nadeau, and H. Labelle, "Inter-trial and test-retest reliability of kinematic and kinetic gait parameters among subjects with adolescent idiopathic scoliosis," *Eur. Spine J.*, vol. 17, no. 2, pp. 204–216, Feb. 2008, doi: 10.1007/s00586-007-0469-9.

[224] T. M. Cook, K. P. Farrell, I. A. Carey, J. M. Gibbs, and G. E. Wiger, "Effects of Restricted Knee Flexion and Walking Speed on the Vertical Ground Reaction Force During Gait," *J. Orthop. Sport. Phys. Ther.*, vol. 25, no. 4, pp. 236–244, 1997, doi: 10.2519/jospt.1997.25.4.236.

[225] T. B. Muniz, R. Moraes, and R. R. J. Guirro, “Lower limb ice application alters ground reaction force during gait initiation,” *Brazilian J. Phys. Ther.*, vol. 19, no. 2, pp. 114–121, 2015, doi: 10.1590/bjpt-rbf.2014.0080.

[226] M. Błażkiewicz, I. Wiszomirska, and A. Wit, “Comparison of four methods of calculating the symmetry of spatial-temporal parameters of gait.,” *Acta Bioeng. Biomech.*, vol. 16, no. 1, pp. 29–35, 2014.

[227] K. F. Weaver, V. Morales, S. L. Dunn, K. Godde, and P. F. Weaver, “Kruskal—Wallis,” in *An Introduction to Statistical Analysis in Research*, John Wiley & Sons, Ltd, 2017, pp. 353–391.

[228] C. Lewis, “Multiple Comparisons,” in *International Encyclopedia of Education*, Elsevier, 2010, pp. 312–318.

[229] R. B. McDonald, “Thermoregulation: Autonomic, Age-Related Changes,” L. R. B. T.-E. of N. Squire, Ed. Oxford: Academic Press, 2009, pp. 977–986.

[230] A. Martinez-Nicolas *et al.*, “Daytime variation in ambient temperature affects skin temperatures and blood pressure: Ambulatory winter/summer comparison in healthy young women,” *Physiol. Behav.*, vol. 149, pp. 203–211, 2015, doi: 10.1016/j.physbeh.2015.06.014.

[231] J. T. Peery, W. R. Ledoux, and G. K. Klute, “Residual-limb skin temperature in transtibial sockets,” *J. Rehabil. Res. Dev.*, vol. 42, no. 2, pp. 147–154, 2005, doi: 10.1682/JRRD.2004.01.0013.

[232] I. Kovač, V. Medved, and L. Ostojić, “Ground reaction force analysis in traumatic transtibial amputees’ gait,” *Coll. Antropol.*, vol. 33, no. SUPPL.2, pp. 107–114, 2009.

[233] A. M. Grabowski and S. D’Andrea, “Effects of a powered ankle-foot prosthesis on kinetic loading of the unaffected leg during level-ground walking,” *J. Neuroeng. Rehabil.*, vol. 10, no. 1, 2013, doi: 10.1186/1743-0003-10-49.

[234] L. Yang, S. E. Solomonidis, W. D. Spence, and J. P. Paul, “The influence of limb alignment on the gait of above-knee amputees,” *J. Biomech.*, vol. 24, no. 11, pp. 981–997, 1991, doi: 10.1016/0021-9290(91)90016-G.

[235] Y. Sagawa Jr., K. Turcot, S. Armand, A. Thevenon, N. Vuillerme, and E. Watelain, “Biomechanics and

physiological parameters during gait in lower-limb amputees: A systematic review," *Gait Posture*, vol. 33, no. 4, pp. 511–526, Apr. 2011, doi: 10.1016/j.gaitpost.2011.02.003.

[236] A. S. O. de C. Soares, E. Y. Yamaguti, L. Mochizuki, A. C. Amadio, and J. C. Serrão, "Biomechanical parameters of gait among transtibial amputees: a review," *Sao Paulo Medical Journal*, vol. 127. scielo, pp. 302–309, 2009.

[237] A. M. Cardenas-Torres, J. Uribe P., J. M. Font-Llagunes, A. M. Hernández, and J. A. Plata, "The Effect of Prosthetic Alignment on the Stump Temperature and Ground Reaction Forces during Gait in Transfemoral Amputees," *Gait Posture*, 2021.

[238] R. B. Davis, S. Õunpuu, D. Tyburski, and J. R. Gage, "A gait analysis data collection and reduction technique," *Hum. Mov. Sci.*, vol. 10, no. 5, pp. 575–587, Oct. 1991, doi: 10.1016/0167-9457(91)90046-Z.

[239] M. H. Schwartz and A. Rozumalski, "The gait deviation index: A new comprehensive index of gait pathology," *Gait Posture*, vol. 28, no. 3, pp. 351–357, Oct. 2008, doi: 10.1016/j.gaitpost.2008.05.001.

[240] M. B. I. Raez, M. S. Hussain, and F. Mohd-Yasin, "Techniques of EMG signal analysis: detection, processing, classification and applications," *Biol. Proced. Online*, vol. 8, no. 1, p. 11, Mar. 2006, doi: 10.1251/BPO115.

[241] R. Jane, P. Laguna, N. V. Thakor, and P. Caminal, "Adaptive baseline wander removal in the ECG: Comparative analysis with cubic spline technique," *Proc. - Comput. Cardiol. CIC 1992*, pp. 143–146, 1992, doi: 10.1109/CIC.1992.269426.

[242] V. Barbero Romero, "ECG baseline wander removal and noise suppression analysis in an embedded platform," Universidad Complutense de Madrid, Madrid, 2008.

[243] T. KK, L. J, T. YJ, Y. CW, L. FY, and Z. Z, "Clustering Analysis of Aging Diseases and Chronic Habits With Multivariate Time Series Electrocardiogram and Medical Records," *Front. Aging Neurosci.*, vol. 12, pp. 1–10, May 2020, doi: 10.3389/FNAGI.2020.00095.

[244] J. H. T. Viitasalo and P. V. Komi, "Signal characteristics of EMG during fatigue," *Eur. J. Appl. Physiol.*

Occup. Physiol. 1977 372, vol. 37, no. 2, pp. 111–121, Jun. 1977, doi: 10.1007/BF00421697.

[245] T. Roland, S. Amsuess, M. F. Russold, and W. Baumgartner, "Ultra-Low-Power Digital Filtering for Insulated EMG Sensing," *Sensors 2019, Vol. 19, Page 959*, vol. 19, no. 4, p. 959, Feb. 2019, doi: 10.3390/S19040959.

[246] L. L. Beranek and T. J. Mellow, "Introduction and terminology," in *Acoustics: Sound Fields and Transducers*, Academic Press, 2012, pp. 1–19.

[247] A. Phinyomark, P. Phukpattaranont, and C. Limsakul, "Feature reduction and selection for EMG signal classification," *Expert Syst. Appl.*, vol. 39, no. 8, pp. 7420–7431, Jun. 2012, doi: 10.1016/J.ESWA.2012.01.102.

[248] J. Chang, D. Chablat, F. Bennis, and L. Ma, "Estimating the EMG response exclusively to fatigue during sustained static maximum voluntary contraction," in *Advances in Intelligent Systems and Computing*, 2016, vol. 489, pp. 29–39, doi: 10.1007/978-3-319-41694-6_4.

[249] T. Y. Fukuda *et al.*, "Root Mean Square value of the electromyographic signal in the isometric torque of the quadriceps, hamstrings and brachial biceps muscles in female subjects," *J. Appl. Res.*, vol. 10, no. 1, pp. 32–40, Mar. 2010, Accessed: Oct. 13, 2021. [Online]. Available: https://go.gale.com/ps/i.do?p=HRCA&sw=w&issn=1537064X&v=2.1&it=r&id=GALE%7CA227012906&sid=googleScholar&linkaccess=fulltext.

[250] P. A. Karthick and S. Ramakrishnan, "Muscle fatigue analysis using surface EMG signals and time–frequency based medium-to-low band power ratio," *Electron. Lett.*, vol. 52, no. 3, pp. 185–186, Feb. 2016, doi: 10.1049/EL.2015.3460.

[251] A. Strazza, F. Verdini, L. Burattini, S. Fioretti, and F. Di Nardo, "Time-frequency analysis of surface EMG signals for maximum energy localization during walking," *IFMBE Proc.*, vol. 65, pp. 494–497, 2017, doi: 10.1007/978-981-10-5122-7_124.

[252] A. Strazza *et al.*, "A Time-Frequency Approach for the Assessment of Dynamic Muscle Co-contractions," *IFMBE Proc.*, vol. 68, no. 2, pp. 223–226, 2019, doi: 10.1007/978-981-10-9038-7_41.

[253] V. von Tscharner, M. Ullrich, M. Mohr, D. C. Marquez, and B. M. Nigg, “A wavelet based time frequency analysis of electromyograms to group steps of runners into clusters that contain similar muscle activation patterns,” *PLoS One*, vol. 13, no. 4, pp. 1–19, Apr. 2018, doi: 10.1371/JOURNAL.PONE.0195125.

[254] U. Rosenblum, I. Melzer, G. Zeilig, and M. Plotnik, “Muscle Activation Profile While Walking with Perturbations,” *bioRxiv*, pp. 1–28, Jan. 2021, doi: 10.1101/2021.01.13.426393.

[255] W. JM, P. SA, N. BM, and von T. V, “Surface EMG shows distinct populations of muscle activity when measured during sustained sub-maximal exercise,” *Eur. J. Appl. Physiol.*, vol. 86, no. 1, pp. 40–47, 2001, doi: 10.1007/S004210100508.

[256] V. von Tscharner, M. Ullrich, M. Mohr, D. C. Marquez, and B. M. Nigg, “Beta, gamma band, and high-frequency coherence of EMGs of vasti muscles caused by clustering of motor units,” *Exp. brain Res.*, vol. 236, no. 11, pp. 3065–3075, Nov. 2018, doi: 10.1007/S00221-018-5356-6.

[257] P. Grosse, M. J. Cassidy, and P. Brown, “EEG–EMG, MEG–EMG and EMG–EMG frequency analysis: physiological principles and clinical applications,” *Clin. Neurophysiol.*, vol. 113, no. 10, pp. 1523–1531, Oct. 2002, doi: 10.1016/S1388-2457(02)00223-7.

[258] N. R. Smalheiser, “ANOVA,” in *Data Literacy*, Academic Press, 2017, pp. 149–155.

[259] M. Halaki and K. Ginn, “Normalization of EMG Signals: To Normalize or Not to Normalize and What to Normalize to?,” *Comput. Intell. Electromyogr. Anal. - A Perspect. Curr. Appl. Futur. Challenges*, Oct. 2012, doi: 10.5772/49957.

[260] M. Y. PM and D. JB, “Voluntary changes in step width and step length during human walking affect dynamic margins of stability,” *Gait Posture*, vol. 36, no. 2, pp. 219–224, Jun. 2012, doi: 10.1016/J.GAITPOST.2012.02.020.

[261] S. M. Bruijn and J. H. van Dieën, “Control of human gait stability through foot placement,” *J. R. Soc. Interface*, vol. 15, no. 143, pp. 1–11, 2018, doi: 10.1098/RSIF.2017.0816.

[262] M. M. A. ; A. A. Khan;, “Electromyography-based Fatigue Assessment During Endurance Testing by

Different Vibration Training Protocols," *Iran. Rehabil. J.*, vol. 19, no. 1, pp. 85–98, 6375, doi: 10.32598/IRJ.19.1.1150.1.

[263] A. Phinyomark, S. Thongpanja, H. Hu, P. Phukpattaranont, and C. Limsakul, "The Usefulness of Mean and Median Frequencies in Electromyography Analysis," *Comput. Intell. Electromyogr. Anal. - A Perspect. Curr. Appl. Futur. Challenges*, Oct. 2012, doi: 10.5772/50639.

[264] J. Fernando Ramírez-Patiño, D. Faviana Gutiérrez-Rôa, & Alexander, and A. Correa-Espinal, "Comfort perception assessment in persons with transfemoral amputation," *DYNA*, vol. 82, pp. 194–202, 2015, doi: 10.15446/dyna.v82n191.44700.

[265] D. A. D. A. Boone *et al.*, "Perception of socket alignment perturbations in amputees with transtibial prostheses," *J. Rehabil. Res. Dev.*, vol. 49, no. 6, pp. 843–854, 2012, doi: 10.1682/JRRD.2011.08.0143.

[266] D. A. Boone *et al.*, "Influence of malalignment on socket reaction moments during gait in amputees with transtibial prostheses," *Gait Posture*, vol. 37, no. 4, pp. 620–626, 2013, doi: 10.1016/j.gaitpost.2012.10.002.

[267] T. Kobayashi, M. S. Orendurff, and D. A. Boone, "Dynamic alignment of transtibial prostheses through visualization of socket reaction moments," *Prosthet. Orthot. Int.*, vol. 39, no. 6, pp. 512–516, 2015, doi: 10.1177/0309364614545421.

[268] S.-S. Lee, S. T. Choi, and S.-I. Choi, "Classification of Gait Type Based on Deep Learning Using Various Sensors with Smart Insole," *Sensors (Basel).*, vol. 19, no. 8, Apr. 2019, doi: 10.3390/S19081757.

[269] L. R, M. T, H. A, and N. K, "Implementation of machine learning for classifying prosthesis type through conventional gait analysis," *Annu. Int. Conf. IEEE Eng. Med. Biol. Soc. IEEE Eng. Med. Biol. Soc. Annu. Int. Conf.*, vol. 2015, pp. 202–205, Nov. 2015, doi: 10.1109/EMBC.2015.7318335.

[270] A. M. Cardenas, C. Isaza, J. Uribe, and A. M. Hernadez, "Gait parameters identification for the differentiation of neurodegenerative diseases using classifiers," *2018 Glob. Med. Eng. Phys. Exch. Am. Heal. Care Exch.*, pp. 1–5, Mar. 2018, doi: 10.1109/GMEPE-PAHCE.2018.8400751.

[271] L. A. Luengas Contreras, “Modelo de alineación estática para prótesis transtibiales,” Universidad Javeriana, Bogotá, 2016.

[272] L. A. Luengas, H. A. Hernandez, and D. C. Toloza Cano, “MVS en la alineación estática de prótesis transtibiales,” *Rev. vínculos*, vol. 14, no. 2, pp. 119–126, Dec. 2017, doi: 10.14483/2322939X.12785.

[273] A. M. Cárdenas, J. Andrysek, J. Uribe P., A. M. Hernández, and J. A. Plata, “Technical and procedural considerations relating to the prosthetic alignment of transfemoral and transtibial prostheses: A systematic review,” 2020.

[274] G. Fiedler, B. A. Slavens, K. M. O’Connor, R. O. Smith, and B. J. Hafner, “Effects of physical exertion on trans-tibial prosthesis users’ ability to accommodate alignment perturbations,” *Prosthet. Orthot. Int.*, vol. 40, no. 1, pp. 75–82, 2016, doi: 10.1177/0309364614545419.

[275] T. Kobayashi, M. S. Orendurff, A. K. Arabian, T. G. Rosenbaum-Chou, and D. A. Boone, “Effect of prosthetic alignment changes on socket reaction moment impulse during walking in transtibial amputees,” *J. Biomech.*, vol. 47, no. 6, pp. 1315–1323, 2014, doi: 10.1016/j.jbiomech.2014.02.012.

[276] Clip Art, “Pelvis Clipart,” *http://www.clipartpanda.com/*, Dec. 13, 2021. http://images.clipartpanda.com/pelvis-clipart-54678_pelvis_lg.gif (accessed Dec. 13, 2021).

[277] Unknown, “TÉCNICAS PARA SABER: Cuerpo Humano CAP. I: HUESOS,” Aug. 13, 2015. http://tecnicasparasaber.blogspot.com/2015/08/cuerpo-humano-cap-i-huesos.html (accessed Dec. 13, 2021).

[278] Wikimedia Commons, “Human Anatomy Kenhub,” *File:Inner hip muscles (preview) - Human Anatomy Kenhub 1.webm*, Jan. 03, 2015. https://commons.wikimedia.org/wiki/File:Inner_hip_muscles_(preview)_-_Human_Anatomy_Kenhub_1.webm (accessed Dec. 13, 2021).

[279] J. Leyva, “How Do Muscles Grow? The Science Of Muscle Growth,” *General Health*, Dec. 31, 2020. https://www.builtlean.com/muscles-grow/ (accessed Dec. 13, 2021).

[280] V. Rajt’úková, M. Michalíková, L. Bednarcíková, A. Balogová, and J. Živčák, “Biomechanics of Lower

Limb Prostheses," *Procedia Eng.*, vol. 96, pp. 382–391, Jan. 2014, doi: 10.1016/J.PROENG.2014.12.107.

Appendix RP.

PROTOCOLO DE REGISTRO DE DATOS

El siguiente documento describe el protocolo y los instrumentos que serán utilizados para el registro de información personal, médica y antropométrica de los voluntarios, los criterios de inclusión-exclusión, los protocolos de registro de electromiografía, la captura de movimiento para el análisis de marcha, gasto metabólico y la grabación con la cámara térmica.

DESCRIPCIÓN GENERAL.

Este estudio busca registrar un conjunto de variables de una población de adultos sanos y con amputación de tipo transfemoral, con el fin de determinar un protocolo que permita la alineación de prótesis transfemorales. El registro de datos se realizará en dos tiempos diferentes, por lo que se solicitará información de contacto. Se capturarán señales de electromiografía superficial, se realizará un análisis de marcha utilizando cámaras infrarrojas, se registrará el gasto metabólico y se medirá la temperatura del muñón utilizando cámaras térmicas. El voluntario debe responder al siguiente cuestionario para definir si cumple con los criterios de inclusión.

Descripción del mecanismo de captación de los participantes

La población seleccionada a participar en el presente estudio incluye adultos sanos y adultos con amputación de tipo transfemoral. El registro de pacientes amputados se realizará bajo la supervisión de la Fundación Mahavir-Kmina. Para los pacientes sanos, como valores de control, se registrarán las señales electromiográficas de las extremidades y se realizará la captura de movimiento.

Procedimiento de registro de pacientes amputados.

Cada paciente deberá manifestar su interés de participar en la investigación.

Los pacientes interesados deberán responder a los criterios de inclusión y exclusión.

Los datos de los ítems 3-5, se recolectarán en el día 1 de la visita a Mahavir-Kmina. Luego de cumplir con los requisitos, se recolectarán datos de contacto.

Nombres:	
Apellidos:	
Dirección:	
Ciudad de residencia:	
Municipio de residencia:	
Teléfono:	
Correo electrónico:	
Edad (años):	
Género:	

Luego se registrará información antropométrica. La medición antropométrica se debe realizar en una camilla, con el paciente en ropa interior y relajado sobre esta.

Peso (Kg):	
Altura (cm):	
Índice de Masa Corporal (IMC):	
Longitud Miembro Inferior sano:	Esta distancia se mide desde la espina iliaca hasta el maléolo medial (pasando a través de la rodilla)
Ancho de pelvis:	Con el paciente acostado supino, se asegura que la pelvis esté correctamente alineada. Identificar los puntos anterior y posterior de las espinas iliacas y se mide la distancia entre estas con el pelvímetro. (escala superior cm)
Altura de la pelvis:	Para medir esto se siguen 3 pasos: Identificar el trocánter mayor. Se flexiona la cadera del paciente a su máxima flexión de la extremidad. Se rota la cadera hacia adentro-internamente. Se ubica el trocánter mayor con los dedos (protuberancia ósea) Se marca el punto con un lápiz de maquillaje.

	Se deja extendida la extremidad. Ubicar el plano horizontal que pasa a través del trocánter mayor. Se utiliza la regla larga para cruzar a través del trocánter mayor. La regla debe quedar de forma paralela a la camilla. La regla más pequeña se ubica perpendicularmente al plano del trocánter. Se ubica la regla entre la espina iliaca anterior superior y el plano del trocánter. Medir la altura entre la espina iliaca anterior superior y el plano del trocánter. Se deja fija la regla pequeña y la regla larga se ubica paralelamente a la espina iliaca anterior superior. Se mide la distancia. Para corroborar la medición, se verifica que la altura de la pelvis y el diámetro de los tobillos sean similares (<2cm).
Altura de la rodilla:	Con el paciente en supino, se flexiona la rodilla a 90° y se verifica con el goniómetro. Se mide todo el segmento, desde parte externa del muslo, paralelo al peroné, pasando por el tobillo hasta la planta del pie.
Ancho de la rodilla:	Se flexiona la rodilla para ubicar el epicóndilo lateral y el medial. Estas prominencias óseas se palpan con la mano. Luego se mide el ancho de la rodilla utilizando el pelvímetro.
Ancho del tobillo:	Con el paciente en la camilla, se flexiona la rodilla y se palpa la articulación del tobillo para ubicar los maléolos lateral y medial. Finalmente se debe medir con el pelvímetro.
Circunferencia del tobillo:	Se mide con el metro flexible el diámetro de la pierna arriba del tobillo.
Circunferencia de pantorrilla	Se mide con el metro flexible el diámetro de la pantorrilla.
Largo del pie sano (cm):	Se mide desde el talón hasta la punta del dedo grueso.
Ancho del pie sano (cm):	Se mide la parte más ancha del pie.

Circunferencia pélvica:	Diámetro del vientre medido rodeando las espinas iliacas.

Luego se registrará información antropométrica. La medición antropométrica se debe realizar en una camilla, con el paciente en ropa interior y relajado sobre esta.

Fecha de amputación:	Día / mes / año
Lado de amputación:	Izquierdo / Derecho
Estado del muñón:	
Ángulo de flexión del muñón:	Con el paciente de pie, se usa el goniómetro para medir el ángulo de inclinación del fémur en relación con la línea vertical anatómica del cuerpo (usar laser o plomada), estando en la máxima posición de extensión, pero sin rotación pélvica.
Ángulo de aducción del muñón:	Con el paciente de pie, se usa el goniómetro para medir el ángulo de inclinación del fémur respecto a la línea vertical, con la pelvis alineada horizontalmente y el fémur en la posición de aducción tan horizontal como sea posible.
Dimensión A-P del muñón:	Se ubica la tuberosidad isquiática, palpando en la parte inferior de la nalga cuando el muslo está flexionado. Se mide desde la parte anterior del tendón del aductor largo al punto más inferior de la tuberosidad isquiática.
Perímetro del muñón:	Se mide horizontalmente, a nivel isquiático y a intervalos de 5 cm. por debajo de este mismo nivel.
Longitud del muñón:	La longitud del muñón se mide desde la tuberosidad isquiática o el trocánter mayor hasta el extremo carnoso (a esto se conoce como longitud actual).
Longitud del muñón efectivo (long. Fémur)	La longitud del muñón efectiva se mide desde la tuberosidad isquiática o el trocánter mayor hasta la extremidad de hueso.

Se deberán realizar algunas mediciones de la prótesis, luego que termine de ser construida.

Longitud de la prótesis:	
Longitud del encaje:	
Longitud de la extremidad con prótesis:	
Altura de unidad articular:	
Largo pie protésico:	
Ancho pie protésico:	
Largo pie sano:	
Ancho pie sano:	

CRITERIOS DE INCLUSIÓN Y EXCLUSIÓN

El siguiente cuestionario busca evaluar los criterios de inclusión o exclusión para tener en cuenta en el proyecto de investigación. Solicitamos su colaboración contestando las siguientes preguntas.

	SI	NO
¿Es usted mayor de edad y menor de 50 años?		
¿Posee historial clínico de enfermedades óseas, cardiacas, respiratorias o problemas de diabetes?		
¿Ha consumido alcohol en las últimas 48 horas?		
¿Consume con algún tipo de droga o alucinógeno?		
¿Sufre de vértigo u otro problema que le afecte el equilibrio?		
¿Se encuentra bajo tratamiento médico?		
¿Toma actualmente algún medicamento que le produce mareos?		
¿Se encuentra en estado de embarazo o proyecta estarlo en los próximos 8 meses?		

Los voluntarios que cumplan alguno de los criterios de exclusión no serán tenido en cuenta en el registro de los datos. A los voluntarios que continúen el proceso se les pedirá que respondan a las siguientes preguntas que recogen datos personales y antropométricos.

PROTOCOLOS Y EQUIPOS A UTILIZAR

A continuación, se da explicación del procedimiento que se seguirá para realizar el registro de los datos y los equipos que se utilizarán para esto.

PROTOCOLO DE ANÁLISIS DE MARCHA

El análisis de marcha estudia la biomecánica, la dinámica y las variables espacio-temporales de los movimientos del cuerpo durante el desplazamiento erguido sobre diferentes superficies.

El cuerpo humano puede modelarse aproximando sus partes en enlaces rígidos interconectados mediante puntos de articulación, para lo cual se utilizan diferentes técnicas. El uso de cámaras infrarrojas y marcadores refractivos permiten realizar esta aproximación, por cual es muy importante definir los lugares en los que se deben localizar los marcadores reflectivos.

Los protocolos para ubicar los marcadores son diversos, sin embargo, el protocolo modificado Helen Hayes [1] y Davis [2] son comúnmente utilizados para el análisis de marcha sana y protésica. En la figura 1 se ejemplifica la ubicación de los marcadores en el protocolo Helen Hayes. Este utiliza 15 marcadores reflectivos que son captados por 6 cámaras infrarrojas ubicas de tal manera que graban en 3D el cuerpo del voluntario. Los marcadores reflectivos cuentan con una cinta ultradelgada y estéril que se usa para adherirla al cuerpo.

Cada uno de los marcadores se pone paralelamente en cada extremidad comenzando desde los pies a la pelvis. Se suministrará a cada voluntario una cuchilla de afeitar nueva que se desechará luego de su uso. Al final de la prueba se suministrará vaselina para que se aplique en las zonas depiladas.

Uno de los investigadores acompañado de personal de Mahavir Kmina realizarán la ubicación de los marcadores en el cuerpo del voluntario. Para tener contacto con el voluntario

se utilizarán guantes médicos plásticos desechables. Se ubicarán cada uno de los siguientes puntos de referencia o prominencias óseas: quinto metatarso, maléolo lateral, cabeza del peroné, epicóndilo lateral, cabeza del trocánter, espina iliaca anterior de la izquierda y de la derecha, la vértebra S1 y la vértebra C7.

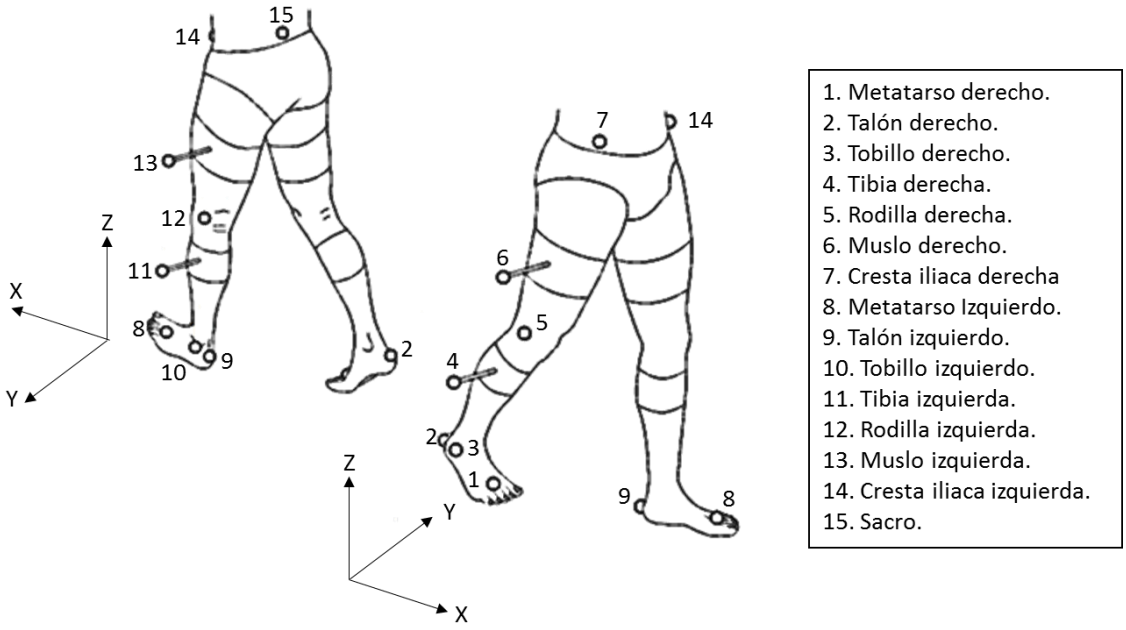

a. Ubicación de los marcadores sobre los miembros inferiores.

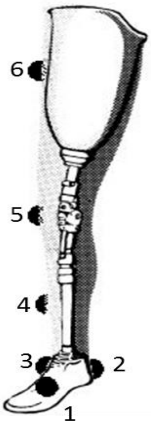

b. Ubicación de los marcadores sobre una prótesis transfemoral

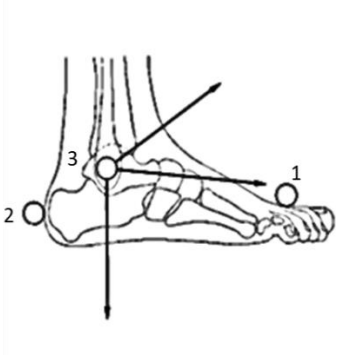

c. Ubicación de los marcadores sobre el pie.

d. Ubicación de los marcadores sobre el pie protésico.

Figura 1. Protocolo Helen Hayes para la captura de movimiento.

Los marcadores se ubicarán de la siguiente manera. A la altura de la pelvis, los marcadores 7 y 14 se ubican a la altura de la espina iliaca anterosuperior derecha e izquierda. El marcador 15 se ubica sobre la unión de la quinta vértebra lumbar y el hueso sacro. A la altura de la mitad del fémur en el muslo izquierdo, se ubica el número 13. En el caso de una miembro protésico, este se colocará paralelamente en el encaje. En la rodilla derecha, sobre el epicóndilo lateral se ubica el número 5. Para el caso de una rodilla protésica, el marcador será ubicado paralelamente a la extremidad sana. En la mitad de la tibia izquierda se adhiere el número 11. Para el tobillo, a la altura del maléolo lateral se ubica el número 10. Sobre el tobillo el número 9 y en el quinto metatarso se ubica el 8. De igual forma se realiza sobre el pie protésico.

En el protocolo Davis se utilizan 22 marcadores. La ubicación se realiza siguiendo el procedimiento anterior. La ubicación se debe realizar en el miembro izquierdo y derecho de la siguiente manera: Un marcador se ubica sobre el quinto metatarsiano, un marcador sobre el talón, otros sobre el maléolo lateral, la cabeza del peroné, el epicóndilo femoral lateral, la cabeza del trocánter, sobre la espina iliaca anterior superior, un único sobre el sacro (vértebra S1), sobre el acromion y finalmente un único marcador en la vértebra C7.

Las imágenes captadas por las cámaras son enviadas a un computador que utiliza el software Smart Analyser (BTS) para determinar la posición exacta del marcador y realizar un análisis espacio-temporal de la marcha del voluntario.

Las siguientes imágenes de referencia muestran los equipos que serán utilizados para la toma de datos y algunas gráficas que se obtienen del software de análisis de marcha.

a. Cámaras infrarrojas. b. Marcadores reflectivos.

Figura 2. Imagen de referencia los equipos de la marca BTS para el registro de movimiento.

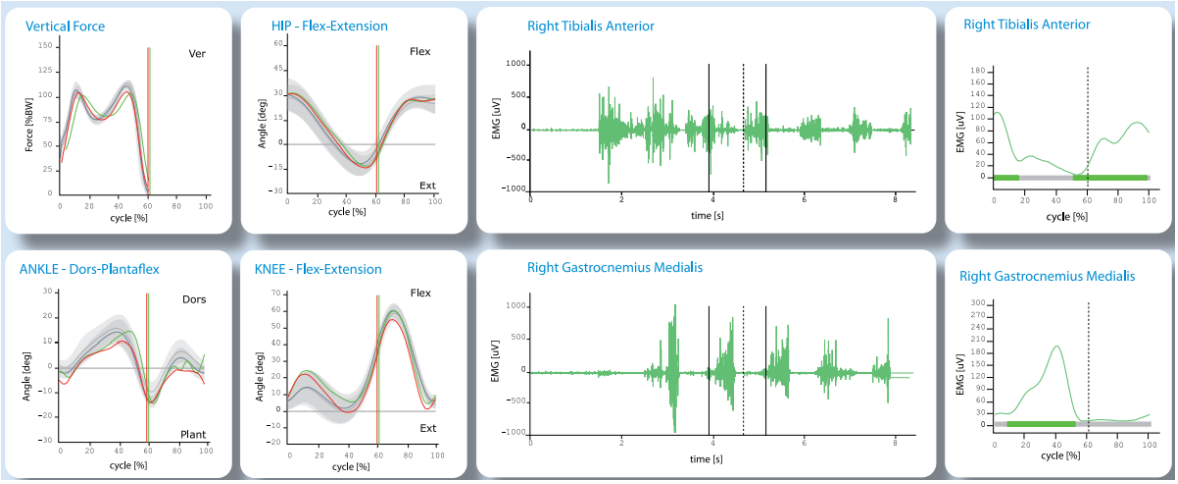

Figura 3. Imagen de referencia de los resultados del análisis de marcha.

PROTOCOLO DE ELECTROMIOGRAFÍA

El registro de electromiografía se realiza sobre un solo miembro para que las medidas puedan compararse con amputados. Los datos se registran sobre un conjunto de músculos de la pierna y el muslo, debido a su importancia para la marcha, sugeridos en [3]. Se utilizan 4 canales del equipo de electromiografía Mobi.

De la pierna:

- Tibial Anterior (TA): Dorsiflexión del tobillo e inversión del pie.
- Gastrocnemio medial (GM): producen flexión plantar del pie y en menor proporción, flexión de la pierna.

Del muslo:

Isquiotibial:

- Bíceps Femoral (BF): Extiende el muslo, flexiona la pierna y la rota lateralmente cuando la rodilla cuando está flexionada.

Cuádriceps: Extensor del miembro inferior

- Recto Femoral (RF): Músculo biarticular que flexiona el muslo y genera extensión de la rodilla.

Para ubicar los electrodos se sigue el siguiente procedimiento sugerido por BTS [4] basado en las referencias [3], [5] y [6]. Para el análisis de marcha se registran los músculos de la pierna y del muslo. A continuación, se presenta el procedimiento completo seguido por BTS, para el cual se utilizan imágenes de referencia tomadas del video explicativo [7].

Para los músculos de la pierna:

- Se pide al paciente que se recueste sobre una camilla.
- Se pide que flexione la rodilla 80° para identificar la cabeza del peroné.
- Se identifica el borde inferior del maléolo lateral.
- Se mide con un metro la distancia entre los puntos. La distancia se divide en 1/4 y se marcan los puntos proximal y distal.
- Se marcan los puntos que se observan en la fotografía.

Figura 4. Ubicación de puntos.

Mientras el paciente flexiona la rodilla, se identifica en la cresta anterior de la tibia en el En el ¼ superior de la pierna. A 1cm aproximadamente del punto se ubica el electrodo en el tibial anterior.

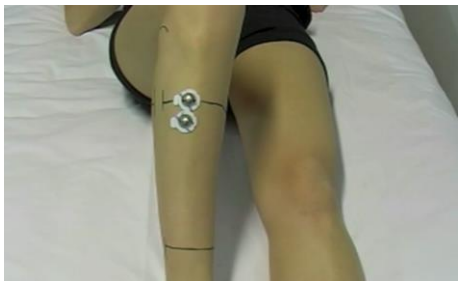

Figura 5. Ubicación del tibial anterior.

Para ubicar gastrocnemio medial, se pide que el paciente en supino y con la rodilla extendida, se marcan en el ¼ superior de la pierna el punto medial y lateral, como se aprecia en la foto.

a) Ubicación del gastrocnemio medial.
Figura 6. Ubicación del Gastrocnemio.

Para los músculos del muslo:

Con la extremidad extendida, se traza una línea sobre el borde superior de la rodilla. Luego se marca la espina iliaca anterior superior. Se mide la distancia completa y se divide entre 2. En este punto se adhieren los electrodos del recto femoral.

Figura 7. Ubicación del recto femoral.

Para el bíceps femoral, se debe seguir la línea entre la tuberosidad isquiática y la cabeza del peroné. Medir la distancia y dividirla entre 3. Se marca el tercio distal y allí se adhieren los electrodos en este punto.

Figura 8. Ubicación del bíceps femoral.

PROTOCOLO DE CAPTURA INFRARROJA

El registro de la temperatura del muñón se realizará mediante la cámara térmica GOBI 640 que puede apreciarse en la siguiente fotografía. Antes de iniciar las pruebas de alineación el paciente reposará por un tiempo de 20 minutos, sin prótesis, y se capturarán 4 fotografías del muñón: lateral, medial, anterior y posterior, para conocer la temperatura de referencia del miembro residual sin ningún esfuerzo.

Figura 9. Cámara Térmica GOBI 640.

El voluntario, luego de una prueba de alineación, deberá retirarse la prótesis e inmediatamente después se tomarán 4 fotos del muñón: de vista lateral, medial, anterior y posterior.

FORMATO DE RECOLECCIÓN DE DATOS

Los siguientes datos se utilizarán únicamente para clasificación y contacto del voluntario durante el registro de los datos. Esta información se solicitará en dos ocasiones, durante la recolección de información para la construcción del protocolo y durante la validación del modelo.

Información de contacto

Nombres:	
Apellidos:	
Dirección:	
Ciudad de residencia:	
Municipio de residencia:	
Teléfono:	
Correo electrónico:	
Edad (años):	
Género:	

Información de antropométrica

Peso (Kg):	
Altura (cm):	
Índice de Masa Corporal (IMC):	
Longitud Miembro Inferior sano:	
Circunferencia pélvica:	
Ancho de pelvis:	
Altura de la pelvis:	
Altura de eje de rotación de la rodilla:	
Ancho de la rodilla:	
Diámetro de la rodilla:	
Altura de eje de rotación de la rodilla:	
Ancho del tobillo:	
Diámetro del tobillo:	
Circunferencia de pantorrilla	
Talla pie sano (cm):	
Longitud de miembro sano:	

Información del miembro residual.

Fecha de amputación:	
Lado de amputación:	
Estado del muñón:	
Ángulo de flexión del muñón:	

Ángulo de aducción del muñón:	
Dimensión A-P del muñón:	
Perímetro del muñón:	
Circunferencia pélvica:	
Longitud del muñón:	

Información de la prótesis.

Longitud de la prótesis:	
Longitud del encaje:	
Longitud de la extremidad con prótesis:	
Altura de unidad articular:	
Largo pie prótesico:	
Ancho pie prótesico:	
Largo pie sano:	
Ancho pie sano:	

Referencias

[1] Leonardo Broche-Vázquez, Roberto Sagaró-Zamora, Claudia Ochoa-Díaz, Antonio Padilha-Lanari-Bó, y Félix A. Martinez-Nariño, «Análisis cinemático y dinámico de las prótesis transfemorales. Implicaciones clínicas,» Ingeniería Mecánica, vol. 19, nº 3, pp. 150-157, 2016.

[2] Ayman Assi, Ismat Ghanem, François Lavaste y Wafa Skalli, «Gait analysis in children and uncertainty assessment for Davis protocol and Gillette Gait Index,» Gait & Posture, vol. 30, nº 1, p. 22–26, 2009.

[3] Yves Blanc y Ugo Dimanico, «Electrode Placement in Surface Electromyography (sEMG) "Minimal Crosstalk Area" (MCA),» The Open Rehabilitation Journal, vol. 3, nº 1, pp. 110-126, 2010.

[4] BTS Bioengineering, «BTS FREEWALK,» [En línea]. Available: http://www.btsbioengineering.com/products/surface-emg/bts-freewalk/. [Último acceso: 08 Febrero 2017].

[5] D. Winter y H. Yack. , «EMG profiles during normal human walking: stride-to-stride and inter-subject variability,» Electroencephalography and Clinical Neurophysiology, vol. 67, nº 5, p. 402–411, 1987.

[6] Annachiara Strazza, Alessandro Mengarelli, Sandro Fioretti, Laura Burattini, Valentina Agostini, Marco Knaflitz y Francesco Di Nardo , «Surface-EMG analysis for the quantification of thigh muscle dynamic,» Gait & Posture, vol. 51, nº 1, p. 228–233, 2017.

[7] «Educational Webinar: BTS GAITLAB - Step3: EMG probes application,» 11 Marzo 2014. [En línea]. Available: http://www.btsbioengineering.com/reserved-area/application_webinars/BTSEW_BTS_GAITLAB-Step2_Anthropometric_measures_and_markers_placement.mov. [Último acceso: 08 Febrero 2017].

[8] ARD Sport Science, «Oxycon Mobile,» [En línea]. Available: http://www.ardsport.com/?uid=171. [Último acceso: 08 Mayo 2017].

[9] Ottobock, «Safety data sheet: 616T/83T - ThermoLyn clear (copolyester),» 01 Enero 2016. [En línea]. Available: https://professionals.ottobockus.com/media/pdf/616T_83T_en-US.pdf. [Último acceso: 08 Febrero 2017].

[10] LimbTex Prosthetic & Orthotic, «LimbTex Petg Diagnostic Socket Material,» 2014. [En línea]. Available: http://www.limbtex.com/plastics/prosthetics/limbplex-petg-diagnostic-socket-material. [Último acceso: 08 mayo 2017].

Appendix IC.

UNIVERSIDAD DE ANTIOQUIA	**ACTA APROBACION PROYECTOS**	**FACULTAD DE MEDICINA**
		CÓDIGO F-017-00
		VERSIÓN 01

Acta de aprobación **No. 008**

Nombre del proyecto: "Evaluación de estrategia combinada para mejorar la adherencia de sujetos amputados por artefactos explosivos (AEI) al uso de prótesis de miembros inferior de bajo costo".

Investigadora Principal: Juliana Uribe Pérez

Versión No 1

Enmienda revisada: NO

Fecha de aprobación**: 24 de mayo del 2018**

El Comité de Ética del Instituto de Investigaciones Médicas se constituyó mediante Resolución del Consejo de Facultad en reunión del 30 de mayo 2008, acta 177 y está regido por los principios éticos vigentes en la Resolución 003480 del 4 de octubre de 1993, la Declaración de Helsinki de 2008, la Asamblea Médica Mundial y el Departamento de Salud y Servicios Humanos del Instituto Nacional de Salud de los Estados Unidos de Norteamérica Resolución 2378 del 2008. En ellos se delinean las normas científicas, técnicas y administrativas para la investigación en seres humanos.

El Instituto de Investigaciones Médicas certifica que:

1. Se revisaron los siguientes documentos en el presente proyecto:
   a. Resumen del proyecto (NO)
   b. Protocolo de investigación (SI)
   c. Formato de recolección de datos (SI)
   d. Formato de consentimiento informado (SI)
   e. Manual del investigador (NO)
   f. Evaluaciones de otros comités de ética (NO)
2. El proyecto fue aprobado por los siguientes miembros: Gabriel Jaime Montoya Montoya, Dra. Sonia del Pilar Agudelo López, Dr. José Antonio García Pereañez, Dra. Olga Lucia Giraldo Salazar, Dra. Paula Andrea Velilla Hernández, María Aurora Gallo Rodríguez y representante de la comunidad.
3. El comité considera que el proyecto no contiene tensiones éticas que vulnere los derechos y el bienestar de los participantes. El riesgo involucrado en el estudio es:
   a) Sin riesgo ( )
   b) Riesgo mínimo (x)
   c) Riesgo mayor que el mínimo ( )
4. El comité considera que tanto la forma de obtención del consentimiento cuando aplica como las medidas tomadas para proteger el bienestar y los derechos de los participantes son adecuadas. No aplica

5. El comité se reserva el derecho de hacer nuevas revisiones del proyecto a solicitud de alguno o algunos de sus miembros o de las directivas institucionales con el fin de revisar lo relacionado con el bienestar y los derechos de los participantes en la investigación.
6. El comité deberá informar a las directivas institucionales correspondientes cualquier evento tocante con faltas de cumplimiento de las obligaciones del investigador en el desarrollo del proyecto, de las solicitudes del comité o suspensiones del proyecto por razones de tipo ético.
7. Se informara a la dirección del Instituto de Investigaciones sobre situaciones como: 1) efectos dañinos que se ocasionen a los participantes de esta investigación; 2) situaciones que signifiquen riesgos para los participantes o para personas independientes; 3) cambios ocurridos en el proyecto que fueran aprobados por el comité; y 4) situaciones distintas que de alguna manera puedan influenciar negativamente el buen desarrollo de la investigación.
8. La aprobación de este proyecto tendrá una duración de un año a partir de la fecha de aprobación; si se debe continuar por más tiempo, deberá someterse a aprobaciones anuales hasta la finalización del mismo. El investigador deberá anexar la documentación pertinente para cada nueva revisión del proyecto por parte del comité.

El investigador deberá informar al comité y al Instituto sobre los siguientes eventos:

a. Cambios que se realicen en el proyecto, los cuales deberán ser aprobados en una nueva sesión del comité.
b. Situaciones imprevistas que puedan implicar riesgos para los participantes.
c. Efectos adversos que ocurran en los participantes, en las 24 horas siguientes a su ocurrencia.
d. Alteraciones del rumbo de la investigación que alteren la adecuada proporción entre riesgos y beneficios.
e. Las decisiones tomadas por comités de ética de otras instituciones que participen en el proyecto.
f. Los informes parciales, finales o de suspensión temporal o permanente del proyecto, con las debidas razones que los justifiquen.

El investigador deberá presentar informes parciales del estudio cada (6) meses.

En este proyecto no se encontraron conflictos de interés por parte de los investigadores.

Sugerencias y comentarios: Favor Si el proyecto pasa a la convocatoria enviar informe de avance noviembre de 2018.

Nota: Para efectos de la investigación sólo podrá utilizarse el Consentimiento Informado avalado, con el sello del Comité de Bioética.

Appendix PA.

Volunteers recorded.

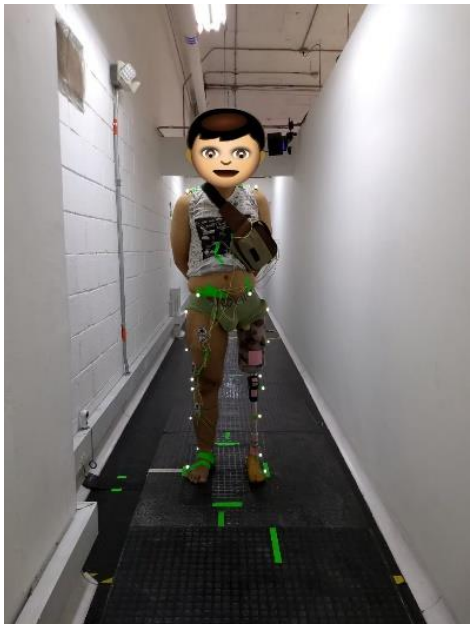

Amputee 1. Male, 34 years old.

Amputation cause: Traffic Accident

Amputee 2. Male, 44 years old.

Amputation cause: Vascular

Amputee 3. Male, 50 years old.

Amputation cause: Gunshot

Amputee 4. Male, 53 years old.

Amputation cause: Traffic Accident

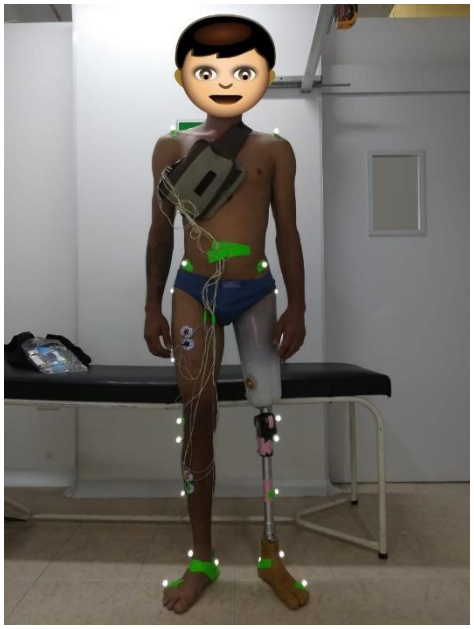

Amputee 5. Male, 29 years old.

Amputation cause: Gunshot

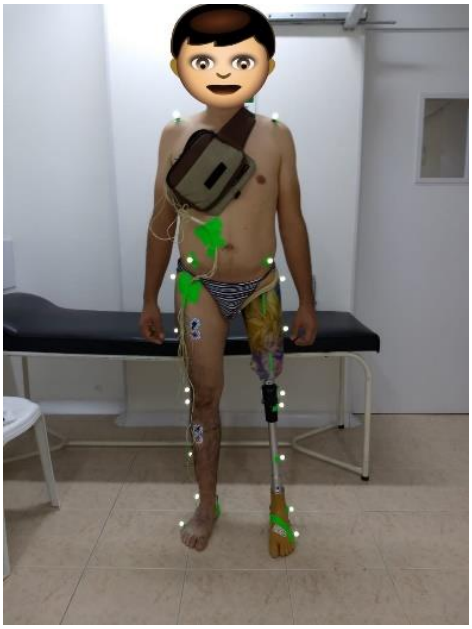

Amputee 6. Male, 33 years old.

Amputation cause: Traffic Accident

Amputee 7. Male, 45 years old.

Amputation cause: Traffic Accident

Amputee 8. Female, 51 years old.

Amputation cause: Traffic Accident

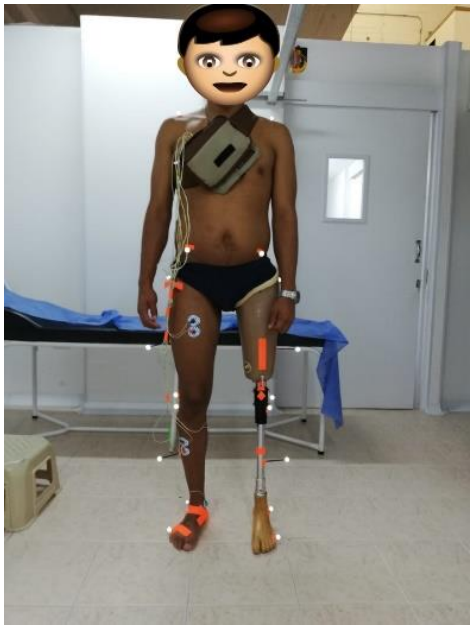

Amputee 9. Male, 25 years old.

Amputation cause: Traffic Accident

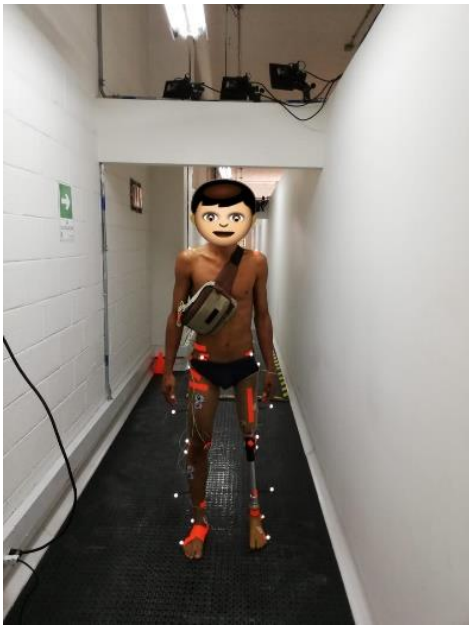

Amputee 10. Male, 35 years old.

Amputation cause: Traffic Accident

Amputee 11. Male, 29 years old.

Amputation cause: Traffic Accident

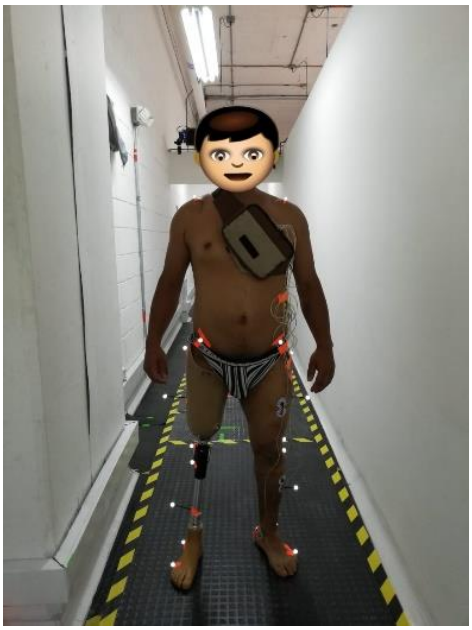

Amputee 12. Male, 34 years old.

Amputation cause: Traffic Accident

Amputee 13. Male, 33 years old.

Amputation cause: Traffic Accident

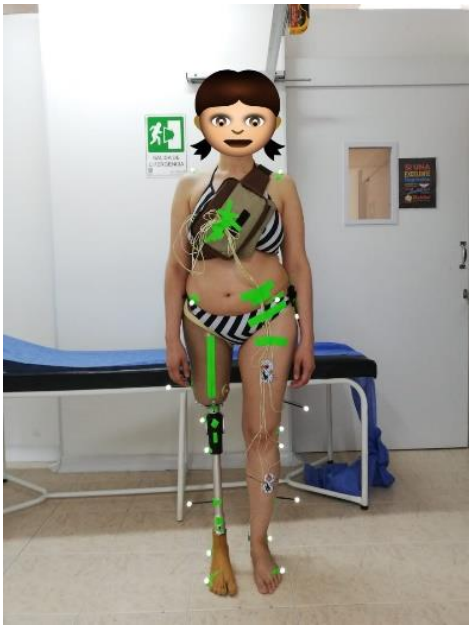

Amputee 14. Female, 30 years old.

Amputation cause: Cancer

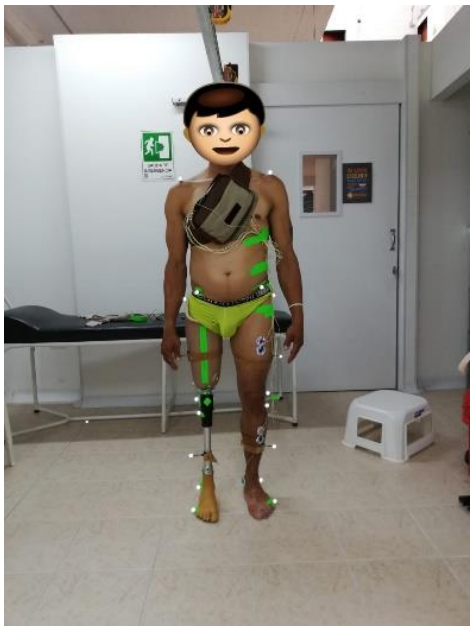

Amputee 15. Male, 35 years old.

Amputation cause: Work Accident

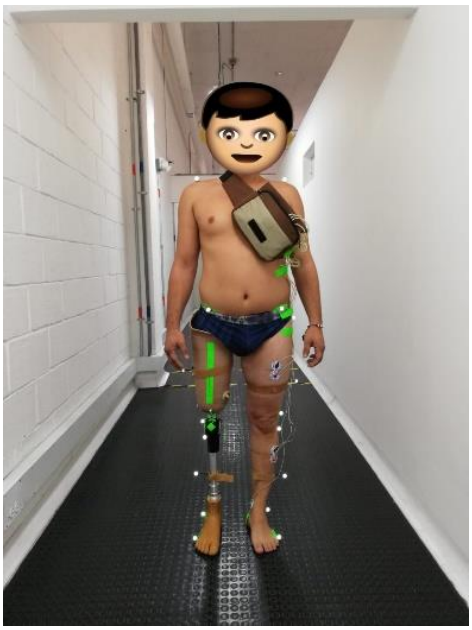

Amputee 6. Male, 37 years old.

Amputation cause: Gunshot

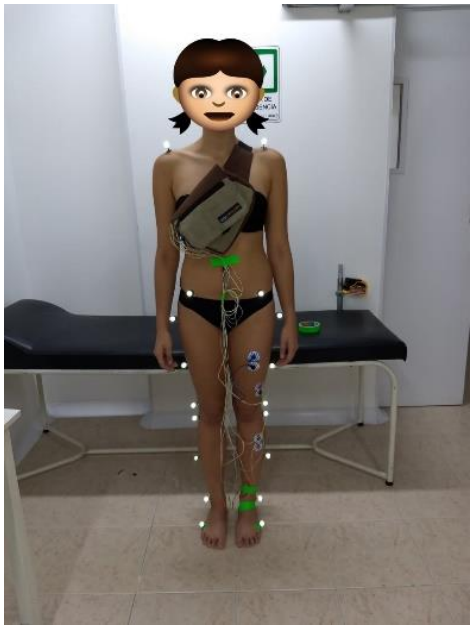

Control 1. Female, 21 years old.

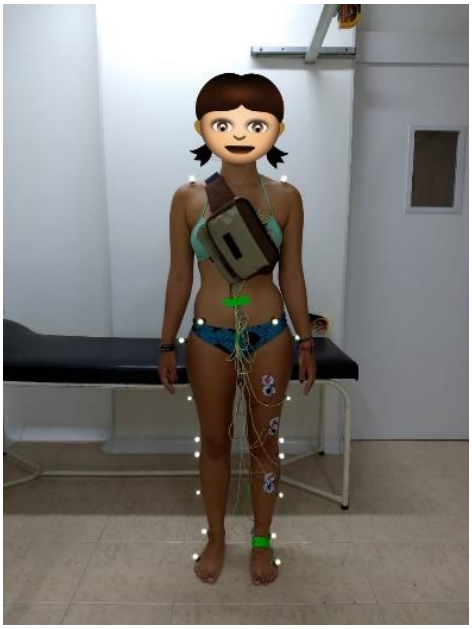

Control 2. Female, 21 years old.

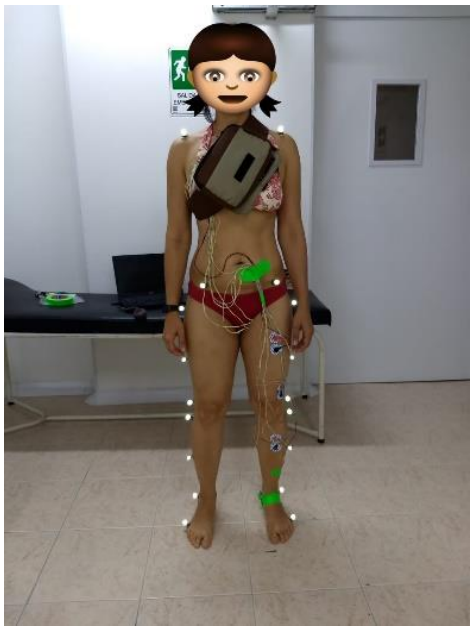

Control 3. Female, 46 years old.

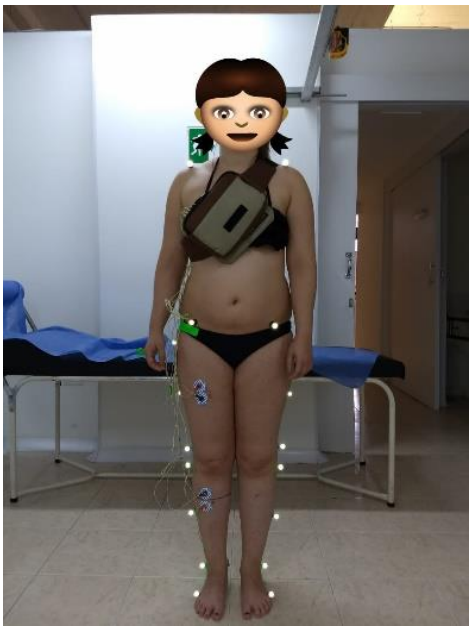

Control 4. Female, 27 years old.

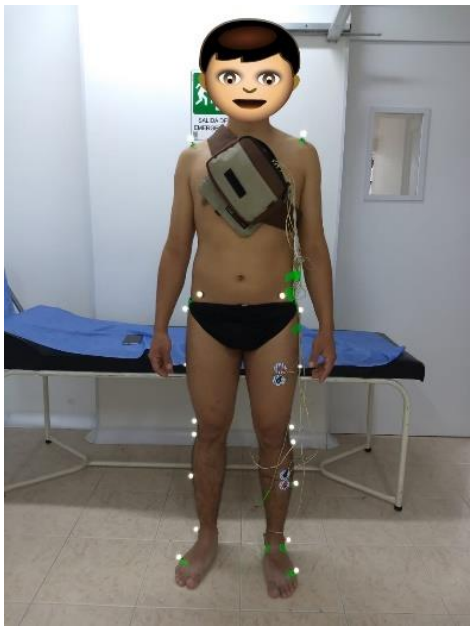

Control 5. Male, 28 years old.

Control 6. Male, 49 years old.

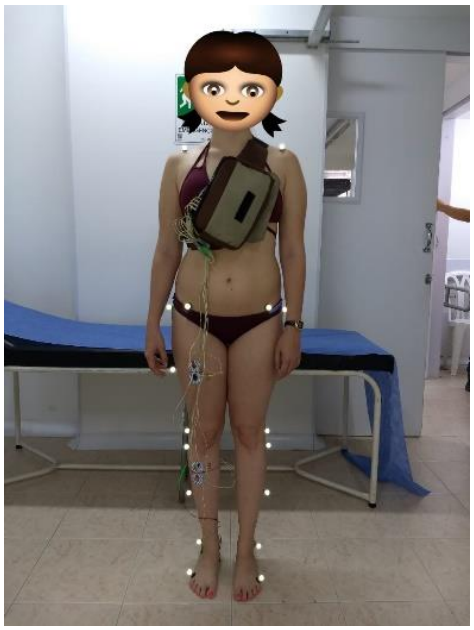

Control 7. Female, 24 years old.

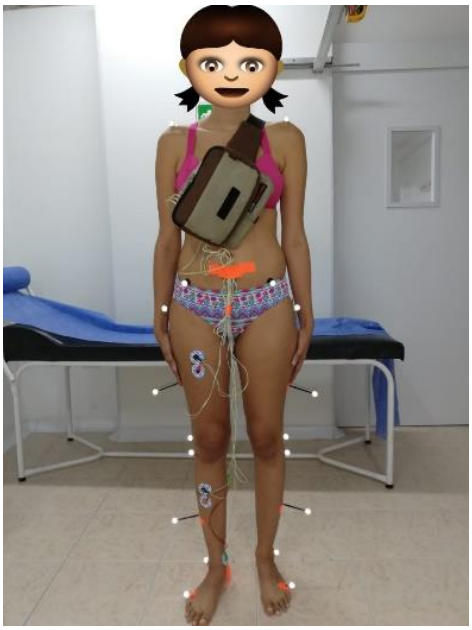

Control 8. Female, 27 years old.

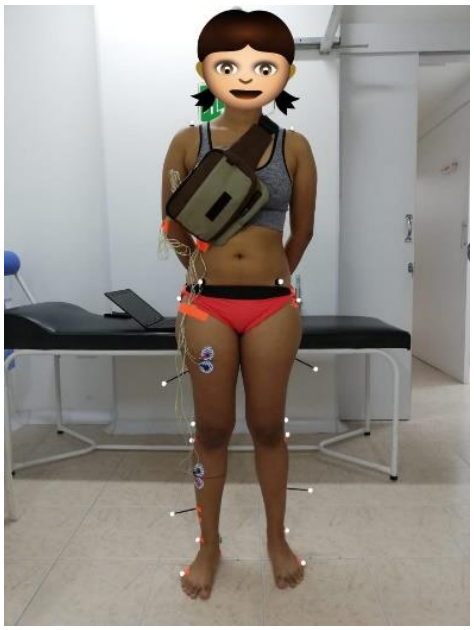

Control 9. Female, 19 years old.

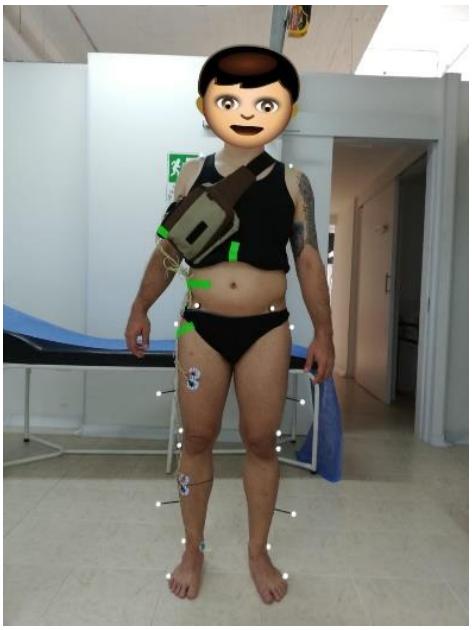

Control 10. Male, 31 years old.

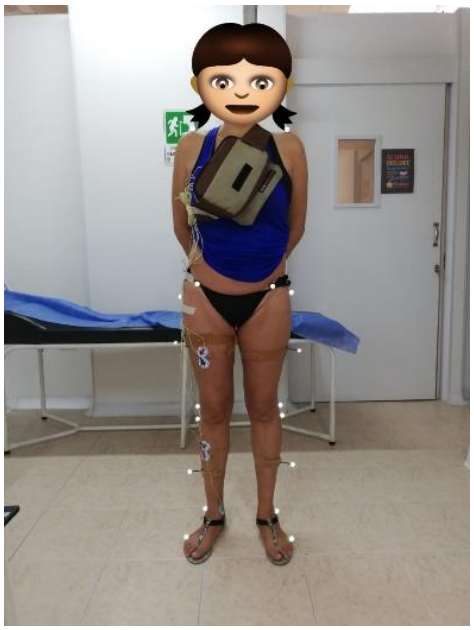

Control 11. Female, 51 years old.

Control 12. Male, 31 years old.

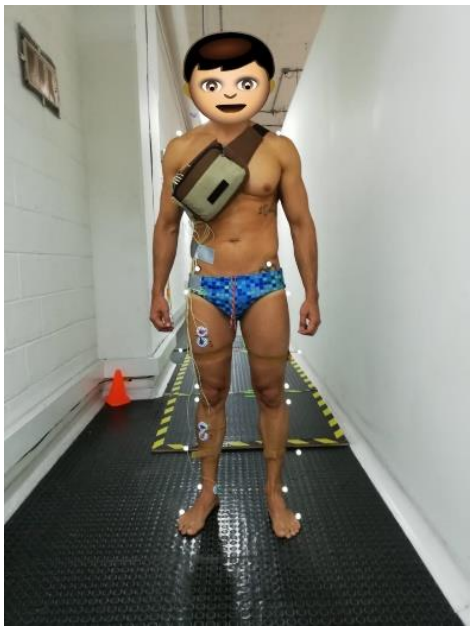

Control 13. Male, 39 years old.

Control 14. Female, 19 years old.

Control 15. Male, 59 years old.

Appendix CS.

PRUEBA DE CONFORT

Mientras lee cada pregunta, recuerde que no hay una respuesta correcta o incorrecta. Solo piense en SU PROPIA OPINIÓN sobre el tema y subraye a lo largo de la línea en cualquier lugar en el que considere sea su opinión, por ejemplo:

¿Qué tan importante es para usted el café en la mañana?

Sin importancia — Extremadamente importante

Luego de comprender la prueba, lea atentamente las siguientes preguntas:

1. Calcule qué tan agotado físicamente se encuentra en este momento.

Extremadamente cansado — Extremadamente relajado

2. Calcule qué tan motivado se encuentra para realizar esta encuesta.

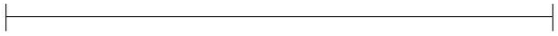

Extremadamente desmotivado — Extremadamente motivado

3. Durante la última prueba, califique el ajuste de su prótesis.

Terrible — Excelente

4. Durante la última prueba, califique su comodidad al estar de pie usando su prótesis.

Terrible — Excelente

5. Durante la última prueba, califique la frecuencia con la que perdió el equilibrio mientras usaba su prótesis.

Todo el tiempo — Nunca

6. Durante la última prueba, calcule qué tanta energía utilizó para usar la prótesis (haciéndolo sentir cansado).

Completamente agotador — Nada en absoluto

7. Durante la última prueba, calcule la sensación de presión o calentamiento ejercidos por la cuenca (socket) en su muñón.

Lo peor posible — Lo mejor posible

PRUEBA DE CONFORT

8. Si tuvo algún dolor en su muñón durante las última prueba, ¿qué tan doloroso fue?.

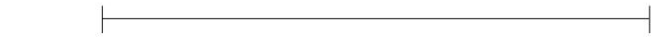

Extremadamente intenso — Extremadamente suave

No tuve dolor ___

9. Durante la última prueba, ¿qué tan molesto fue el dolor en su muñón?

Extremadamente molesto — Nada en absoluto

No tuve dolor ___

10. Tuvo algún dolor en su pierna o pie no amputado durante la última prueba, ¿Qué tan doloroso fue?

Extremadamente intenso — Extremadamente suave

No tuve dolor ___

11. Durante la última prueba, ¿qué tanto le incomodó el dolor en su otra pierna o pie?

Extremadamente molesto — Nada en absoluto

No tuve dolor ___

12. Durante la última prueba tuvo algún dolor en la espalda, ¿qué tan doloroso fue?

Extremadamente intenso — Extremadamente suave

No tuve dolor ___

13. Durante la última prueba, ¿qué tan molesto fue el dolor de espalda para caminar?

Extremadamente molesto — Nada en absoluto

No tuve dolor ___

14. Durante la última prueba, calcule con qué frecuencia se sintió frustrado con su prótesis.

Todo el tiempo — Nunca

15. Durante la última prueba, calcule su capacidad para caminar usando su prótesis.

No pude caminar — No tuve problema

16. Durante la última prueba, califique qué tan satisfecho estuvo con su prótesis.

Extremadamente insatisfecho — Extremadamente satisfecho

17. Durante la última prueba, califique la satisfacción con la que caminó usando su prótesis.

Extremadamente insatisfecho — Extremadamente satisfecho

PRUEBA DE CONFORT

Utilice las siguientes figuras para ubicar y resaltar cualquier lugar en el que hubiese sentido dolor durante la prueba.

MIEMBRO RESIDUAL IZQUIERDO

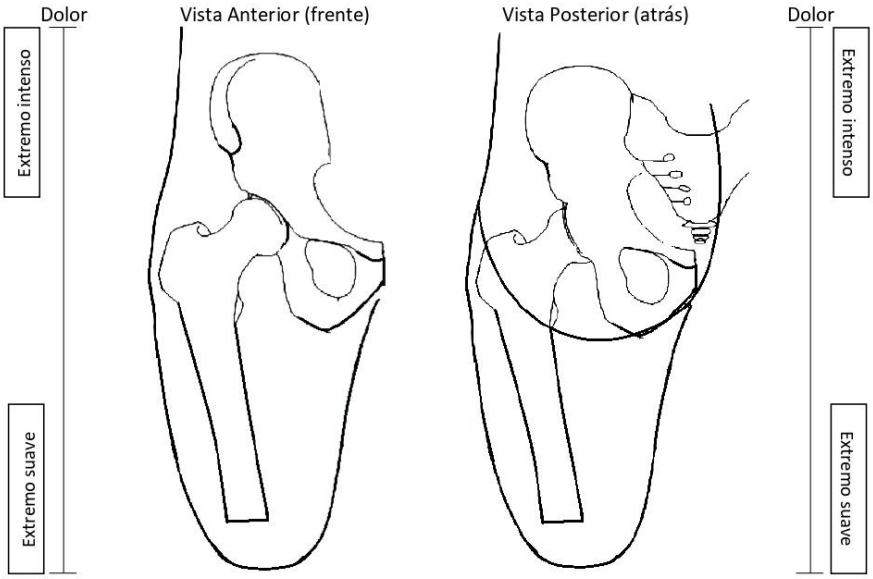

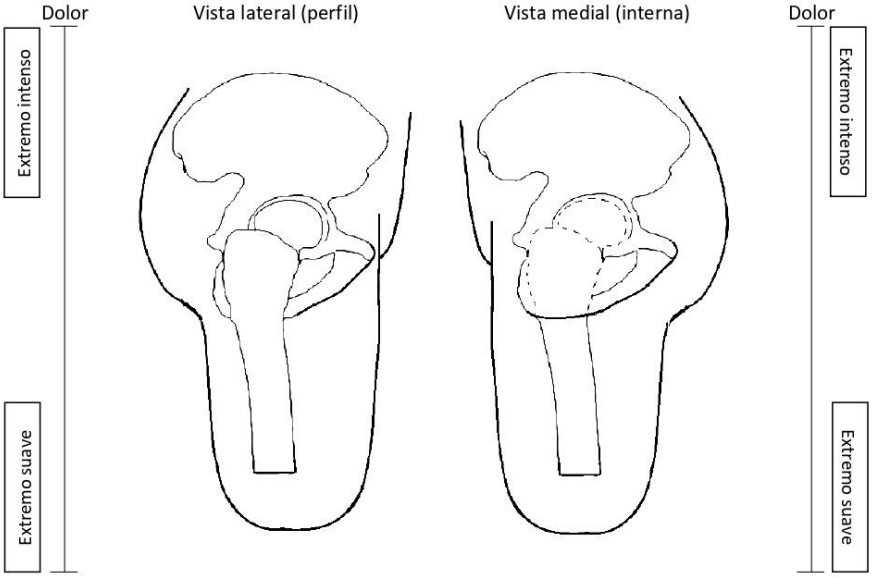

Appendix MLA.

2018 GLOBAL MEDICAL ENGINEERING PHYSICS EXCHANGES/PAN AMERICAN HEALTH CARE EXCHANGES (GMEPE / PAHCE)

Gait Parameters Identification for the Differentiation of Neurodegenerative Diseases using Classifiers

A. M. Cárdenas[1], C. Isaza[2], J. Uribe[1], A. M. Hernadez[1]
[1]GIBIC, Department of Bioengineering
[2]SISTEMIC, Department of Electronic Engineering
Emails: andresm.cardenas, victoria.isaza, juliana.uribep, alher.hernandez (@udea.edu.co)
Engineering Faculty, Universidad de Antioquia UdeA, Calle 70 No. 52-21, Medellín, Colombia

Abstract — **Degenerative nerve diseases affect the neuromusculoskeletal system, which has implications for human gait. The study of the pathological gaits using gait analysis has been performed for the disease characteristics extraction and disease classification. This paper presents a statistical analysis of gait parameters of healthy volunteers, patients with Parkinson's disease, Amyotrophic Lateral Sclerosis and Huntington. Using the statistical analysis, a set of descriptive variables was selected. Descriptors such as the mean of the temporal parameters of gait, the energy cost, and some correlated variables such as gender, age and body mass index were used. As classification methods Discriminant Analysis and fuzzy C-means were implemented. The Linear Discriminant Analysis classifies 100% of the Parkinson's disease cases, 90% of Amyotrophic Lateral Sclerosis, 87.5% of healthy and 89.47% of Huntington patients. The fuzzy c-means achieved a lower classification of 62.5% of Parkinson 60%, 60% of ALS and 42.1% Huntington; however, the information from the membership matrix gives important information to give a final clinical diagnosis. The energy cost in the stance phase increased, and the gait speed decreased for critical conditions. Depending on the disease type, the cadence decreases. The variability of the data of Amyotrophic Lateral Sclerosis and Huntington's involves an intra-subject analysis.**

Keywords — **Neurodegenerative diseases, gait recognition, fuzzy c-means, linear discriminant analysis, pattern analysis**

I. Introduction

Neurodegenerative diseases are disorders characterized by a progressive and accelerated degeneration or death of neurons of the nervous system. This causes limitations in movement, balance, speech, and memory [1]. Diseases such as Parkinson's disease (PD), Amyotrophic Lateral Sclerosis (ALS) and Huntington's disease (HD) severely affect the mobility and gait [2][3].

Usually symptoms like a weakness, loss of sensation, among others [4], cause posture problems, clumsy movements and asymmetry movements [5]. In the Parkinson's disease (PD) the problems of balance and coordination in gait are common [6]. For the Amyotrophic Lateral Sclerosis (ALS) the damage of neuromotor system results in motor dysfunction and muscle weakness [7]. The Huntington's disease (HD) is characterized by fast, sudden and uncontrollable facial movements, spasmodic movements, slow, bradykinesia and an unstable gait [8].

Gait analysis allows for the assessment of repetitive patterns in neurodegenerative diseases. Generally, the studies have been done since the extraction of characteristics and the clinical analysis, to provide an early diagnosis. The characteristics extraction presented by Melo Roiz et al. in [9], used a statistical analysis of spatial-temporal gait variables of subjects with PD and healthy adults. They found significant differences for the speed and length of the stride, the initial contact and the maximum extension in the terminal contact, as well as in the maximum flexion in the middle swing. A similar statistical study was conducted by Sofuwa et al. in [10]. They found a significant reduction in gait length, gait speed, ankle and hip force. These characteristics can help in the diagnosis of neurodegenerative diseases. Delval et al. in [11] evaluated the gait initiation cycle in Huntington's disease. Statistical test such as the Mann-Whitney U-test was applied. They studied the kinetic, spatial, temporal and angular variables. They found akinesia in both types of initiation for HD and hypokinesia.

The automatic diseases classification of diseases is showed by Bilgin's in [12]. They use the discrete Wavelet transform to extract six frequency bands of the signals of feet forces. They use a Bayesian Naïve classifier and the discriminant analysis technique. The classification result was maximum classification of 90.93% of PD, ALS, HD and healthy groups. In the Xiaa's et al. [13] the methods used were Support Vector Machines, Random Forest, Multilayer Perceptron and the K Nearest Neighbor. They used nine statistical descriptors: the minimum and maximum values, the mean, standard deviation, among others. The highest accuracy classification rate was 96.83% between healthy and diseased subjects. Other kinds of algorithm such as radial function neural networks [14] have classified 93.75% of diseases, as well as Neuro-fuzzy [15], the fractal dynamics [16], the bi-clusters technique [17] have made it possible to understand the clinical pathological gait.

Although the clinical statistical analysis reveals clinically relevant information, this information is poorly used to the automatic gait classification nowadays. We consider the statistical analysis and clinical information to find more informative descriptors with higher correlation

PORTO, PORTUGAL; MARCH 19–24, 2018
978-1-5386-5475-0/18/$31.00 ©2018 IEEE
ISBN: 978-1-5386-5475-0
IEEE CATALOG NUMBER: CFP1818G-ART

Appendix PKM.

Parametric Modeling of Kinetic-Kinematic Polycentric Mechanical Knee

A.M. Cárdenas[1], J. Uribe[1] and A.M. Hernández[1]

[1] Bioinstrumentation and Clinical Engineering Research Group - GIBIC, Bioengineering Department, Engineering Faculty, Universidad de Antioquia UdeA; Calle 70 No. 52-21, Medellín, Colombia
(andresm.cardenas, alher.hernandez, juliana.uribep)@udea.edu.co

Abstract— **The transfemoral amputation involves the loss of the knee joint, which is recognized as a common and complex case. The knee is replaced by a polycentric mechanism, which is exposed to high levels of structural stress. Therefore, mathematical models of the mechanics knees are commonly used to kinetic analysis and simulation and determine possible failures. This paper describes the procedure for determining a kinematic model of a four-bars polycentric knee using a geometric analysis and the Grashof Law for a double rocker. The kinetic model was found using parametric, linear and nonlinear identification techniques, for this were used knee force and angle data supplied by the free database Orthoload. The model couples the kinetics and kinematics ARX structure, these can represent bending angles 110 ° and the total force exerted on the instantaneous center of rotation of the knee.**

Keywords— **Biomechanics, kinematics, nonlinear dynamical systems, prosthetics, prosthetic limbs, system identification.**

I. Introduction

The amputation is a progressive problem associated with different causes like work or traffic accidents [1], diseases [2] and war [3]. Regardless of the cause, unilateral lower limb amputation is a common case [4], assorted according to amputation height [5].

The transfemoral prosthesis is a mechanical assistance device for above knee (AK) amputees. This prosthetic system consists of five parts: prosthetic foot, shank, knee unit, socket and suspension [6]. Each of these elements is subjected to different mechanical stresses decreasing the life cycle of elements, affecting mobility and patient confidence [7]. The mechanical knee facilitates patient mobility, improves gait performance and stability of the amputee during their activities of daily living [8]. The prosthetic knees are characterized by monocentric and polycentric mechanisms, providing greater or lesser flexion and extension of the joint [9].

The polycentric knees have different rotation axes, which converge in the instant center of rotation (ICR). These knees are used by it's biomechanics versatility, presenting good performance in the stance and swing phase gait, allowing greater confidence, stability, bending and factly.

A typical four bar knee is shown in Fig 1. This is characterized by four center cranks A, B, OB y OA linked by OA-A, A-B, B-OB, OA-OB, conform 4 links a, b, c, d respectively. Mechanical linkage configuration is based on Law of Grashof mechanisms, where the length of each link is determined to have a full joint revolution [10].

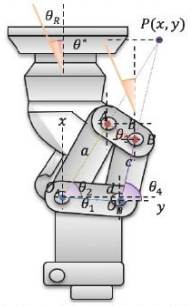

Fig 1. Extended knee geometry: links, articulation angles and instant center of rotation.

The knee should support the weight of the body and additional loads during gait cycles. The resulting forces stabilize the body and achieve the displacement during the phases of gait. If known the knee force magnitude and direction, is possible to choose a correct construction material, simulate the gait performance and estimate possible structural problems.

Two forms of analysis are discussed in this paper, kinematic and kinetic. To find kinetic model, the study is conducted with data from healthy patients, as suggested in [11]. Data is collected from 8 test subjects with an average weight of 100kg and different system identification techniques are evaluated. To find kinematic model, a geometric analysis of four- bar mechanism is done. The resulting model allows provides information about the ICR, marked with a *P(x,y)*.

Mohsen and colleagues [12] designed a method to parameterize a polycentric knee four-bars using the ICR and the floor reaction forces of (FRF) during gait (the initial contact, the support phase and voluntary bending before takeoff foot). To determine an appropriate measures and angles, a genetic algorithm uses FRF data of an amputee patient to parameterize the model of the knee.

The four-bars knee model and the optimal geometry of the joints are presented in [13]. They use the Grashof Law, the

I. Torres et al. (eds.), *VII Latin American Congress on Biomedical Engineering CLAIB 2016, Bucaramanga, Santander, Colombia, October 26th -28th, 2016*,
IFMBE Proceedings 60,
DOI: 10.1007/978-981-10-4086-3_150